

University of Louisville

ThinkIR: The University of Louisville's Institutional Repository

Electronic Theses and Dissertations

12-2016

Glutathione s-transferase p in glucose homeostasis in mice.

Shubha Ghosh Dastidar

Follow this and additional works at: <https://ir.library.louisville.edu/etd>



Part of the [Endocrinology Commons](#)

Recommended Citation

Ghosh Dastidar, Shubha, "Glutathione s-transferase p in glucose homeostasis in mice." (2016). *Electronic Theses and Dissertations*. Paper 2561.

<https://doi.org/10.18297/etd/2561>

This Doctoral Dissertation is brought to you for free and open access by ThinkIR: The University of Louisville's Institutional Repository. It has been accepted for inclusion in Electronic Theses and Dissertations by an authorized administrator of ThinkIR: The University of Louisville's Institutional Repository. This title appears here courtesy of the author, who has retained all other copyrights. For more information, please contact thinkir@louisville.edu.

GLUTATHIONE S-TRANSFERASE P IN GLUCOSE HOMEOSTASIS IN MICE

By

Shubha Ghosh Dastidar
B.S., University of Pune, 2004
M.S., Bangalore University, 2006
M.S., University of Louisville, 2012

A Dissertation
Submitted to the Faculty of the
School of Medicine of the University of Louisville
in Partial Fulfilment of the Requirements
for the Degree of

Doctor of Philosophy in Biochemistry and Molecular Biology

Department of Biochemistry and Molecular Genetics
University of Louisville
Louisville, Kentucky

December 2016

Copyright 2016 by Shubha Ghosh Dastidar

All rights reserved

GLUTATHIONE S-TRANSFERASE P IN GLUCOSE HOMEOSTASIS IN
MICE

By

Shubha Ghosh Dastidar

B.S., University of Pune, 2004

M.S., Bangalore University, 2006

M.S., University of Louisville, 2012

A Dissertation Approved on

November 11, 2016

by the following Dissertation Committee

Aruni Bhatnagar Ph.D

Daniel J. Conklin Ph.D

Russell A. Prough Ph.D

Bradford G. Hill Ph.D

Alan Cheng Ph.D

DEDICATION

To the fond memory of my father, Salil Ghosh Dastidar.
For being the first teacher in my life and imparting on me the
importance of education.

Papa, I miss you and think of you often, but I know that
you walk beside me always.

To my loving mother, Munmun Ghosh Dastidar.
Ma, you have made everything possible for me.
Your sacrifices remain my strongest motivation.

To my beloved friend, Maronda Dowdy.
Through good times and bad, I am eternally grateful for your
kindness, wisdom and unwavering support.

ACKNOWLEDGEMENTS

I am most grateful to my advisors, Dr. Aruni Bhatnagar and Dr. Daniel J. Conklin, for providing the financial support, guidance and flexibility for my scientific pursuits. Dr. Bhatnagar's intuitive understanding and encouragement were extremely helpful, and his assistance in improving my existing research was critical to the end result. Of course, this project would not have been possible without the support and insight of Dr. Conklin. His knowledge and expertise in the area of aldehyde metabolism and GSTs have proven invaluable throughout the course of this academic journey.

My sincere gratitude extends to all members of my thesis committee and to everyone in the Biochemistry Department at the University of Louisville for their discussion, criticism, and support of my data. Dr. Russell A. Prough was always an encouraging and understanding presence in discussing research and career objectives. Dr. Bradford G. Hill gave me invaluable advice on reorganizing the hypothesis for my Exam I proposal on Hutchinson-Gilford Progeria Syndrome, an important step that influenced the positive outcome of my qualifying examination. I thank Dr. Alan Cheng for being willing to serve on my committee and for his inputs. I would especially like to thank Dr. Barbara J. Clark and Dr. Ronald G. Gregg for their encouragement and understanding over the past few years.

I am indebted to past and present members of the Diabetes and Obesity Center for providing an eclectic and fun place to work. Gregg A. Shirk has been a steady experienced hand in assisting with animal experiments, and I am truly grateful for his continuing friendship. Dr. Ganapathy Jagatheesan has played a key role in this project through his insightful discussions of my research. I appreciate Dr. Petra Haberzettl lending her expertise in purifying the acrolein

adduct antibody. Thanks to David Hoetker for sharing his knowledge in a variety of research techniques. Jasmit Shah was an esteemed desk neighbor who provided invaluable assistance with the Spearman's correlation analyses. Dr. Anuradha Kalani was a nurturing post-doctoral influence who taught me various aspects of data presentation. Lastly, I thank all my fellow graduate students for their support over the years.

I reserve my deepest gratitude and appreciation for my family and friends for understanding my self-imposed exile as part of the academic preparation needed to complete this important project. I am eternally grateful for my mother, who has unconditionally supported my dreams; this dissertation is as much her accomplishment as it is mine. Many thanks go to my friends at OASIS for forming a supportive network throughout my years in Louisville. Lastly, I want to thank my dear friends, Maronda and her family, for their support, company and love during this journey toward the PhD. She made it possible for me to face the challenges and uncertainty of research with a smile.

ABSTRACT

GLUTATHIONE S-TRANSFERASE P IN GLUCOSE HOMEOSTASIS IN MICE

Shubha Ghosh Dastidar

November 11, 2016

High calorie diets have fostered the current pandemic of obesity and comorbid conditions of non-alcoholic fatty liver disease (NAFLD), systemic insulin resistance (IR) and type 2 diabetes (T2D). Hepatic glutathione S-transferases (GSTs) are dysregulated in obesity, NAFLD and diabetes. The multifunctional GST pi isoform (GSTP) catalyzes acrolein metabolism and inhibits JNK (c-Jun NH₂-terminal kinase). The purpose of this study was to test specifically whether GSTP deficiency disturbs glucose homeostasis in mice. Hepatic GST proteins were downregulated by short-term high fat diet (HFD) in wild type (WT) mice concomitant with glucose intolerance, increased hepatic JNK activation and protein-acrolein adducts. To address whether GSTP contributes specifically to HFD-induced sequelae, metabolic phenotype of GSTP-null mice was assessed. Body composition, fasted levels of blood glucose and insulin were similar in WT and GSTP-null mice. However, the study revealed that GSTP-null mice were glucose intolerant. GSTP-null mice were glucose intolerant. Furthermore, this defect in glucose homeostasis was due not to peripheral IR but to an impaired capacity to increase plasma insulin level in response to hyperglycemia. In exploring the effect of insufficient insulin release, the pyruvate tolerance test

(PTT) revealed greater PTT AUC in GSTP-null mice, indicating enhanced hepatic glucose output. Glucose intolerance was positively correlated with the level of pyruvate intolerance. However, no differences were found in fasting mRNA levels of the gluconeogenic enzymes: phosphoenolpyruvate carboxykinase (*Pepck*) and glucose-6-phosphatase (*G6pc*) between WT and GSTP-null livers. Treatment of GSTP-null mice with the JNK inhibitor, SP600125, attenuated hepatic gluconeogenesis compared with vehicle-treated littermate controls. Collectively, these data illustrate a novel role of GSTP in glucose handling via JNK regulation and hepatic gluconeogenesis – a heretofore unrecognized function. Thus, future studies are warranted for studying how GSTP dysregulation influences the metabolic complications of human obesity, NAFLD and diabetes.

TABLE OF CONTENTS

DEDICATION.....	iii
ACKNOWLEDGEMENTS.....	iv
ABSTRACT.....	vi
LIST OF FIGURES.....	xi
LIST OF TABLES.....	xii
CHAPTER I.....	1
GENERAL INTRODUCTION.....	1
LITERATURE REVIEW.....	1
Disease Statistics of the West: An Emerging Epidemic.....	1
Disease Statistics around the World: Perils of Urbanization.....	1
'Diabetes: A Disease of Paradoxes'.....	2
Overarching Research Goals.....	3
Natural Progression and Pathophysiology of Type 2 Diabetes.....	3
Oxidative Stress, Lipid peroxidation and Aldehydes.....	6
Glutathione S-transferases.....	7
Obesity, Diabetes and Glutathione S-transferases.....	8
Glutathione S-transferase P.....	11
Regulation of GSTP Expression.....	12
Transcription factor.....	12
Hormonal.....	13
Epigenetics.....	15
microRNA.....	15
Interleukin-6.....	16
GST Polymorphisms and Diabetes.....	16
GSTP and Acrolein Detoxification.....	18
GSTP in Cell Signaling: JNK Activation and Protein S-glutathionylation.....	20
JNK Activation in Obesity and Diabetes.....	22
SUMMARY AND PROJECT OBJECTIVES.....	23

SPECIFIC AIMS	27
THESIS DESCRIPTION.....	28
CHAPTER II	29
EXPERIMENTAL PROCEDURES.....	29
Management of Mouse Colony.	29
High Fat Feeding.....	30
Organ Analyses.....	33
Fasting Blood Glucose Measurements.....	33
Body Composition.	34
Metabolic Profile.....	34
Metabolic Tests.	35
I. Glucose Tolerance Test.	35
II. Pyruvate Tolerance Test.	36
III. Insulin Tolerance Test.	37
Insulin Signaling in vivo.	37
Glucose and Pyruvate-stimulated Insulin Secretion in vivo.	38
JNK Inhibitor Treatment in vivo.	41
Complete Blood Cell Count.	44
Protein Quantification by Immunoblotting.....	44
Histology.	47
Real-Time Quantitative PCR.	47
Biochemical Analyses.	49
Liver Triglycerides and Total Cholesterol.	49
Statistical Analysis.....	50
CHAPTER III	51
EFFECT OF OBESITY ON GLUTATHIONE S-TRANSFERASE-P ABUNDANCE AND FUNCTION	51
INTRODUCTION.....	51
STUDY OBJECTIVE	52
RESULTS.....	53
DISCUSSION.....	75

CHAPTER IV	81
GLUTATHIONE-S-TRANSFERASE-P IN GLUCOSE HOMEOSTASIS: ROLE OF JNK ACTIVATION	81
INTRODUCTION.....	81
STUDY OBJECTIVE	87
RESULTS.....	87
DISCUSSION.....	138
CHAPTER V	145
CONCLUSIONS AND FUTURE DIRECTIONS	145
REFERENCES.....	156
CURRICULUM VITAE	167

LIST OF TABLES

TABLE	PAGE
1. Oligonucleotide primers for qRT-PCR and RT-PCR analysis.....	49
2. Metabolic and plasma parameters of male WT and GSTP-null mice.....	92
3. Spearman's Rank Correlation Coefficients of hepatic gluconeogenic and inflammatory marker mRNAs in WT and GSTP-null mice.....	132
4. Spearman's Rank Correlation Coefficients of hepatic gluconeogenic and inflammatory marker mRNAs in JNK inhibitor-treated GSTP-null mice.....	139

LIST OF FIGURES

FIGURE	PAGE
Figure 1. Scheme illustrating the postulated project hypothesis	25
Figure 2. Experimental design of HFD study in WT and GSTP-null mice	32
Figure 3. Experimental design of GSIS-PSIS study.....	40
Figure 4. Experimental Design of JNK inhibitor study.....	43
Figure 5. Diet-induced obesity in WT mice	56
Figure 6. Effect of HFD on GTT and indirect calorimetry in WT mice	59
Figure 7. Effect of HFD on GST abundance in WT mice	63
Figure 8. Effect of HFD on hepatic GSTP in WT mice.....	65
Figure 9. Effect of HFD on adipose depot GSTP in WT mice.....	68
Figure 10. Effect of HFD on protein-acrolein adducts in WT mice.....	71
Figure 11. Effect of HFD on JNK phosphorylation in WT mice	74
Figure 12. Scheme: Effect of HFD on hepatic GSTP in WT mice.....	79
Figure 13. Scheme: Biochemical pathway of gluconeogenesis	84
Figure 14. GTT and indirect calorimetry in GSTP-null mice on NC diet.....	93
Figure 15. Diet-induced obesity in GSTP-null mice	96
Figure 16. GTT and indirect calorimetry in GSTP-null mice on HF diet	99
Figure 17. Hepatic GSTA and GSTM abundance in GSTP-null mice.....	101
Figure 18. Hepatic triglycerides and cholesterol in GSTP-null mice on HF diet	103
Figure 19. Protein-acrolein adducts in GSTP-null mice on NC diet.....	106

Figure 20. Protein-acrolein adducts in GSTP-null mice on HF diet.....	108
Figure 21. Protein-acrolein adducts in GSTP-null mice on HF diet.....	110
Figure 22. Hepatic ER-stress markers in GSTP-null mice.....	113
Figure 23. JNK phosphorylation in GSTP-null mice on NC diet.....	115
Figure 24. JNK phosphorylation in GSTP-null mice on HF diet	117
Figure 25. Insulin signaling in peripheral tissues in GSTP-null mice	120
Figure 26. Hepatic gluconeogenesis by PTT in GSTP-null mice	122
Figure 27. Glucose and pyruvate-stimulated insulin secretion in GSTP-null mice	127
Figure 28. Gluconeogenic and inflammatory markers in GSTP-null mice	130
Figure 29. Effect of JNK inhibitor on hepatic gluconeogenesis by PTT in GSTP- null mice	134
Figure 30. Effect of JNK inhibitor on gluconeogenic and inflammatory markers in GSTP-null mice	136
Figure 31. Scheme illustrating the summary of project findings.....	140

CHAPTER I

GENERAL INTRODUCTION

LITERATURE REVIEW

Disease Statistics of the West: An Emerging Epidemic

The incidence and prevalence of obesity, T2D and liver disease have soared dramatically in the Western world over the past two decades with the current rates of adult and pediatric obesity reported to be an estimated 20–30% of the US population [1] [2-4]. According to NHANES reports, more than one-third (34.9% or 78.6 million) of U.S. adults are obese and 68% are overweight or obese [5]. Obesity is a major driver of the T2D epidemic, hepato-biliary and gallbladder diseases, cardiovascular pathologies, neurodegenerative disorders, asthma, and a variety of cancers [6]. In addition, obesity is often accompanied by hepatic steatosis, which is part of the spectrum of NAFLD, currently the most common liver disorder in the US [2]. A strong association between NAFLD and T2D has been demonstrated: more than 90% of obese patients with T2D have NAFLD [7]. In addition, around 20% of patients with NAFLD progress to non-alcoholic steatohepatitis (NASH), liver cirrhosis and failure [8, 9].

Disease Statistics around the World: Perils of Urbanization

Once considered a disease of the West, T2D and NAFLD are an escalating epidemic in South Asia and in the Western Pacific Region [10-12]. The International Diabetes Federation has predicted that the number of individuals with diabetes will increase from 240 million in 2007 to 380 million in 2025, with more than 60% of them belonging to Asia, because it remains the world's most populous region.

A multitude of interrelated factors have fostered the diabetes pandemic, including rapid industrialization and urbanization and the ensuing lifestyle changes [10, 13]. The effect of the intrauterine environment and the resulting epigenetic changes may also underlie increased risk of T2D and other chronic diseases in adult life [14, 15]. Epigenetic changes being transmittable to future generations become intergenerational. Impaired fasting glucose (IFG) and impaired glucose tolerance (IGT) are high-risk conditions for diabetes and cardiovascular disease [16]. China and other countries in Western Pacific Region have a high prevalence of IGT [17].

‘Diabetes: A Disease of Paradoxes’

Several lines of evidence support that obesity promotes clusters of risk factors that potentiate IR and, obese individuals experience substantially elevated comorbidities. However, not all obese individuals develop cardiometabolic abnormalities, thus presenting the paradox of the “metabolically healthy obese” or “insulin sensitive obese” subjects who are protected against complications of T2D [18, 19]. Such individuals do not exhibit increased oxidative stress in

visceral adipose tissue and maintain increased levels of antioxidant enzymes. In contrast, NAFLD and/or T2D are reported in an estimated 60% of the young, lean urban population in Asian communities [10, 20, 21]. Taken together, the dynamics of the diabetes epidemic pose the conundrum that not all obese progress to diabetes and not all diabetics are obese, implicating genetic and/or environmental factors as likely determinants governing interindividual susceptibility.

Overarching Research Goals

Diabetes and its complications are preventable and highly treatable. A randomized trial in China demonstrated that dietary and exercise intervention reduced diabetes risk by 31% to 46% in individuals with IGT (reviewed in [10] and references therein). In observational studies and randomized trials conducted in Asia and Europe, control of multiple risk factors reduced cardiorenal complications and all-cause mortality by 50% to 70% in individuals with T2D [10]. Therefore, a better understanding of the pathophysiology of T2D holds great promise. In particular, investigations focused on the differences between obese insulin sensitive, obese insulin resistant and lean diabetic subjects or animal models that recapitulate these attributes of the human disease can delineate key factors that either contribute to or prevent the development of IR.

Natural Progression and Pathophysiology of Type 2 Diabetes

Elevated blood glucose levels take the center stage in the definition of diabetes mellitus. The word *Diabetes* stems from the Greek root meaning *to siphon*, to represent the frequent urination observed in patients, while the term *mellitus* has its origins in the Latin word for honey, referring to the sweet taste of urine in these patients. The nomenclature incorporates the diverse pathophysiologic events resulting in the characteristic hyperglycemia. Type 1 diabetes is an autoimmune disease resulting in the death of pancreatic β cells and usually manifests early in life. It is associated with symptoms such as frequent urination, weight loss, and increased plasma levels of ketone bodies and little or no circulating insulin. Type 1 diabetes account for 10% of the total diabetic population of the United States. In contrast, T2D results from IR, defined as the lack of responsiveness to insulin in peripheral tissues such as muscle, fat and liver.

Diabetes is diagnosed clinically by elevated fasting plasma glucose over 126 mg/dL where the normal range in humans is 70-110 mg/dL [22]. Alternatively, an oral glucose tolerance test can detect T2D as elevated plasma glucose over 200 mg/dL two hours after administering a 75 g glucose load [23]. A longer term marker of blood glucose levels is glycated hemoglobin A1c (HbA1c), which normally accounts for approximately 5% of circulating hemoglobin and in diabetic patients is found at 7% or greater abundance. The metabolic derangements underlying T2D include decreased insulin-stimulated glucose uptake in fat and muscle, increased hepatic glucose production and impaired

pancreatic β cell function as determined by insulin secretion (Berne, R.M. and M.N. Levy, Physiology. 3rd ed. 1993, St. Louis: Mosby Year Book xiv, 1071).

Interrogating the natural progression of T2D in humans requires elucidation of the relationship between plasma glucose and insulin levels in relation to insulin resistance and secretion. A stepwise increase in plasma glucose occurs during progressive glucose intolerance with a corresponding increase in plasma insulin response. Subjects with IGT are able to mount an elevated insulin secretory response and prevent development of hyperglycemia. Due to obesity, inactivity, aging and genetic factors, IR increases. Pancreatic beta cells respond to IR by increasing insulin secretion in the normal physiological state to maintain normoglycemia. In susceptible individuals β cell function begins to decline. This decline of β cell function -- in the face of usually severe but stable IR -- leads to first postprandial hyperglycemia and then fasting hyperglycemia. Most individuals can maintain a high degree of compensatory insulin secretion throughout their life to prevent development of T2D. The failure of adequate beta cell compensation underlies the onset of frank T2D. The proportion of individuals (obese or otherwise) that is unable to adequately compensate become diabetic.

For patient therapy, guidelines target maintaining FPG levels within the normal range of 70-110 mg/dL (5-7 mM) or glycated hemoglobin A1c below 7%. To counter the deleterious effects of hyperglycemia, therapeutic interventions for T2D are aimed at decreasing glucose production in the liver or increasing glucose consumption in peripheral tissues.

Oxidative Stress, Lipid peroxidation and Aldehydes

Obesity is a state of chronic oxidative stress and inflammation, key determinants of the causal progression to diabetes and liver disease [24]. Oxidative stress is defined as a significant imbalance between antioxidant defenses and pro-oxidative reactive oxygen species (ROS) in favor of the latter, resulting in (often) cellular dysfunction. Substantial evidence implicates ROS as key perpetrators of metabolic dysfunction [25]. ROS, such as hydroxyl radicals, are highly reactive and cause direct oxidative modification of proteins, lipids, carbohydrates and DNA. Membrane lipids are extremely susceptible to free radical-mediated injury. ROS initiates peroxidation of polyunsaturated acyl chains of membrane phospholipids to result in Hock cleavage and subsequent formation of lipid-derived reactive aldehydes of various chain lengths such as trans-4-hydroxy-2-nonenal (4-HNE), trans-4-oxo-2-nonenal (4-ONE), acrolein, malondialdehyde, glyoxal, crotonaldehyde, and 2-hexenal [26]. Even transient increases in ROS levels lead to accrual of lipid peroxidation products. Aldehydes are highly reactive and covalently modify cysteine, histidine or lysine residues of proteins in a process generically referred to as protein carbonylation with deleterious consequences for protein function and stability. For example, 4-HNE and acrolein modification of proteins can inhibit their activity and cause protein degradation [27-29]. Consistent with the view that ROS-mediated injury can be attributed in part to lipid-derived aldehydes, almost 7% of AFABP in adipose tissue was covalently modified by 4-HNE in obese insulin-resistant C57Bl/6J mice, resulting in a decreased binding affinity for fatty acids [30]. Increased plasma protein

carbonyls, as a biomarker of systemic oxidative stress, was positively correlated with IR in obese patients [31] and was significantly decreased following treatment [32, 33]. As a result of these (and many more) findings, there has been a surge in interest in evaluating how aldehyde metabolism and protein carbonylation may serve as a mechanistic link between oxidative stress and IR. Investigating the mechanisms and consequences of oxidative stress in insulin-responsive tissues is vital to uncovering novel determinants of disease progression.

Glutathione S-transferases

The capability of cells to counter oxidative stress is primarily mediated through antioxidant response elements (AREs), which are largely under the control of the transcription factor nuclear factor E2-related factor 2 (Nrf2) which, under pro-oxidative conditions, induces expression of phase I and II metabolizing enzymes and transporters pivotal to cellular detoxification [34, 35]. Glutathione S-transferases (GSTs) are a multigene multifunctional family of dimeric phase II detoxification enzymes that catalyze the conjugation of reduced GSH to reactive endogenous and exogenous electrophiles [36]. GSTs can be found in the cytosol, mitochondria, and microsomal membranes of most tissues throughout the body [36]. Based on their amino acid sequence and substrate specificity, eight classes of GSTs (namely GST alpha, mu, pi, theta, sigma, zeta, kappa and omega) have been identified in mammals. Although less than 10% of the primary sequence is conserved, all GST isozymes have a similar topology and two domains responsible for protein folding. The N-terminal domain (residues 1–80)

comprises one third of the protein and forms the G-site. It is composed of four β -sheets with three flanking α -helices, a structural motif common to thioredoxin, and other proteins that have evolved to bind GSH or cysteine [37]. This region contains a catalytic tyrosine, serine, or cysteine residue that directly interacts with the thiol group of GSH [37]. Distinct from their capacity to mediate cellular detoxification, several GSTs have been ascribed additional cellular functions such as cell signaling, as molecular carriers ('ligandins') [38], peroxidase enzyme activity and modulation of calcium channels and ryanodine receptors [39]. In keeping with their critical role as cellular "caretaker" proteins, metabolic syndrome is associated with altered GST expression and function in liver and adipose tissue. Studies of GSTs during progression of obesity, diabetes and NAFLD in humans and animal models have reported both increased and decreased GST expression in vivo as described in the following sections. The impact of NAFLD on GST expression and activity appears to be isoform and, possibly, species specific as reviewed in detail by Merrell and Cherrington [40].

Obesity, Diabetes and Glutathione S-transferases

Similar to NAFLD, the effects of obesity and diabetes on hepatic GST expression and activity are inconclusive. An increase in hepatic GST activity was reported in streptozotocin-induced diabetic mice, but not in spontaneously (db/db and ob/ob) or alloxan-induced diabetic mice [41, 42]. In contrast, Thomas et al. (1989) reported that hepatic GST activity was decreased in diabetic rats and restored by insulin administration [43]. The reason for this discrepancy remains unknown but

may be due, in part, to the use of primarily nonselective GST enzymatic activities as indirect indicators of GST expression. Kim et al. demonstrated that insulin and glucagon regulate, in an opposing manner, the expression of alpha-class GSTs and that glucagon completely inhibits pi class GST expression in primary cultured rat hepatocytes, suggesting that hepatic GST expression may be decreased during diabetes [44]. GSTA4 is downregulated specifically in adipose tissue of obese, insulin-resistant humans and murine models, and also in 3T3-L1 adipocytes treated with tumor necrosis factor (TNF)- α [30, 45, 46]. Mitochondria from both GSTA4-silenced 3T3-L1 adipocytes and adipose tissue of GSTA4-null or obese C57BL/6J mice accumulate ROS and exhibit compromised respiration, resulting in impaired glucose and lipid homeostasis. This suggests that TNF- α -induced downregulation of GSTA4 is a major determinant linking inflammation with oxidative stress and IR [45]. Boden et al. performed a detailed analysis of subcutaneous fat biopsies from six lean and six obese nondiabetic subjects and observed an upregulation of GSTP along with ER stress-related unfolded protein response (UPR) proteins such as calreticulin, protein disulfide-isomerase A3 by proteomic analysis [47]. The authors also confirmed by western blot, an upregulation of several UPR stress-related proteins, including calnexin and phospho-JNK-1, a downstream effector of ER stress. Furthermore, RT-PCR analysis revealed upregulation of the spliced form of X-box-binding protein-1, a potent transcription factor and part of the proximal ER stress sensor inositol-requiring enzyme-1 pathway, demonstrating evidence of ER stress-activation of JNK as a possible link between obesity, IR, and inflammation in human subjects.

Grant et al. reported perturbations in GSTs in examining global gene expression profiles of adipose tissue in dogs during the transition from a lean to obese phenotype [48]. The authors fed high fat diet to female beagles and collected subcutaneous adipose tissue biopsies, blood, and DEXA measurements at 0, 4, 8, 12, and 24 weeks of feeding. They found that, among other genes, GSTP was induced at all time points, while GSTM4, GSTT2 and GSTO1 showed increased expression at 4 and 8 weeks, which then decreased to baseline levels or lower at 12 and 24 weeks. Interestingly, the highest food intake occurred at 4 and 8 weeks which led the authors to conclude that the induction of GSTM4, GSTT2 and GSTO1 may be due to metabolic stress associated with adipose tissue expansion and lipid storage. In contrast, some reports have also documented a decrease in GSTs during obesity and attributed it to increased oxidative stress. Kirpich et al. reported a decrease in hepatic GSTP and GSTM protein in high-fat lard diet-fed C57Bl/6J mice [49]. In a separate study, investigators fed male Wistar rats a cafeteria diet, described as a fat-rich hyper caloric diet containing pate, chips, chocolate, bacon, biscuits, and chow in a proportion of 2:1:1:1:1:1 (65% calories from fat), for 65 days and examined the expression of over 12,500 transcripts in epididymal adipose by DNA microarray [50]. Redox and stress proteins were among the pathways down-regulated in obese animals with a 2.6-3.2 fold downregulation of GSTP transcript. Miller et al. determined effects of dietary composition on obesity in mice by feeding either a high-carbohydrate diet (HC; 10% fat energy) or a high-fat energy-restricted diet (HFR; 60% fat energy) for 18 weeks. Further, to identify obesity-associated genes with persistently

altered expression following weight reduction, mice were fed either a standard low-fat diet (LF; 10% fat energy), an unrestricted high-fat diet (HF; 60% fat energy), or a HF diet followed by weight reduction (WR) [51]. Microarray analysis identified global differences in adipocyte gene expression patterns with downregulation in several GSTs. In conclusion, specific GST isozymes appears to be dysregulated with metabolic disease progression.

Glutathione S-transferase P

The GST Pi isoform (GSTP) has been ascribed diverse catalytic and non-catalytic functions relevant to metabolic disease [36]. GSTP catalyzes the Michael addition of acrolein to glutathione with high specificity as a substrate to facilitate its detoxification [52]. GSTP is overexpressed in many human tumors, and is a well-documented cancer biomarker [[53] and references therein]. In humans, the dimeric GSTP is the most abundant GST isozyme in most tissues, although it is reported to be absent from hepatocytes with its expression in liver restricted to a few specialized cell types, including biliary epithelial and Ito cells [54]. Despite this, it is clearly a major hepatic protein as it produces abundant discernible spots on Coomassie blue-stained 2-DE gels of normal human liver [55]. Expression of GSTP in hepatocytes has been shown to increase in certain liver pathologies, such as alcoholic liver disease [54]. In contrast, in mice, GSTP1 is the most abundant of the GST isoforms in normal liver [36]. In addition, a second GSTP isoform (GSTP2) is expressed as a product of a distinct gene located in tandem with GSTP1 on chromosome 19. A GSTP1/2 knockout mouse

model was created to study the function of GSTP in vivo. GSTP-deficient (GSTP-null) did not show any obvious phenotype, although some null mice had higher body weights than controls [56]. Studies using GSTP-null mice have elucidated GSTP to be an important metabolic determinant of 7,12-dimethylbenz anthracene (DMBA)-induced carcinogenesis [56], APAP-induced hepatotoxicity [57], allergic airways disease [58], tobacco-induced endothelial dysfunction [59], cyclophosphamide-induced urinary bladder and cardio-toxicity [60] and more recently myocardial sensitivity to ischemia-reperfusion injury [61, 62]. GSTP was also found to be a major GST isoform in the heart, lung and aorta and contributed significantly to total GST conjugating activity in those tissues. The relative abundance of GSTP protein in other major tissues germane to obesity and diabetes, such as skeletal muscle, adipose tissue depots and pancreas has not been examined.

Regulation of GSTP Expression

The following section encompasses in brief the current understanding of each regulatory mechanism of GSTP, with emphasis on the known and anticipated contribution to obesity and diabetes. GSTP expression may be regulated by any (or a combination) of the following mechanisms: Transcription factors (Nrf2), epigenetics, microRNA, and hormonal, all of which are affected by metabolic stress states such as obesity and diabetes.

Transcription factor

GSTP gene expression is highly inducible and regulated at the transcriptional level by the activation of nuclear factors that sense electrophilic stressors of different origin and bind specific sequences of GST promoter region, such as the antioxidant responsive element (ARE). Nuclear factor erythroid 2-related factor (Nrf2) is one of the most well-characterized transcription factors recognized to stimulate the induction of GSTP as well as of other cytosolic GSTs and phase II genes (reviewed in [63]). Nrf2 is activated by electrophiles through the Keap1-Nrf2 pathway. In normal liver cells, Keap1, a cytoplasmic effector, binds to Nrf2 in the cytoplasm, causing the rapid degradation of the latter in the cytoplasm. This releases the interaction of Nrf2-Keap1 and promotes nuclear accumulation of Nrf2 to lead to the activation of detoxification enzyme genes, such as GSTs and NQO1 [63].

Hormonal

The human *GSTP* promoter region contains a TATA box, two SP1 sites, an insulin response element, and an antioxidant response element within an AP1 site [64]. The relative influence of hormones versus oxidative stress during diabetes may be critical for regulation of *GSTP* expression and activity. It is interesting to note that glucagon and insulin were shown to modulate *GSTP* expression in isolated rat hepatocytes [44]. The addition of insulin increased alpha-class GST protein levels, whereas alpha- and pi-class GST protein levels were markedly decreased in hepatocytes cultured with glucagon. In contrast, mu-class GST protein expression was unaffected by insulin or glucagon treatment. This study demonstrated that insulin and glucagon regulate, in an opposing

manner, the expression of alpha-class GSTs and that glucagon completely inhibits pi class GST expression in vitro, suggesting that hepatic GST expression may be decreased during diabetes. Relationships between antioxidant enzymes and insulin are not unprecedented. However, these effects were measured in vitro and may be unrelated to the in vivo physiologic perturbations or be insufficient to cause them, making simple associations in humans difficult. Nonetheless, it is interesting to consider that altered pancreatic hormone levels in insulin resistant states such as diabetes and NAFLD in humans can affect hepatic GSTP (and other GSTs) protein expression or activity.

GSTP1 promoter contains an insulin response element motif [65]. The insulin response element (IRE) in a gene promoter contains a T(A/G)TTT motif essential for insulin inhibition of transcription. Insulin-mediated suppression of hepatic GSTP through this IRE motif in diabetes via an as yet unidentified transcription factor is an attractive notion. In addition to conferring insulin inhibition, the IRE is required for maximal glucocorticoid stimulation. IRE sequence, location, and function are conserved among the human, rat and mouse IGFBP-1 promoters, further underscoring the importance of this element. Interestingly, the gluconeogenic enzyme, PEPCK also contains the IRE motif. Insulin inhibits and glucocorticoids stimulate hepatic expression of PEPCK and tyrosine aminotransferase (TAT). IREs mapped to the PEPCK and TAT gene promoters resemble the human and rat IGFBP-1 IREs by requiring the same T(G/A)TTT motif for maximal insulin inhibition and glucocorticoid stimulation of promoter activity. This suggests that the same protein(s) binds the T(G/A)TTT

sequence to confer insulin and glucocorticoid responsiveness to these genes. Identifying such novel transcription factor(s) (and co-activators, co-repressors) may reveal if insulin and glucocorticoids regulate hepatic expression of proteins such as GSTP, PEPCK (and many more) in vivo. Collectively, these observations illustrate the complex interwoven mechanisms of regulation of pancreatic hormones, gluconeogenic enzymes and hepatic GSTs that remain to be uncovered. Antioxidant mouse models are valuable for investigating such relationships.

Epigenetics

GSTP is frequently inactivated by acquired somatic CpG island promoter hypermethylation in multiple cancer subtypes including prostate, breast, liver, and blood cancers [66]. Epigenetically-mediated GSTP1 silencing is associated with decreased cellular detoxification capability. Epigenetic modification of GSTP is now considered not only a biomarker but a potential determinant of cancer progression.

microRNA

Recent studies suggest that microRNAs may regulate GSTP expression. miR-133b reduced GSTP1 expression by 2.1 fold in prostate cancer cells [67]. miR-513a-3p sensitized human A549 lung adenocarcinoma cells to chemotherapy by targeting GSTP1 [68]. miR-133a repressed the expression of GSTP1 at mRNA and protein levels [69]. Similar findings were observed in human bladder cancer [70] and lung squamous cell carcinoma [71]. Because diet-induced obesity and

diabetes is associated with dysregulation of microRNAs, regulation of hepatic GSTP abundance by microRNAs following HFD is plausible.

Interleukin-6

GSTP1 has recently been shown to be an IL-6 target gene [72]. Inhibition of GSTP1 activity by an IL-6 or IL-6 receptor mAb correlated with increased platinum (and paclitaxel) sensitivity in renal cancer cells [73]. Plasma IL-6 is elevated in obesity and is a well-known mediator of inflammation-induced insulin resistance and hepatic gluconeogenesis via JNK pathway. [74, 75]. Therefore, it will be interesting to consider the possibility of a relationship between IL-6 and GSTP in vivo in obese states.

GST Polymorphisms and Diabetes

T2D is a multifactorial disease that is influenced by environmental risk factors, lifestyle habits and genetic susceptibility. Human GSTs are polymorphic, and genetic variations and deletion genotypes of GSTs are relatively prevalent in human populations. GSTP1 maps to chromosome 11q13 [76], a locus linked to the development of diabetes [77, 78]. Four haplotypes of GSTP that differ structurally and functionally owing to variation in two residues have been determined and characterized, as follows: GSTP haplotype A (WT), with Ile105 and Ala114; haplotype B, with Val-105 and Ala-114; haplotype C, with Val-105 and Val-114; and haplotype D, with Ile-105 and Val-114. The presence of valine at position 105, which is part of the H-site, was shown to disrupt the water hydrogen-bonding network, thereby allowing GSTP to accommodate less bulky substrates [79]. Polymorphic forms of human GSTP1 differ in their ability to

metabolize acrolein [80]. The I105V variant has a reduced ability to conjugate electrophilic species with reduced glutathione, leading to lower enzyme activity towards normal GSTP substrates and may therefore sensitize cells to free radical-mediated toxicity. While the presence of valine at position 114 does not affect the standard GSTP activity, the V105/V114 haplotype is a more potent inhibitor of JNK activity than the wildtype haplotype (I105/A114) [81]. Thus, interindividual susceptibility to oxidative stress may well be contingent upon population differences in GSTP expression and function. However, interpretation of GST polymorphism studies is subject to the caveat that GSTs are inducible enzymes. Induction of one GST could offset the contribution of the other GST-null or polymorphic allele, as illustrated by the increased expression of GSTP in individuals lacking GSTM (a common polymorphism in Caucasians), presumably as a compensatory defense mechanism against carcinogens [82]. Nonetheless, recent studies in diverse population groups have reported significant association of both the GSTM1 and GSTT1 null genotypes with the risk of developing T2D [83-93]. Two reports studying North Indian and Egyptian subjects respectively were the only ones demonstrating a significant association of the GSTP SNP (A313G) with T2D [83, 94]. Although these correlative results remain nascent, the principle that genetic variation may play a role in diabetes susceptibility takes on a greater relevance in light of the connections between GSTP and protein carbonylation, and S-glutathionylation and JNK kinase regulation, processes pivotal to glucose homeostasis. Therefore, well-designed animal studies are needed to delineate a causal and tissue-specific contribution of GSTs to

diabetes. In this regard, GSTP-null mice are an important model to probe GSTP-specific roles under controlled conditions that are not affected by the variables that confound epidemiologic studies.

GSTP and Acrolein Detoxification

Although GSTP catalyzes conjugation of glutathione with different electrophilic substrates, the enzyme has particularly high affinity for small unsaturated aldehydes, such as acrolein [20, 52, 95]. Acrolein is an unsaturated aldehyde that readily reacts with cellular nucleophiles such as glutathione and cysteine and histidine side chains of proteins. Acrolein toxicity could be attributed to the high reactivity of the α,β -unsaturated structure of the aldehyde, because addition of nucleophiles such as glutathione to the site of unsaturation attenuates acrolein reactivity and toxicity. Although acrolein reacts spontaneously with glutathione, this reaction is catalyzed by GSTP increasing the rate (600-fold) of conjugation of acrolein with GSH [52]. Thus, enzymatic conjugation by GSTP facilitates and enhances the detoxification and removal of acrolein and other related aldehydes [52]. The physiological relevance of this metabolic proclivity is supported by studies in rodents that demonstrate a role for GSTP in protection against cardiovascular toxicity of direct acrolein exposure and acrolein-containing tobacco smoke as well as cyclophosphamide-induced urotoxicity and cardiotoxicity, and myocardial ischemia/reperfusion injury [59-62]. Among all the $\alpha\beta$ -unsaturated aldehydes, acrolein is by far the strongest electrophile and reacts 100-fold more rapidly with thiols than 4-HNE [96, 97]. Humans are exposed to acrolein per oral (food and water), respiratory (cigarette smoke, automobile

exhaust, and biocide use) and dermal routes, in addition to endogenous generation (metabolism and lipid peroxidation). Acrolein has been implicated in several disease states, including spinal cord injury, multiple sclerosis, Alzheimer's disease, cardiovascular disease, diabetes mellitus, and neuro-, hepato-, and nephro-toxicity. At the cellular level, acrolein exposure has diverse toxic effects, including DNA and protein adduction, oxidative stress, mitochondrial disruption, membrane damage, endoplasmic reticulum stress, and immune dysfunction [reviewed in [98]]. Much has been elucidated and written about the contribution of acrolein and protein-acrolein adducts in disease development/ progression [reviewed in [98, 99]]. However, free acrolein in tissues is highly volatile and reactive, which renders accurate detection and quantification of endogenous acrolein challenging. The existing methods require complicated approaches using carbonyl derivatizing reagents, as elucidated with murine hearts [61]. Alternatively, as an index of acrolein toxicity, protein acrolein adducts are estimated in plasma and tissues by immunological analyses such as Western blotting and dot blotting. Accordingly, dietary obesity in mice was associated with increased tissue and plasma levels of protein-acrolein adduct [100]. Acrolein-insulin adducts was shown to reduce both its hypoglycemic effects in rats and glucose uptake in 3T3-L1 adipocytes. Also, urinary acrolein correlated with glycated hemoglobin HbA1c in type-2 diabetic individuals [101]. Although reports documenting the involvement of acrolein toxicity in diabetes are sparse and a definitive role is not currently discernable, in light of the pathological importance of acrolein, alterations in acrolein metabolism and detoxification due

to GSTP dysregulation in obesity and diabetes may have important consequences.

GSTP in Cell Signaling: JNK Activation and Protein S-glutathionylation

Distinct from its role in detoxification, GSTP has also been ascribed further roles in a variety of cellular functions such as in regulation of stress-induced cell-signaling. Through protein-protein interactions via its C-terminus, GSTP can sequester c-jun N-terminal kinase (JNK) and act as a negative regulator of this stress kinase [102]. Oxidative stress can destabilize the GSTP-JNK complex leading to an activation of downstream targets of JNK. Embryonic fibroblasts from GSTP-null mice exhibited JNK activation and a higher basal JNK activity compared with those from wild type mice [102]. The interaction between GSTP and JNK was also demonstrated in cell lines using apoptosis as an indicator of JNK activation. Accordingly, the protection of dopaminergic neurons against dopamine-induced apoptosis was attributed to an increase in the expression of GSTP and the subsequent suppression of JNK activity [103]. Conversely apoptosis was shown to increase in a human leukemia Jurkat cell line following etoposide treatment, which was ascribed to the dimerization of GSTP resulting in the release of JNK from the GSTP-JNK complex and thus increased JNK activity [104].

GSTP content is high in normal male mouse liver (~500 µg/g) [105], which results it being in excess of the K_d for the GSTP-JNK association [106]. Thus, JNK might be expected to be totally inactive in vivo. The observation of

constitutive JNK activity in wild type liver is attributed to the fact that under basal conditions cellular GSTP content consists of both monomers and homodimers of which only the former binds JNK [102]. Accordingly, GSTP-null mice exhibit constitutive JNK activity and expression of specific phase II detoxification enzymes and antioxidant proteins that are downstream JNK targets [107]. Thus, GSTP serves as a sensor of intracellular changes in redox potential and has the capacity to regulate kinase pathways. Pharmacologically, this interaction served as the basis for development of the anti-cancer GSTP inhibitor, Ezatiostat hydrochloride (Telintra) [108].

In addition, GSTP catalyzes the forward protein S-glutathionylation reaction (i.e. the addition of GSH), a reversible post-translational modification that alters protein conformation and charge to impact function and/or subcellular localization [53]. Selective modification can affect proteins including, enzymes, receptors, structural proteins, transcription factors and transport proteins and may also alter a variety of protein-protein interactions. For example, glutathionylation of activated aldose reductase in ischemic mouse heart was demonstrated to be mediated by GSTP [109]. Furthermore, GSTP is itself susceptible to S-glutathionylation. Most approaches lack the sensitivity to identify the proteins and pathways regulated by S-glutathionylation under basal conditions in whole organisms. McGarry et al reported the quantification and identification of S-glutathionylated target proteins from murine liver, using a highly sensitive methodology combining high-accuracy proteomics with tandem mass tagging [110]. Significant enrichment of S-glutathionylated mitochondrial

and Krebs cycle proteins suggests an involvement of this modification in energy metabolism processes in vivo. However, little overall difference between the hepatic protein S-glutathionylation profiles between wild-type and GSTP-null mice was demonstrated [111]. The authors concluded that whereas GSTP may be an important determinant of protein S-glutathionylation in response to oxidative/nitrosative stress, its role as a fundamental component of the S-glutathionylation process is limited. Compared with wild-type mice, only a subset of proteins with significantly altered peptide ratios were identified in GSTP-null mice [111].

JNK Activation in Obesity and Diabetes

The JNK signaling pathway is of prominent relevance to metabolic disease. JNK is a mitogen-activated protein kinase that can activate a variety of signal cascades through its phosphorylation of transcription factors [112]. In both dietary and genetic mouse models of obesity, exacerbated JNK activity potentiates IR in peripheral insulin-target tissues [113]. IR is attributed to multiple triggers such as increased pro-inflammatory cytokines, induction of ER stress and increased plasma free fatty acids [114]. At the molecular level, several stress-responsive serine/threonine protein kinases are activated by these stimuli, including JNK and inhibitor of nuclear factor- κ B kinase (IKK β), which both target the insulin receptor substrate (IRS)-1 for serine phosphorylation. As a result, IRS-1 recruitment to insulin-bound insulin receptor is inhibited, thereby preventing activation of the insulin-signaling cascade. Consistent with this, JNK-deficient

mice are protected from HFD-induced obesity and IR [75, 115]. Furthermore, recent reports substantiate the involvement of JNK in insulin secretion in pancreatic β -cells [116-123]. JNK is involved in the loss of pancreatic β -cells induced by pro-inflammatory cytokines, and *jnk1* deficiency or treatment with JNK inhibitors prevents IL-1 β -induced apoptosis of islets and insulin-secreting cell lines [116, 124, 125]. *Jnk1*-deficient pancreatic islets show increased GIIIS and protection against FFA-induced inhibition of glucose-triggered insulin gene transcription [117]. Moreover, JNK inhibition enhances the survival of islets subjected to transplantation protocols [121, 122]. Finally, JNK activation was sufficient to inhibit insulin receptor signaling but not elicit β -cell death and, hence, promote IR in pancreatic β -cells in vivo [126].

SUMMARY AND PROJECT OBJECTIVES

High-calorie diets have fostered the current pandemic of obesity and comorbid conditions of IR and diabetes. Efforts to better define the genetic and environmental risk factors are crucial. Obesity, diabetes and NAFLD are associated with dysregulation of glutathione S-transferases (GSTs). By virtue of its roles in aldehyde detoxification and JNK kinase regulation, the GST pi isoform is well poised to respond to oxidative and metabolic stress elicited by dietary or genetic nutrient excess. We hypothesized that the ability of GSTP to modulate JNK has a selective role in glucose homeostasis and served as the premise for the design of this study. Although epidemiological reports suggest this possibility,

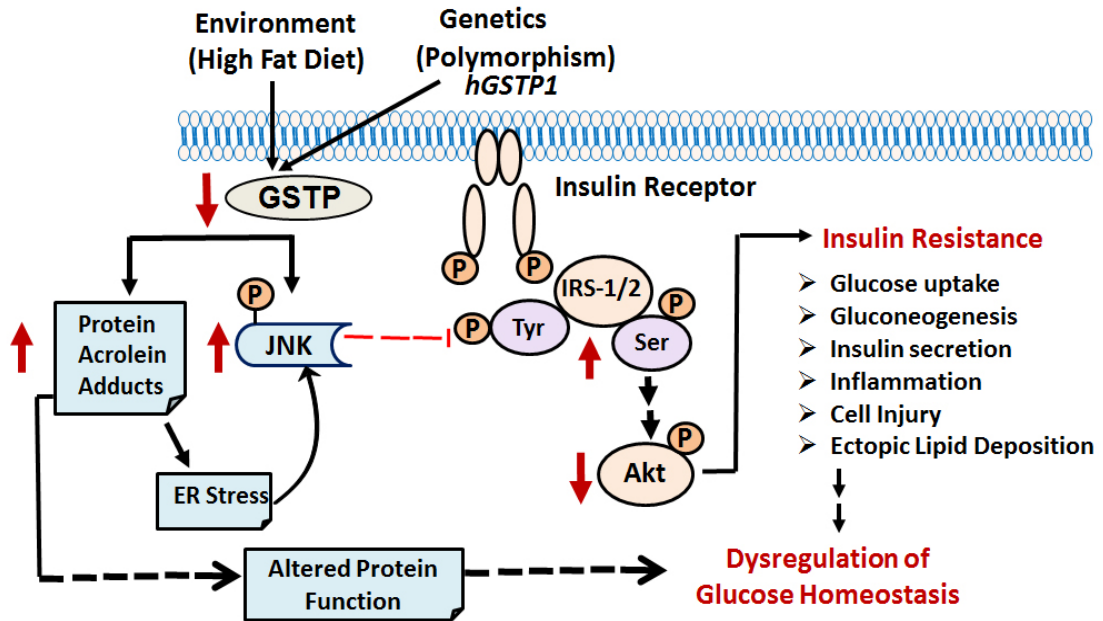
there is no direct evidence for a functional involvement of GSTP in specific pathophysiological pathways that underlie the clinical features of diabetes.

HYPOTHESIS: Decreased GSTP expression and/or function impairs systemic glucose handling and insulin sensitivity to promote progression towards impaired glucose tolerance via formation of increased protein-acrolein adducts and/or enhanced JNK phosphorylation to lead to blunted Akt signaling (Figure 1). To test this hypothesis, we conducted animal studies and addressed the following specific aims:

FIG. 1. Hypothetical scheme of the postulated role of Glutathione S-transferase P in glucose homeostasis via its function(s) in acrolein metabolism and JNK regulation.

Consumption of high fat diet would result in the downregulation of the antioxidant enzyme, glutathione S-transferase P (GSTP) in metabolic tissues. Decreased GSTP abundance would lead to deficits in its function (s) of acrolein metabolism and JNK sequestration. Decreased acrolein metabolism would form increased protein-acrolein adducts that may have deleterious consequences for proteins critical for maintaining glucose homeostasis. Additionally, increased protein-acrolein adducts could also lead to enhanced JNK activation via the ER-stress pathway. Distinct from its role in aldehyde metabolism, decreased GSTP in obesity could also result in increased JNK activation via inhibitory IRS-1/2 serine phosphorylation. JNK activation is well known to impair insulin sensitivity (and secretion) to lead to glucose intolerance via its effect on multiple pathways as outlined in the schematic. This may have implications for human polymorphic variants of GSTP with altered functionality.

Figure 1. Scheme illustrating the postulated project hypothesis



SPECIFIC AIMS

SPECIFIC AIM 1: To determine the effects of early diet-induced obesity on GSTP expression and function in insulin-sensitive tissues.

We assessed the effect of high fat diet on GSTP (and other GSTs) abundance, protein-acrolein adducts and phospho-JNK abundance in insulin-sensitive tissues in relation to glucose intolerance and IR in mice.

SPECIFIC AIM 2: To define the contributions of GSTP in vivo to obesity, inflammation and blood glucose homeostasis.

Next, we used whole-body GSTP-null mice to more directly evaluate the putative requirement of GSTP for blood glucose homeostasis. We determined the effects of GSTP-deficiency on body composition, glucose tolerance, insulin sensitivity and metabolic profiles under normal chow and high fat-fed conditions. These whole-body measurements were combined with assessment of phospho-JNK abundance and protein acrolein adducts to identify cellular mechanisms. To date, HFD-induced dysregulation in multiple GSTs have been reported, but none has yet demonstrated a role for a GST in glucose homeostasis in vivo.

SPECIFIC AIM 3: To test the effect of JNK inhibitor, SP600125, on glucose homeostasis and inflammation in GSTP-null mice.

Finally, we probed the role of JNK activation by testing the effect of JNK inhibitor, SP600125, on hepatic glucose output in GSTP-null mice.

Here, we show that hepatic GSTP is markedly suppressed in both dietary and genetic models of obesity-induced IR and that genetic deletion of GSTP leads to glucose intolerance. Furthermore, glucose intolerance in GSTP-deficient mice is due to increased hepatic glucose production mediated, at least in part, by insufficient insulin release and not IR. Finally, suppression of the JNK pathway significantly reduces hepatic glucose output in GSTP-null mice.

THESIS DESCRIPTION

This thesis is divided in five chapters representing the conceptual and experimental framework. Chapter I is a focused review of the literature relating to obesity, diabetes and glutathione-S-transferases as well as the thesis objective, approach to the hypothesis and the structure of the thesis. Chapter II is a detailed description of the experimental procedures used for all studies. Chapter III describes studies that apply the diet-induced obesity model to address Specific Aim 1. Chapter IV describes our efforts to explore the in vivo contribution of GSTP to obesity and diabetes by using GSTP-null mice to address Specific Aim 2. The chapter further describes the JNK inhibitor intervention study to address Specific Aim 3. Chapter V summarizes the overall conclusions derived from this thesis work and presents recommendations for future work.

CHAPTER II EXPERIMENTAL PROCEDURES

Management of Mouse Colony. C57BL/6 and age-matched male *db/db* mice were purchased from the Jackson Laboratories (Bar Harbor, Maine, USA). All mice in the present study were housed either in the Research Resources Facilities located in the MDR (Medical Dental Resources) and Baxter II Biomedical Research Buildings at University of Louisville, Louisville, KY, USA. GSTP-null mice, generated on a MF1 background strain using homologous recombination [56], were bred for >12 generations with C57BL/6J mice as previously described [61]. Mice heterozygous for the targeted locus (F1) were crossed to generate wild-type (WT) and KO littermates. After weaning, genotypes were housed separately. Mice were housed at five or fewer per cage. Only male mice were used for experiments. Mice were fed normal chow diet (NCD, 12.5% kcal fat; catalog #D12450, Research Diets, New Brunswick, New Jersey, USA) unless otherwise specified. The GSTP-null mice were genotyped using primers that amplified the region between exons 5 and 6 of GSTP1 and a region in the lacZ gene to identify a null allele. The mice were healthy and reproduced in a Mendelian fashion. All animals were housed in specific pathogen-free facilities, in 20–22°C temperature controlled rooms on a standard 12-h light and dark cycle and were allowed ad libitum access to water and food. All procedures involving mice were performed in accordance with the Declaration of Helsinki and with the Guide for the Care and Use of Laboratory Animals as adopted and promulgated

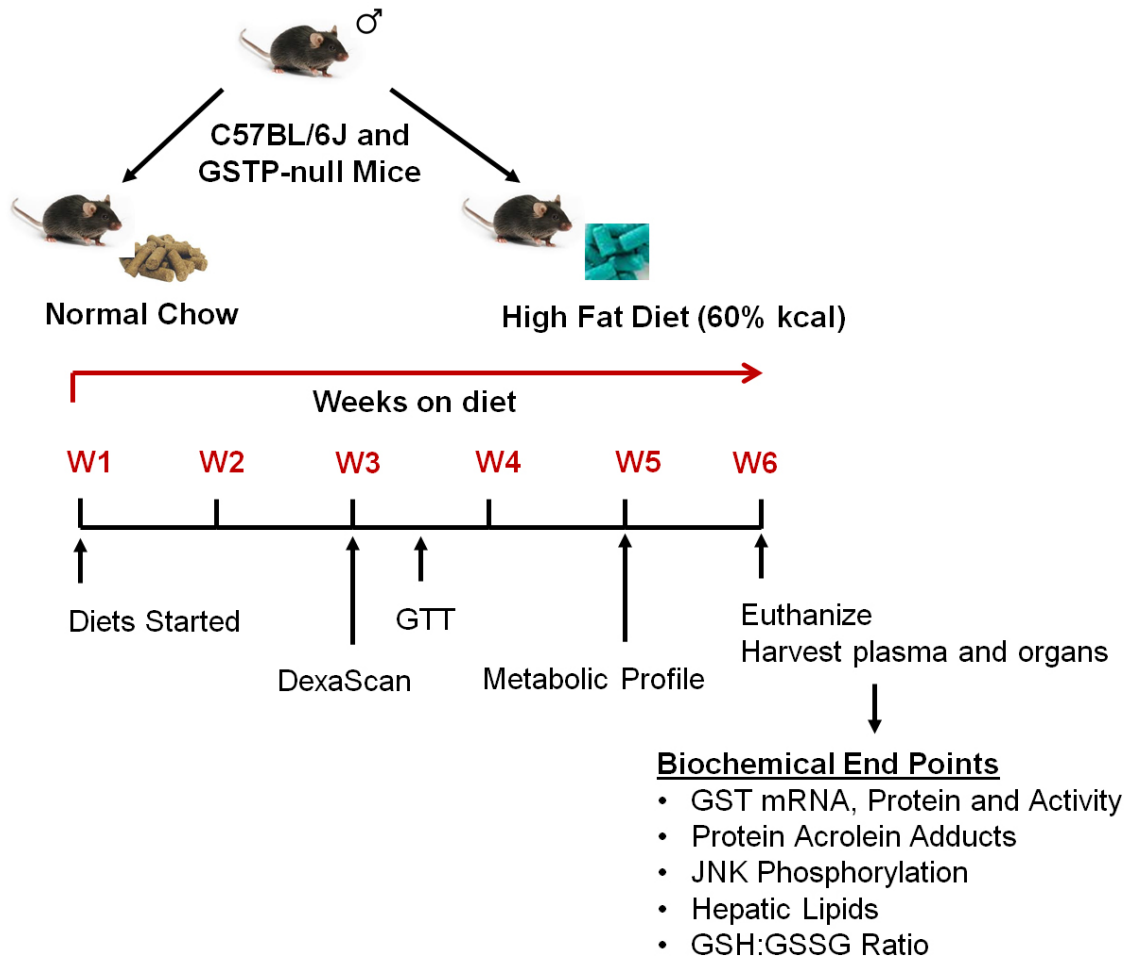
by the U.S. National Institutes of Health. All treatment protocols were in compliance with the University of Louisville IACUC.

High Fat Feeding. Feeding of western diets in rodents induces body weight gain, adiposity and IR and is used as a model to study how nutrient excess elicits the progression of metabolic syndrome. It is well established that C57Bl/6 mice are “obesity prone” as well as are “susceptible to insulin resistance and glucose intolerance” [127]. Eight-week old male C57BL/6J and GSTP-null mice were fed normal chow (NC) diet or a high fat diet (HFD; 60% kcal, #D12492 Research Diets, New Brunswick, New Jersey, USA; 42% kcal, TD.88137, Harlan Teklad, Madison, Wisconsin, USA). In each group, a minimum total of 5 mice were used. Body weights and blood glucose (fasting and non-fasting) were recorded bi-weekly. Body composition was assessed at 3 weeks, glucose tolerance tests were performed at 3.5 weeks and metabolic profile assessed at 5 weeks during the diet study (Figure 2).

FIG. 2. Schematic illustrating the experimental design and end-points of diet-induced obesity study in WT and GSTP-null mice.

Eight-week old male C57BL/6J and GSTP-null mice were fed normal chow (NC) diet or a high fat diet (HFD; 60% kcal, $n=5-7$ per group) for 6 weeks. Body weights were recorded bi-weekly. Body composition was assessed at 3 weeks by dual energy X-ray absorptiometry (DexaScan). Glucose tolerance test (GTT) was performed at 3.5 weeks and metabolic profile was assessed at 5 weeks during the diet study. At the end of the feeding protocol, mice were euthanized and blood (plasma) and tissues were harvested. Tissues such as liver, skeletal muscle and adipose depots representing visceral (epididymal, retroperitoneal), subcutaneous (white suprascapular) and brown (perivascular, PVAT; brown interscapular, iBAT) adipose were harvested for further biochemical analyses as outlined.

Figure 2. Experimental design of HFD study in WT and GSTP-null mice



For the long-term HFD study, C57 mice fed NC or HF (60% kcal) for 16 weeks were purchased from Jackson Labs (n=5 per group). At the end of each feeding protocol, mice were euthanized (sodium pentobarbital i.p., 40 mg/kg body weight) and plasma and tissues were harvested. Animals were fasted for 6 h with free access to water, prior to euthanization. Tissues such as liver, skeletal muscle and adipose depots representing visceral (epididymal, retroperitoneal), subcutaneous (white suprascapular) and brown (perivascular, PVAT; brown interscapular, iBAT) adipose were harvested, weighed and snap-frozen (-80C) for further biochemical analyses. Sections of epididymal adipose and liver were formalin-fixed (10% neutral buffered formalin) for histological analyses of cell size or inflammatory cell infiltration. Liver sections were embedded and frozen in OCT compound (optimal cutting temperature; Tissue-Tek-Catalog #4583; Thermo Fisher Scientific, Atlanta, Georgia, USA) at -80C for Oil Red O staining to assess lipid accumulation.

Organ Analyses. Body and organ (liver, adipose tissue depots and heart) wet weights (nearest milligram) were recorded, and individual organs were snap-frozen in liquid nitrogen and stored at -80°C.

Fasting Blood Glucose Measurements. Blood glucose was measured using Accu-Check Aviva glucose monitor on blood collected from tail snips. Fasting regimens for blood glucose measurements in all our studies were performed according to recommended guidelines [128]. Since mice predominantly eat at night (dark cycle) and have a very high metabolic rate, overnight fasting a mouse is a major metabolic stress. Short-term fasting is more physiological and results

in reduced metabolic stress. A five- to six-hour fast is sufficient to assess whether fasting glucose levels are normal. Since mice tend to nibble throughout the day, mice rarely go into a “true” fast. Therefore, measuring glucose concentrations in the fed state is informative as well.

Body Composition. Obesity is primarily a result of increased fat mass. To determine the effect of HFD on changes in lean and fat body mass, chow and fat-fed mice were subjected to densitometry using Dual Energy X-ray Absorptiometry (DEXA). The DEXA scanner (PIXImus, LUNAR, Madison, WI, USA) offers a relatively non-invasive method to measure body composition in small rodents and is ideal for longitudinal studies requiring repeated measurements on the same mouse. Briefly, animals were anesthetized with isoflurane (5% for induction and 1–2% for maintenance), placed in the prone position, and scanned on the densitometer. Measurements included total mass, total fat mass, total lean mass, and body fat percentage. DEXA scans were also performed prior to all metabolic tests (GTT, PTT, and ITT) to enable glucose/pyruvate/insulin dosing based on lean body mass as recommended [128].

Metabolic Profile. The effect of HFD on metabolic profiles was evaluated by indirect calorimetry (TSE PhenoMaster System, Chesterfield, Missouri, USA). Volume of oxygen consumption (VO_2) and carbon dioxide production (VCO_2), as well as spontaneous locomotor activity, were simultaneously assessed in mice housed individually with free access to food and water. VO_2 consumption and VCO_2 production were measured every 10 min for a total of 24 h and was

normalized to body weight (and lean mass) to determine the respiratory quotient and energy expenditure. Food intake was determined continuously via scales located within the sealed-cage environment. Home-cage locomotor activity was determined using a multidimensional infrared light-beam system with beams scanning the bottom and top levels of the cage and activity being expressed as beam breaks. Data during the light and dark cycles were calculated separately.

Metabolic Tests. Whole-body glucose homeostasis was assessed by intraperitoneal glucose tolerance test (GTT). The glucose tolerance test (GTT) measures the clearance of an intraperitoneally injected glucose load in conscious mice and is used to detect disturbances in glucose metabolism. The intraperitoneal Insulin Tolerance Test (ITT) is a variant of the GTT in which insulin is injected instead of glucose to assess the hypoglycemic effect of insulin as a measure of peripheral insulin sensitivity. The intraperitoneal Pyruvate Tolerance Test (PTT) is a variant of the GTT in which the gluconeogenic precursor, pyruvate, is injected instead of glucose.

- I. **Glucose Tolerance Test.** The GTT (intraperitoneal or oral) is commonly used in the diagnosis of diabetes in both humans and rodents. The ability to quickly normalize the hyperglycemia following injection of a glucose bolus provides integrated information about glucose-induced insulin secretion by the pancreatic β cells and insulin sensitivity in the liver and peripheral organs. Mice were fasted for 6 h with free access to water (8 A.M.-2 P.M.). Each mouse was individually weighed immediately prior to glucose administration and glucose doses (D-glucose, Sigma Aldrich)

were calculated and prepared as a 1 mg/g lean body mass bolus in 100 μ l of total final volume in sterile saline. Mouse tails were gently cleansed and swabbed. A small incision was made at the tip of the tail for the collection of blood. An initial blood glucose level reading ($t= 0$) was taken prior to injection using the Accu-Chek Aviva Plus Glucose Meter. After the initial pre-glucose reading, mice were injected intraperitoneally with the predetermined dose. Glucose readings were recorded at 5, 15, 30, 60, 120 min following the injection. The glucose readings were averaged within genotypes at each time point, giving the mean \pm SEM. Glucose disposal was estimated by calculating the areas under the glucose disposal curves (AUC) using the trapezoidal rule. AUC was calculated by subtracting the average baseline area of each group from each individual AUC.

- II. **Pyruvate Tolerance Test.** Mice were fasted overnight for 16 h with free access to water. Each animal then received an intraperitoneal injection of pyruvate (2 mg/g lean body mass in 200 μ l of total final volume in sterile saline). Blood samples were taken from the tail vein before glucose injection (0 min) and at 15, 30, 60, 120 min after the injection. The 30 min glucose appearance rate was calculated from the delta blood glucose values at 0 and 30 min respectively. The glucose readings were averaged within genotypes at each time point, giving the means \pm S.E. Area under the curve for PTT was calculated similar to that of the GTT.

III. **Insulin Tolerance Test.** Age-matched mice were fasted for 6 h and then injected intraperitoneally with Humulin (1.5 units/kg, lean mass, Elli Lilly, Indianapolis, Indiana, USA). Glucose readings were recorded at 0, 30, 60, 90, and 120 min post-injection. The glucose readings were averaged within genotypes at each time point, giving the means \pm S.E.

Insulin Signaling in vivo. To assess insulin sensitivity, mice were fasted for 6 h (3 A.M-9 A.M) and blood glucose was recorded (baseline; $t = 0$ min), following which an intraperitoneal insulin bolus (1.5U/kg lean body mass) was administered using sterile saline as diluent in a total volume of 100 μ l per injection. After 15 min, blood glucose was recorded ($t = 15$ min) and skeletal muscle, liver and adipose were excised and snap frozen in liquid nitrogen. The Δ blood glucose between 0 min and 15 min was calculated to assess insulin effectiveness. For analysis of insulin-stimulated PKB/Akt phosphorylation, tissues were pulverized in liquid nitrogen and homogenized in buffer A containing proteinase and phosphatase inhibitors. The homogenates were centrifuged at 13,000 rpm for 20 min, and the supernatant protein (50 μ g) was analyzed by SDS-PAGE and immunoblotting with antibodies that detect phospho-Akt (Ser473) and total Akt (Cell Signaling, Danvers, Massachusetts, USA), the distal end of the insulin signaling pathway.

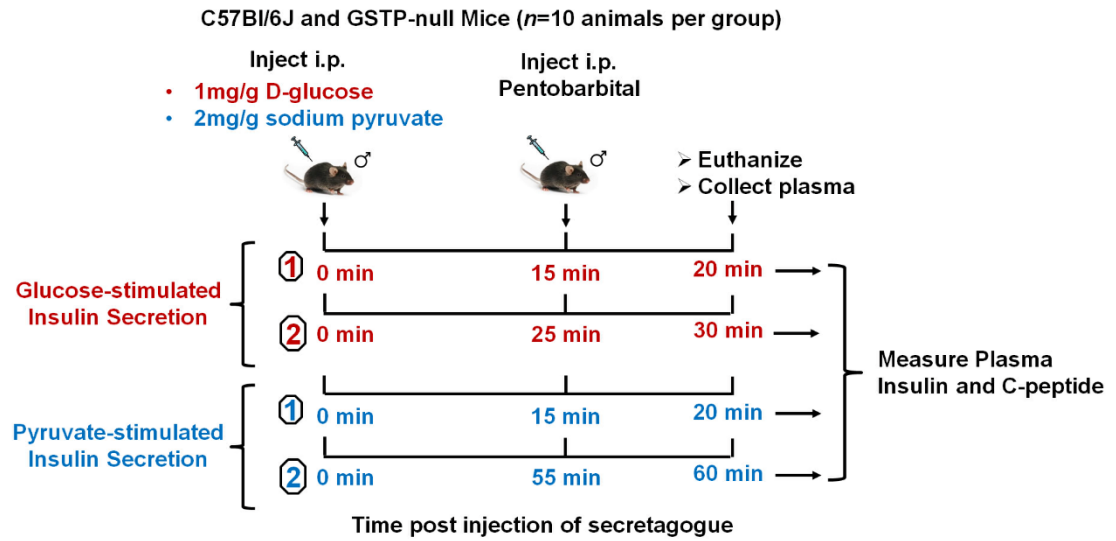
HOMA-IR and HOMA- β , as surrogate indices of insulin resistance and β -cell function were computed as follows: HOMA-IR: fasting insulin (μ U/ml) \times fasting glucose (mmol/ml)/22.5; HOMA- β : $20 \times$ fasting insulin (μ U/ml)/fasting glucose (mmol/ml) - 3.5.

Glucose and Pyruvate-stimulated Insulin Secretion in vivo. The peak insulin secretion and action has been reported in the literature to be within ~25-30 min following glucose bolus administration in mice. The half-life of insulin in mice is ~10-15 min and that of the pro-insulin cleavage product, C-peptide is ~30 min. Hence, we chose to address glucose-stimulated insulin secretion (GSIS) at two early time points, 20 min and 30 min post glucose bolus challenge in age-matched WT and GSTP-null mice. Literature reports suggested that pyruvate-stimulated insulin secretion and expression of gluconeogenic enzymes were altered at 60 min post injection [129]. Hence, we chose to address pyruvate-stimulated insulin secretion (PSIS) at an early time point, 20 min (similar to GSIS) and at 60 min post pyruvate bolus challenge in age-matched WT and GSTP-null mice. Since baseline 6 h fasted plasma insulin values were not found to vary between WT and GSTP-null mice in multiple independent experiments, we considered it appropriate to examine the time points of GSIS and PSIS in separate cohorts of mice to decrease procedural stress of repeated blood sampling and enhance reliability of measurements. For each time point a minimum of 10 mice per group were used. As in all experiments with GSTP-null mice in our study, multiple litters were represented. Detailed schematic of the GSIS and PSIS protocol is presented in Figure. 3. Briefly, mice were fasted for 6 h and administered a glucose or pyruvate bolus. Mice were anesthetized with sodium pentobarbital and blood (plasma) was collected and frozen at -80C for future insulin and c-peptide measurements at each time point of interest. Livers were also harvested and snap-frozen.

FIG. 3. Schematic illustrating the experimental design of glucose and pyruvate-stimulated insulin and C-peptide secretion in WT and GSTP-null mice.

WT and GSTP-null mice ($n=10-12$ animals per group) were fasted for 6 h or 16 h and were administered intraperitoneally a glucose (for GSIS) or pyruvate (for PSIS) bolus respectively. Mice were anesthetized with sodium pentobarbital and blood was harvested at indicated time points. Plasma was frozen at -80°C for future insulin and c-peptide measurements. Livers were also harvested and snap-frozen.

Figure 3. Experimental design of GSIS-PSIS study

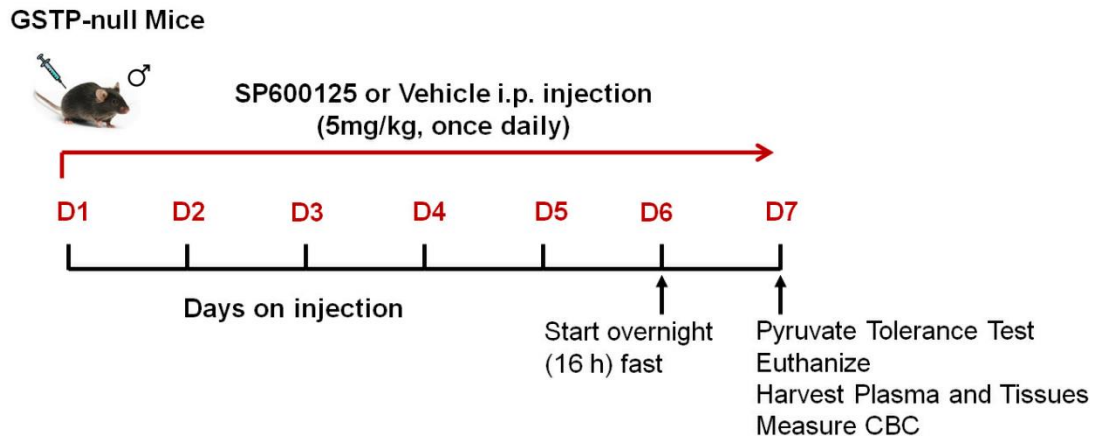


JNK Inhibitor Treatment in vivo. GSTP-null mice were separated into two groups with 12 animals in each group. Group 1 was vehicle control and littermate mice were included in Group 2 for treatment with the anthrapyrazolone inhibitor of JNK, SP600125 (Figure 4). A total of nine cages were used for this study to represent mice from various litters. SP600125 was dissolved in dimethyl sulfoxide (DMSO) (Sigma) at a stock concentration of 20 mg/ml (optimal solubility of the drug in the solvent as reported by Sigma-Aldrich). The drug was administered at a dose of 5 mg/kg/day/injection, diluted with sterile saline such that the final total volume per injection remained 100 μ l to avoid possible toxicity with higher injection volumes. The vehicle control consisted of DMSO diluted with sterile saline and was delivered in the same volume using BD Insulin Syringes (12.7 mm needle). Vehicle and SP600125 were administered by intraperitoneal injection once a day (P.M. except on day 7) for 7 continuous days. Proper dissolution of the drug in the solvent was ensured before each injection to avoid possible precipitation of the drug from the solution. Body weights of mice were recorded daily. Any loss in body weight equal to or more than 10 percent of their previous weight, perhaps due to effects of drug on food and drink intake, was considered a toxic effect and was set as an exclusion criteria for the study. To evaluate the effect of JNK inhibitor on hepatic gluconeogenesis, pyruvate tolerance test (PTT) was performed. Mice were fasted for 16 h overnight on day 6, with free access to water. On day 7, baseline 16 h fasting blood glucose was recorded and final SP600125 injection was administered

FIG. 4. Schematic illustrating the experimental design of JNK inhibitor intervention study in GSTP-null mice.

GSTP-null mice ($n=12$ animals per group) were treated intraperitoneally with JNK inhibitor (SP600125; 5 mg/kg, once daily) or vehicle (DMSO diluted with saline) for 7 consecutive days. Littermate mice were treated in pairs for all drug and vehicle injections. Body weights of mice were recorded daily to assess for potential drug toxicity. Animals were fasted overnight for 16 h on day 6 of the study for performing a pyruvate tolerance test (PTT) on day 7. On treatment day 7, following the last drug injection, animals were administered a pyruvate bolus and blood glucose recorded at pre-defined time-points for the PTT. Mice were anesthetized immediately with sodium pentobarbital and euthanized. Blood (plasma) and liver were harvested and frozen at -80°C . Blood was also used for complete blood count analysis

Figure 4. Experimental design of JNK inhibitor study



in the A.M, 2 h following which PTT was performed. Mice were euthanized immediately and tissues (liver, skeletal muscle and epididymal adipose) and plasma were collected and stored at -80C for further biochemical studies. 100 µl of blood was used for complete blood count analyses.

Complete Blood Cell Count. CBC was measured in blood collected from GSTP-null mice from the JNK inhibitor study. Blood was sampled in ethylenediaminetetraacetic acid-containing tubes and leukocytes quantitated using a Hemavet.

Protein Quantification by Immunoblotting.

Protein abundance was measured in mouse tissue lysates by immunoblots using appropriate buffers.

Buffer Composition.

Buffer A (Tissue lysis buffer): RIPA buffer-10 mM Tris 7.2, 150 mM NaCl, 5 mM EDTA, 1% Triton X100, 1% sodium deoxycholate, 5 mM sodium orthovanadate, 50 mM NaF, supplemented with 1:100 protease inhibitor mixture, 1:100 phosphatase inhibitor mixture (Sigma Aldrich).

Buffer B (Tissue lysis buffer): 25 mM HEPES, pH 7.0, 1 mM EDTA, 1 mM EGTA, 1% Nonidet P40, 1% SDS, supplemented with 1:100 protease inhibitor mixture, 1:100 phosphatase inhibitor mixture.

Buffer C (Wash buffer and Antibody dilution buffer): TBST buffer was composed of 1X TBS (10 mM Tris 7.5, 150 mM NaCl) and 0.1% Tween 20.

Buffer D: 5X Laemmli buffer (312.5 mM Tris base, pH 6.8, 10% glycerol, 11.5% SDS, 0.1% bromophenol, and 50 mM N-ethylmaleimide)

Stock solutions of running buffer and transfer buffer were prepared as 10X solutions and stored at room temperature prior to use. Stock solution of running buffer consisted of 10X Tris/Glycine/SDS Buffer. Stock solution of transfer buffer was made with 24.7 mM Tris and 191.8 mM glycine diluted in water to a 10X concentration. Working running buffer was prepared to a 1X concentration by dilution of 10X Buffer in Milli-Q water. Working transfer buffer was prepared at a 1500mL volume composed of 300mL methanol, 150mL 10X transfer buffer, and 1050uL MilliQ water. Prior to use, working transfer buffer was chilled for 15 approximately 45 minutes at 4C.

For GSTA, GSTM, GSTP, phospho-Akt and phospho-JNK Western blots:

Frozen tissues (liver, skeletal muscle and adipose tissue) were pulverized using a metal tissue pulverizer that was cooled in liquid nitrogen. Aliquots of pulverized tissue were homogenized in buffer A to result in a 10 percent lysate (w/v), sonicated, and centrifuged (13,000 RPM, 20 min, 4°C). The lysate was sonicated for 10 seconds, and centrifuged at 13,000 RPM for 20 minutes. Protein concentration was determined in the supernatant using Bio-Rad reagents. Protein samples were prepared in buffer C with DTT (250mM) and heat-denatured at 95°C for 10 min. Samples were subjected to SDS PAGE (120V), transferred to polyvinylidene fluoride membranes at 77 volts for 2 h at 4°C. The membranes were blocked with 5% BSA or milk in TBST for 1 h in room temperature followed by overnight incubation with primary antibodies: anti-

phospho-SAPK/JNK; anti-SAPK/JNK; 1:1000 which recognizes both 46 and 54 kDa JNK isoforms (Cell Signaling Technology, Danvers, Massachusetts, USA); GSTP (BD Biosciences, 1:1000, San Jose, California, USA); GSTA and GSTM (kind gift from Dr. R. Prough (Univ. of Louisville)). The membranes that were probed for phospho-JNK and phospho-Akt were stripped with buffer D and incubated with antibodies for the respective total proteins or loading controls.

For protein-acrolein adducts Western blots: Frozen tissues (adipose, liver, skeletal muscle) were pulverized and suspended in buffer B, sonicated, and centrifuged (13,000 rpm, 20 min, 4°C). Protein samples were prepared in buffer C without any reducing agents and heat-denatured at 95°C for 10 min. Samples were subjected to SDS PAGE, transferred to polyvinylidene fluoride membranes, blocked in 5% milk in TBST for 1 h at room temperature, and incubated overnight with an IgG-purified rabbit polyclonal antibody (1: 1000-2000) that recognizes keyhole limpet hemocyanin acrolein antigen (1:1000) (gift from Dr. P. Burcham, University of Western Australia).

For all immunoblots, antibody binding was detected with appropriate secondary antibodies (anti-mouse HRP-conjugated IgG and anti-rabbit HRP-conjugated IgG; Cell Signaling). All immunoblots were developed using chemiluminescence (ECL system (Pierce, Illinois, USA) and detected with a Typhoon 9400 variable mode imager (GE Healthcare). Quantification of band intensities was performed using Image Quant TL software (GE Healthcare).

Histology. For immunohistochemical staining, formalin-fixed, paraffin-embedded liver sections (5 μ m) were stained with anti-GSTP1 antibody (1:1,500; Novocastra).

Real-Time Quantitative PCR. RNA was isolated using Qiagen kit (Valencia, California, USA) and reverse transcribed using Bio-Rad (Richmond, California, USA) cDNA kit. QRT-PCR was performed with ABI Prism 7700 and SYBR green (Bio-Rad) detection of amplified products. Relative mRNA expression was estimated by the $\Delta\Delta$ Ct method [130] using *Rplp0* as an internal standard [131]. GSTs were assessed using validated primers for *Gstp1*, *Gstm4.1* and *Gsta4*, as representative isoforms of the respective GST class. All primer sequences for the GST isoforms, ER stress, inflammatory and gluconeogenic markers examined are provided in Table 1.

Table 1. Oligonucleotide Primers

Gene name	Accession #	Forward primer	Reverse primer
<i>Mip- 1alpha</i>	NM_011337.2	5'- ACTGACCTGGAAGTGAATG CCTGA-3'	5 '- GTGGCTACTTGGCAGCAAACAG -3'
<i>Mcp-1</i>	NM_011333.3	5'- ATGCAGGTCCCTGTCATG- 3'	5'-GCTTGAGGTGGTTGTGGA-3'
<i>Il-1beta</i>	NM_008361.3	5'- CTCCATGAGCTTTGTACAA GG-3'	5'-TGCTGATGTACCAGTTGGGG- 3'
<i>Il-6</i>	NM_031168	5'- CTCTGGGAAATCGTGGAA AT-3'	5'- CCAGTTTGGTAGCATCCATC- 3'
<i>Pepck</i>	NM_011044.2	5'- ATCTTTGGTGGCCGTAGAC CT-3'	5'- CCGAAGTTGTAGCCGAAGAA- 3'
<i>G6pc</i>	NM_008061.4	5'- AGGAAGGATGGAGGAAGG AA-3'	5'- TGGAACCAGATGGGAAAGAG-3'
<i>Grp78</i>	NM_022310.2	5'- CACGTCCAACCCCGAGAA- 3'	5'-ATTCCAAGTGCGTCCGATG-3'
<i>Herp</i>	NM_022331.1	5'- CGTTCAGACAGAGGCCAG TTC-3'	5'-CTCGAGGACCACCATCATCC- 3'
<i>Xbp-1</i>	NM_013842.2	5'- TTACGGGAGAAAACCTCAC GGC-3'	5'- GGGTCCAACCTTGTCCAGAATGC- 3'
<i>Gsta4</i>	NM_010357.3	5'- TGATTGCCGTGGCTCCATT TA-3'	5'- CAACGAGAAAAGCCTCTCCGT-3'
<i>Gstm4.1</i>	NM_026764.3	5'- AGCTCACGCTATTCGGCT G-3'	5'- GCTCCAAGTATTCCACCTTCAGT -3'
<i>Gstp1</i>	NM_013541.1	5'- ATGCCACCATACACCATTG TC-3'	5'-GGGAGCTGCCCATACAGAC-3'
<i>Rplp0</i>	NM_007475.5	5'- AGATTCGGGATATGCTGTT GGC-3'	5'- TCGGGTCCTAGACCAGTGTTTC-3'

Biochemical Analyses. Plasma total cholesterol, HDL-cholesterol, LDL-cholesterol and triglycerides were measured using respective reagents (Wako, Richmond, Virginia, USA) with the COBAS MIRA PLUS Analyzer (Roche Diagnostics, Indianapolis, Indiana, USA). Total hepatic cholesterol and triglycerides were extracted using the method of Bligh and Dyer (1959) [132] and measured using commercial reagents (Wako, Richmond, Virginia, USA). Total hepatic GST conjugating activity towards the substrate 1-chloro-2,4-dinitrobenzene (CDNB) was measured by a colorimetric assay (Cayman Chemicals, Ann Arbor, Michigan, USA). Plasma insulin and C-peptide levels were measured by commercial kits (Merckodia, Winston Salem, North Carolina; Crystal Chem, Downers Grove, Illinois, USA respectively). To measure fasting plasma insulin levels, mice were fasted for 6 h. Blood was collected from anesthetized mice by left ventricular cardiac puncture and centrifuged at 3,000 × g for 20 min. The clarified plasma layer was transferred to a new tube, snap-frozen, and stored at –80 °C. On the day of the assay, the plasma samples were thawed and centrifuged (4000Xg, 5 min at 4C). Standard curves were performed with each assay. Assays were performed in duplicate, and the insulin/C-peptide values for all of the replicates of a single sample were calculated and the averages for all samples within a treatment or genotype group were used to calculate the means ± SEM. The lower limit of detection for the insulin assay was 0.025µg/L for a 25 µl sample.

Liver Triglycerides and Total Cholesterol. To examine hepatic lipid accumulation, total hepatic cholesterol and triglycerides were extracted using the

method of Bligh and Dyer (1959) and measured using commercial reagents (Wako, Richmond, Virginia, USA).

Statistical Analysis. Statistical analyses were performed using GraphPad Prism software (La Jolla, California, USA). Data are presented as mean \pm SEM.

Comparisons between two groups were performed by *Student's t-test* or Mann-Whitney U-test while multiple groups were compared using one-way or two-way ANOVA with Bonferroni's post hoc test as appropriate. Spearman's Rank Correlation Coefficients were computed using R software [133]. $P < 0.05$ was considered to indicate statistically significant differences.

CHAPTER III
EFFECT OF OBESITY ON GLUTATHIONE S-TRANSFERASE-P ABUNDANCE
AND FUNCTION

INTRODUCTION

Obesity and type 2 diabetes (T2D) are major public health concerns worldwide. While lifestyle choices and lack of exercise are important risk factors for weight gain, high calorie diets are a key factor fueling the current pandemic of obesity and comorbid conditions of non-alcoholic fatty liver disease (NAFLD), systemic insulin resistance (IR) and T2D [1-4]. Poor dietary habits promote a cluster of risk factors for development of T2D and cardiovascular disease. More than one-third (34.9% or 78.6 million) of U.S. adults are obese and 68% are overweight or obese [5]. According to the CDC reports in 2015, nearly 30 million Americans have diabetes [134]. However, not all obese individuals develop cardiometabolic abnormalities, suggesting that key environmental/genetic factors contribute to the development of IR [18, 19]. For example, NAFLD and/or T2D are reported in an estimated 60% of the urban population including young, lean individuals in Asian communities [2, 10]. Likewise, several studies in rodents indicate that obesity and insulin resistance may be distinct sequelae of nutrient excess. Given that obesity, thus, is not a prerequisite for development of diabetes, the early

metabolic changes governing interindividual susceptibility need to be investigated.

Accumulating evidence suggests that obesity, NAFLD and diabetes are all linked with aberrant hepatic expression of glutathione S-transferase (GSTs) isozymes [40, 49, 135]. The GSTs are a multigene family of abundant and ubiquitous phase II enzymes [36] that primarily catalyze glutathione (GSH) conjugation of toxic, unsaturated aldehydes such as acrolein and 4-hydroxynonenal (4HNE). Given that consumption of high calorie diets results in oxidative stress-mediated metabolic formation of 4-HNE and acrolein [45, 46], a loss of GST activity in vivo may be detrimental. Consistent with this idea, downregulated GSTA in obese, insulin-resistant humans or HFD-fed mice results in increased protein-HNE adducts (carbonylated proteins) in adipose [45, 46]. Furthermore, human *GSTM1*, *GSTT1* and *GSTP1* gene polymorphisms (i.e., altered GST activity) [80, 81] are associated with increased risk of T2D [84, 88, 89, 136]. Accumulation of protein-aldehyde adducts, which can diminish protein function and trigger endoplasmic reticulum (ER) stress [98, 137], is a proposed mechanistic link between oxidative stress, inflammation and IR [45, 46]. Considered together, altered GSTs may represent an early causal change that provokes metabolic disease progression.

STUDY OBJECTIVE

The GST Pi (GSTP) isoform has diverse catalytic and non-catalytic functions potentially relevant to metabolic disease [36]. For example, GSTP specifically

catalyzes GSH conjugation to acrolein facilitating its detoxification [95]. Similarly, diet-induced obesity in mice downregulates hepatic GSTP [49], increases levels of tissue and plasma protein–acrolein adducts [100], and urinary acrolein level correlates with glycated hemoglobin in T2D subjects [101]. Distinct from its catalytic function, GSTP binds and inhibits c-Jun NH₂-terminal kinase (JNK) activation [102]. GSTP-null mice exhibit constitutive JNK activation in liver and lung [107]. Moreover, excessive JNK activation in response to multiple triggers mediates IR [114, 138, 139], and JNK-deficient mice are protected from HFD-induced obesity and IR [75, 113, 115]. The specific role of GSTP in JNK activation and development of insulin resistance has not been addressed. Thus, we hypothesized that GSTP dysregulation contributes to metabolic derangements of diet-induced obesity, perhaps through protein-acrolein adduct formation and/or JNK activation. Using the commonly used diet-induced obesity model in mice, we studied effects of high fat diet on GSTP abundance and function(s) in insulin-responsive tissues.

RESULTS

Short-term high fat diet leads to increased adiposity, insulin resistance, glucose intolerance and altered systemic metabolism.

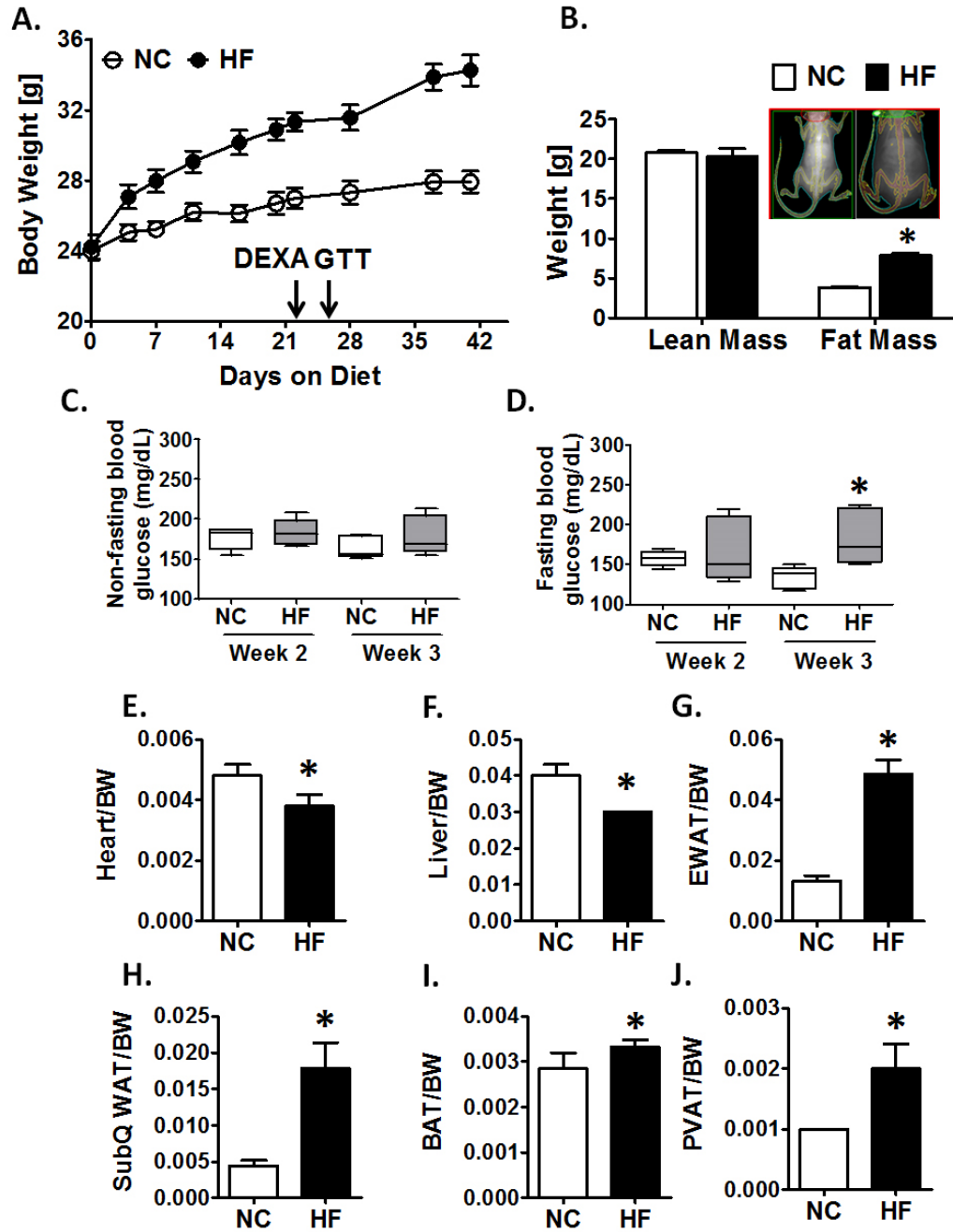
Numerous studies indicate that GSTs are dysregulated in diet-induced obesity and in human NAFLD, yet whether altered GSTs are mechanistically involved in the development of glucose intolerance is unclear. So, to gain insight, eight

week-old male C57BL/6J (WT) mice were fed NC or HFD (60 kcal% fat), with ad libitum access to both diets. Four days into the diet regimen, mice on the HFD exhibited significantly greater weight gain (1.04 ± 0.09 g in NC, 2.84 ± 0.16 g in HF, $p < 0.05$, $n = 5$) which persisted throughout the six weeks of the diet study (Fig. 5A). Since obesity is primarily a result of increase in fat mass, mice were subjected to DEXA at 3 weeks to estimate body composition. Dexascan analysis showed a 2-fold increase in fat mass in HF-fed mice compared to chow-fed mice (Fig. 5B), typical of this commonly utilized model of diet-induced obesity [127].

FIG. 5. Short-term diet-induced obesity in WT mice.

(A) Absolute weekly body weight (BW) of mice fed normal chow (NC) and high-fat diet (HF, 60% kcal fat) ad libitum for 6 weeks. Dual-energy X-ray absorptiometry (DEXA) analysis and glucose tolerance test (GTT) were performed at 3 or 3.5 weeks of diet study, respectively (see arrows). **(B)** Lean and fat mass content as measured by DEXA. *Inset:* Representative DEXA images. **(C)** Fed and **(D)** Fasting (6h) blood glucose at weeks 2 and 3 of diet study measured by tail vein. **(E-J)** Organ to body weight ratios at the end of the diet study. Values are mean \pm SEM ($n = 5$ per group). BW, body weight; EWAT, epididymal white adipose tissue; SubQ WAT, subcutaneous white adipose tissue; BAT, brown adipose tissue (interscapular); PVAT, perivascular adipose tissue. * $P < 0.05$, NC vs. HF by Mann-Whitney U test. NC, open symbols or bars; HF, filled symbols or grey bars.

Figure 5. Diet-induced obesity in WT mice

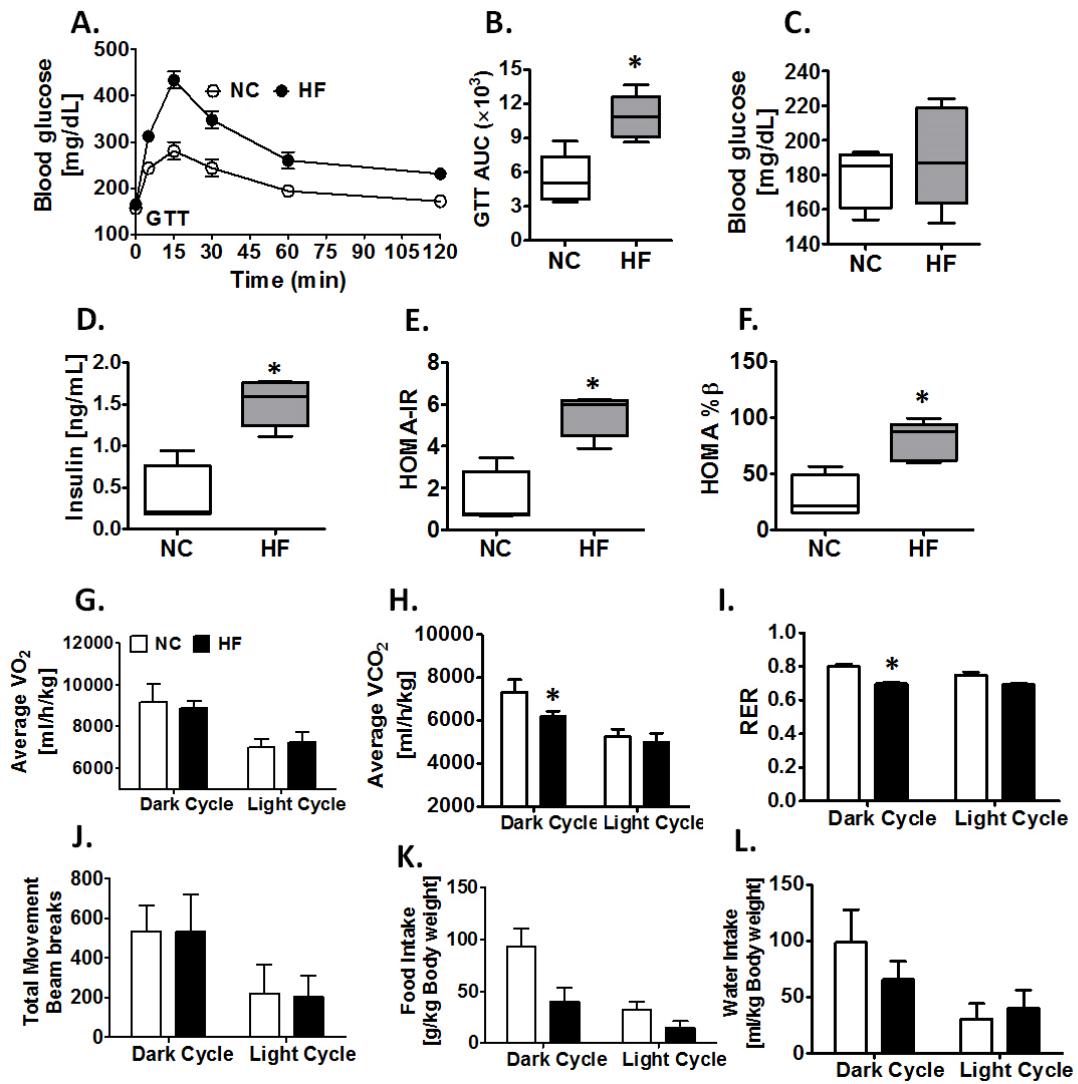


As a primary screen to evaluate glucose homeostasis, fasted and fed blood glucose was measured each week. After 3 weeks of HF feeding, we observed a significant elevation in fasting blood glucose concentrations in obese mice compared with controls (NC, 133.8 ± 6.176 mg/dL vs HF, 184.2 ± 15.47 mg/dL, $n=5$ per group, $p<0.05$; Fig. 5D), suggesting onset of glucose intolerance or insulin insensitivity. Therefore, to examine the glucose tolerance status, GTT was performed. Following a six hour fast, mice were administered an intraperitoneal glucose bolus (1 mg/g lean mass) to evaluate blood glucose excursions. Since the primary site of glucose disposal, skeletal muscle (lean mass), is relatively unaltered by HF feeding, it is recommended to normalize glucose doses on the basis of lean mass and not total body weight to avoid overdosing obese animals [128]. Our serial use of DEXA enabled estimation of lean mass to calculate glucose doses for GTT studies. Mice fed HF for 3.5 weeks demonstrated worsened glucose tolerance compared with chow-fed mice, as assessed by GTT AUC (NC, 5406 ± 953.6 mg/dL*time vs. HF, 10870 ± 868.2 mg/dL*time, $n = 5$ per group, $p<0.05$; Fig. 6A-B). Consistent with IGT, surrogate markers of IR such as fasting plasma insulin, HOMA-IR and HOMA- β were also elevated in obese mice (Fig. 6D-F).

FIG. 6. Short-term diet-induced obesity and glucose intolerance in WT mice.

Glucose tolerance test (GTT), glycemic indices and indirect calorimetry measurements shown for WT mice fed NC and HF diet. **(A)** For GTT, mice were fasted for 6 h and injected intraperitoneally with glucose bolus (1 mg/g of lean mass), blood glucose measured by tail vein, and **(B)** the area under the curve (AUC) was calculated. **(C)** Fasting blood glucose (6 h) and **(D)** plasma insulin concentrations were measured from blood collected at the end of the diet study. **(E)** HOMA-IR and **(F)** HOMA % β were calculated from fasting blood glucose and insulin as described. Metabolic parameters were measured by indirect calorimetry in 12 week-old WT and GSTP-null mice using a PhenoMaster system: **(G)** oxygen consumption (VO_2); **(H)** carbon dioxide production (VCO_2); **(I)** respiratory exchange ratio (RER); **(J)** total activity (movement); and **(K, L)** food and water intake. Values are mean \pm SEM ($n = 5$ per group). HOMA-IR and HOMA-% β , homeostasis model assessment-estimated insulin resistance and β -cell function indices. * $P < 0.05$, NC vs. HF by Mann-Whitney U test. NC, open symbols or bars; HF, filled symbols or grey bars.

Figure 6. Effect of HFD on GTT and indirect calorimetry in WT mice



To determine how diet affects systemic metabolism, mice fed either NC or HFD for 5 weeks were placed in metabolic chambers to assess metabolic profile by indirect calorimetry. Measurements included oxygen consumption (VO₂), carbon dioxide production (VCO₂), food and water intake, and physical activity. As shown in Fig. 6F and G, average VCO₂ values were decreased in HF-fed mice compared with mice fed NC. The respiratory exchange ratio (RER) was also decreased in mice fed HF compared with NC-fed mice (Fig. 6H). Physical activity, measured by total beam breaks (Fig. 6I), ambulatory counts (Fig. 6J), and fine movements (Fig. 6K), was not significantly different between groups.

Effect of obesity on glutathione-S-transferase expression and activity in insulin-responsive tissues.

To evaluate HFD effects on GSTs, we measured mRNA and protein abundance of major GST isozymes in insulin-responsive tissues. The mRNAs of the GST family (*Gsta4*, *Gstm4.1* and *Gstp1*) were decreased in livers of mice fed HFD (6 weeks, 60% kcal) compared with NC (Fig. 7A-C). Western blotting for GSTA, GSTM, and GSTP confirmed mRNA data (Fig. 7D-E). Surprisingly, GSTP abundance was not diminished by HFD in skeletal muscle and epididymal adipose tissue (Fig. 3G). In addition, we also found a significant decrease in GSTP protein abundance and total GST activity in interscapular brown adipose tissue (BAT) which may have implications for BAT inflammation and mitochondrial function (Fig. 3I, J and K). Similarly, hepatic GSTP protein was significantly decreased in both WT mice fed a different HF composition (42% kcal; 4-12 weeks) and in diabetic *db/db* mice (~70%; Fig. 8A, B). Consistent with

HFD-induced downregulation of GSTP protein, positive GSTP immunohistochemical staining was substantially decreased (and restricted to portal triad region) in livers of HFD-fed mice (42% kcal; 12 weeks; Fig. 8C-D). Furthermore, hepatic total GST activity towards the substrate CDNB and GSTP-specific activity (for substrate, ethacrynic acid) was significantly decreased in mice fed HF (42% kcal) for 12 weeks (Fig. 8C, D). To summarize, hepatic GSTP abundance and GST activity were markedly reduced in both HFD-induced and a genetic model of obesity and IR. Overall, these data are consistent with prior measurements of hepatic GSTs in fat-fed animals [49] and collectively illustrate the significance of hepatic GST suppression as an early change that can augment susceptibility to diet-induced glucose intolerance

FIG. 7. Short-term diet-induced obesity and Glutathione S-transferases (GST) expression and activity in insulin-sensitive organs.

(A) *Gsta4*, **(B)** *Gstm4.1*, and **(C)** *Gstp1* mRNA expression (normalized to *Rplp0*) in liver of NC and HF-fed C57BL6/J mice (n=6-8 per group). **(D)** Representative Western blots of liver lysates for GSTA, GSTM and GSTP and respective **(E)** densitometric analyses (n=5-13 per group). **(F)** Hepatic GST activity measured with 1-chloro-dinitrobenzene (CDNB) as substrate (n=10-11 per group). Representative Western blots for GSTP in **(G)** gastrocnemius skeletal muscle (SKM), epididymal white adipose tissue (WAT) and **(I)** interscapular brown adipose tissue (BAT) lysates and **(H, J)** densitometric analyses. **(K)** GST activity in BAT measured with CDNB as substrate. “Null” indicates liver homogenate of GSTP-null mice used as negative control. Values are mean \pm SEM. **P* < 0.05, NC vs. HF or vs *db/db* by Mann-Whitney U test. NC, open symbols or bars; HF, filled symbols or bars.

Figure 7. Effect of HFD on GST abundance in WT mice

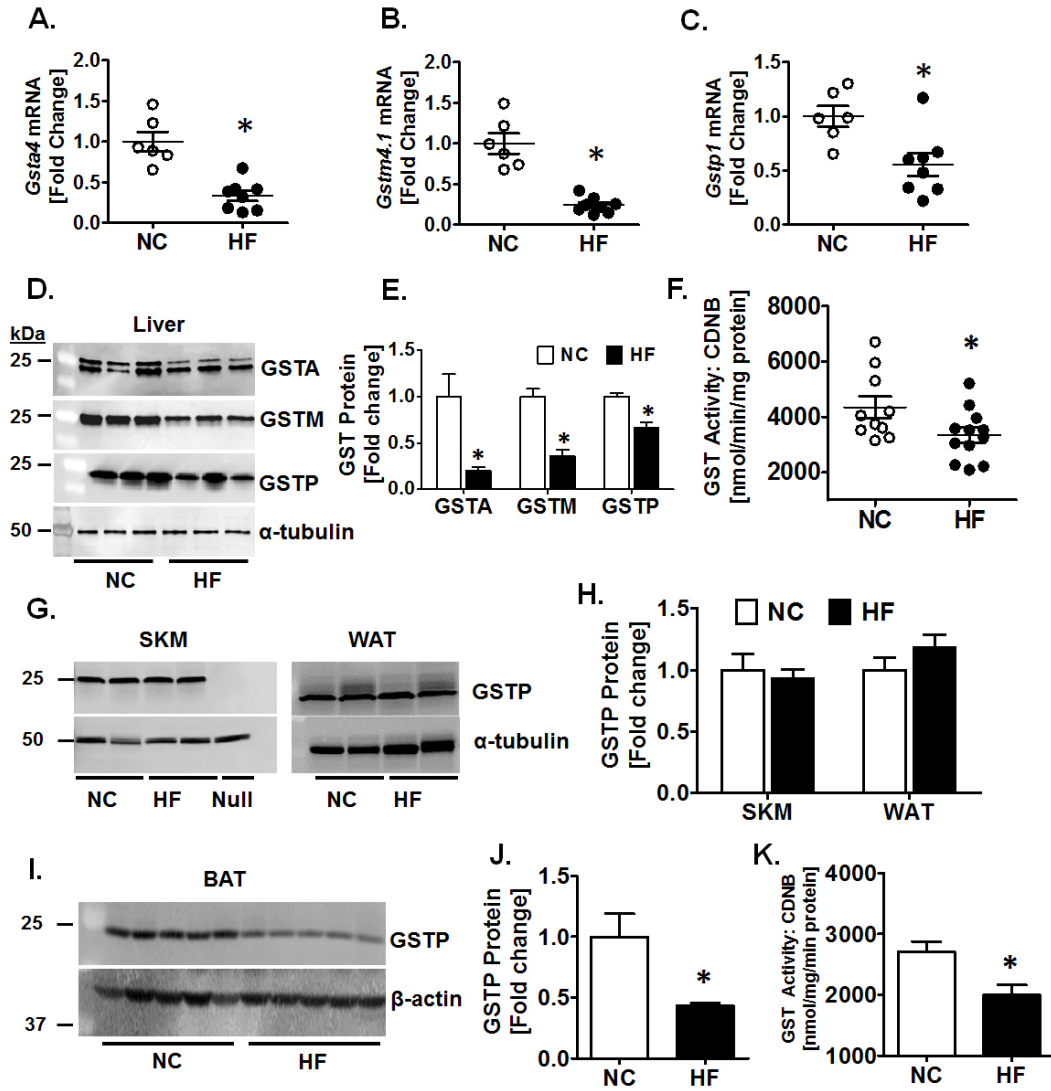
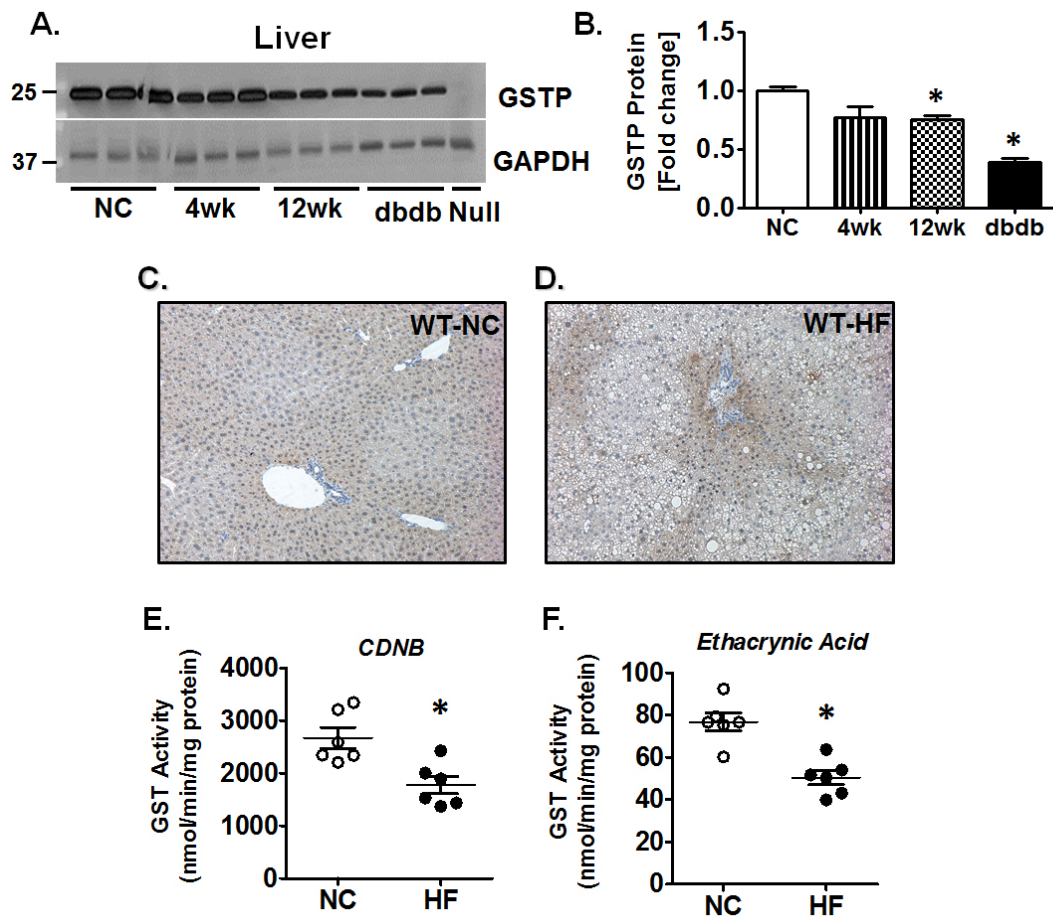


FIG. 8. Long-term diet-induced obesity and hepatic GSTP expression and activity in WT mice.

(A) Hepatic GSTP abundance in C57BL/6J mice fed either a NC or HF diet (42% kcal fat) for 4–12 weeks, and GSTP in age-matched *db/db* mice, and **(B)** densitometric analyses ($n=3$ per group). **(E, F)** Representative histology images of immunohistochemical staining for GSTP in livers of NC and HF (42% kcal, 12 weeks, 100X). Hepatic GST activity measured with **(E)** 1-chloro-dinitrobenzene (CDNB) and **(F)** and ethacrynic acid as substrate in NC and HF-fed mice from the 12 weeks cohort ($n=6$ per group). Values are mean \pm SEM. $*P < 0.05$, NC vs. HF by Mann-Whitney U test. NC, open symbols or bars; HF, filled symbols or bars.

Figure 8. Effect of HFD on hepatic GSTP in WT mice



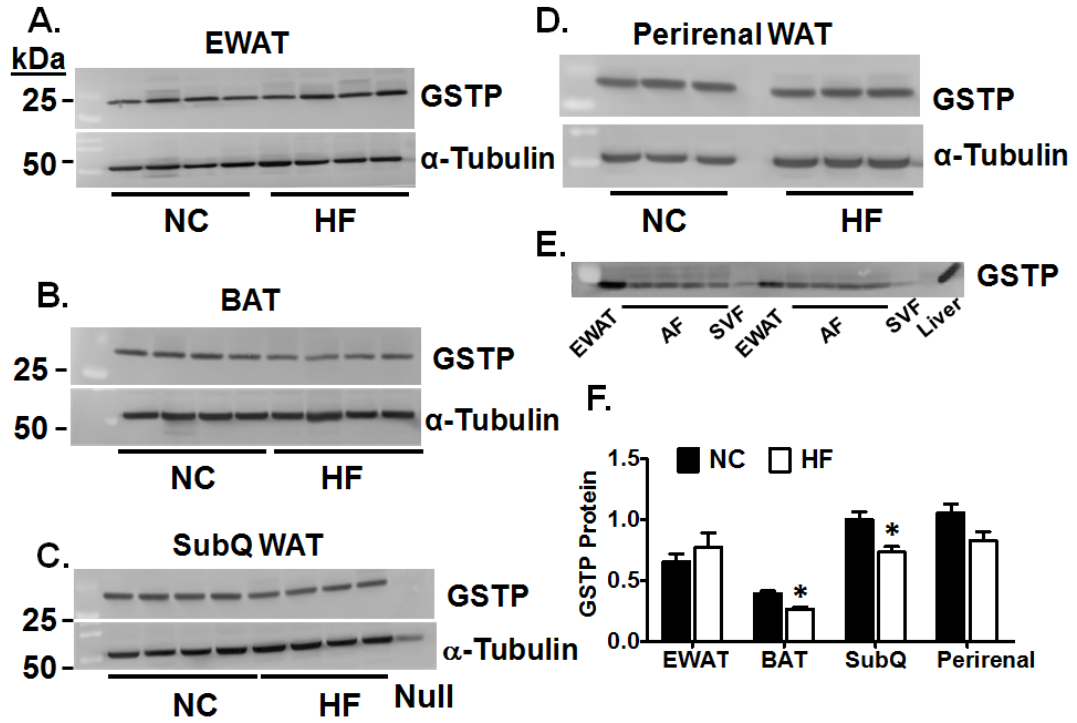
Effect of prolonged high fat diet on GSTP abundance in adipose depots.

In separate studies, we investigated the effect of long-term high fat feeding (16 weeks, 60% kcal) on GSTP abundance in adipose tissues depots in WT mice. Our rationale to study depot-specific effects was based on the knowledge that, not all adipose depots are equally susceptible to inflammation and do not confer the same risk of CVD in obese, diabetic individuals. Visceral adipose tissue (VAT) confers a higher risk of metabolic syndrome and incident cardiovascular disease than subcutaneous adipose (SAT). Recently, perivascular adipose tissue (PVAT) has been proposed to be a potential link between diabetes and CVD. Also, brown adipose tissue (BAT) transplantation significantly decreased body weight and improved glucose metabolism and insulin sensitivity. Therefore, we evaluated whether long-term HFD affected GSTP abundance differently in adipose depots compared with NC-fed mice. Similar to short-term HFD, GSTP abundance was unaltered in epididymal adipose tissue, but was significantly decreased in BAT (Fig. 9A, B). Interestingly, decrease in GSTP abundance was also observed in subcutaneous and perirenal adipose tissue. Furthermore, we confirmed that GSTP was present in the adipocyte fraction of adipose tissue (Fig. 9E). Potential implications of GSTP dysregulation in adipose depots in obese states remain to be investigated.

FIG. 9. Long-term diet-induced obesity and protein abundance of GSTP in adipose tissue depots in WT mice.

Normal chow (NC) and high fat diet (HF)-fed (60% kcal fat, 16 weeks) C57BL/6J mice were purchased from JAX (n=4 per group). Representative Western blots for GSTP in **(A)** epididymal white (EWAT), **(B)** interscapular brown (BAT), **(C)** subcutaneous white (SubQ-WAT) and **(D)** perirenal white adipose tissues and respective **(F)** densitometric analyses. **(E)** Western blot for GSTP in lysates from epididymal white adipose tissue (EWAT) and adipocyte (AF) and stromal vascular fraction (SVF). Values are mean \pm SEM. * $P < 0.05$, NC vs. HF or vs *db/db* by Mann-Whitney U test. NC, open symbols or bars; HF, filled symbols or bars.

Figure 9. Effect of HFD on adipose depot GSTP in WT mice



Obesity results in increased protein-acrolein adduct formation and JNK activation in the liver.

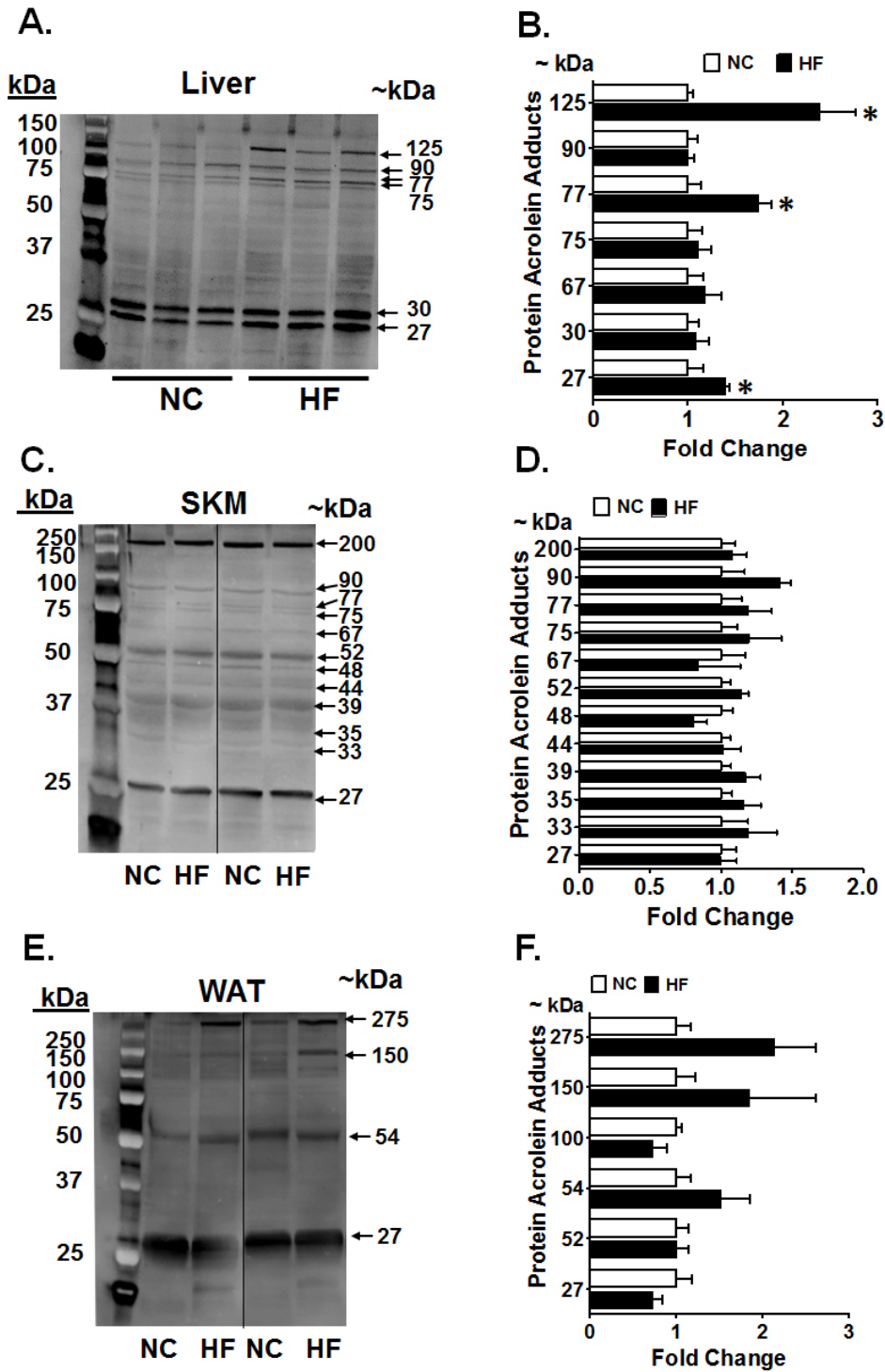
Because GSTs are multifunctional proteins that contribute to the metabolism of environmentally-, drug- and lipid-derived toxic aldehydes, such as acrolein and 4HNE [36], yet also modulate stress signaling, e.g., JNK [102], we hypothesized that decreased GST abundance may deleteriously alter one or both of these pathways in livers of HFD-fed mice.

Insufficient GSTP activity may induce deficits in acrolein metabolism leading to increased accumulation of protein acrolein adducts. Acrolein-induced protein crosslinking can inhibit protein function or affect protein folding leading to ER stress and the unfolded protein response (UPR) [98]. Indeed, recent studies have demonstrated acrolein-induced ER stress and UPR. ER stress-activation of JNK is a link between obesity, inflammation and insulin resistance [138, 140]. Consistent with our hypothesis, HFD compared with NC significantly increased abundance of several hepatic protein-acrolein adducts, i.e., $M_r \cong 125$ kDa, +2.5 fold; $M_r \cong 77$ kDa, +2.0 fold and $M_r \cong 27$ kDa, +1.5 fold (Fig. 10A). Relative abundance of adducts was quantified by normalizing the intensity of the specific protein band to the signal intensity of total protein by Amido black staining for the entire lane.

FIG. 10. Protein-acrolein adducts in normal chow and high-fat diet fed WT mice.

Representative Western blots of protein-acrolein adduct bands in **(A)** liver, **(C)** gastrocnemius skeletal muscle, and **(E)** epididymal adipose tissue and respective **(B, D, F)** densitometric analyses. Values are mean \pm SEM ($n=5$ per group). * $P < 0.05$, NC vs. HF by Mann-Whitney U-test. NC, open bars; HF, filled bars.

Figure 10. Effect of HFD on protein-acrolein adducts in WT mice



This HFD effect was selective for the liver as levels of protein-acrolein adducts were unchanged in adipose and skeletal muscle (Fig. 10B, C) – organs where GSTP was not downregulated by HFD.

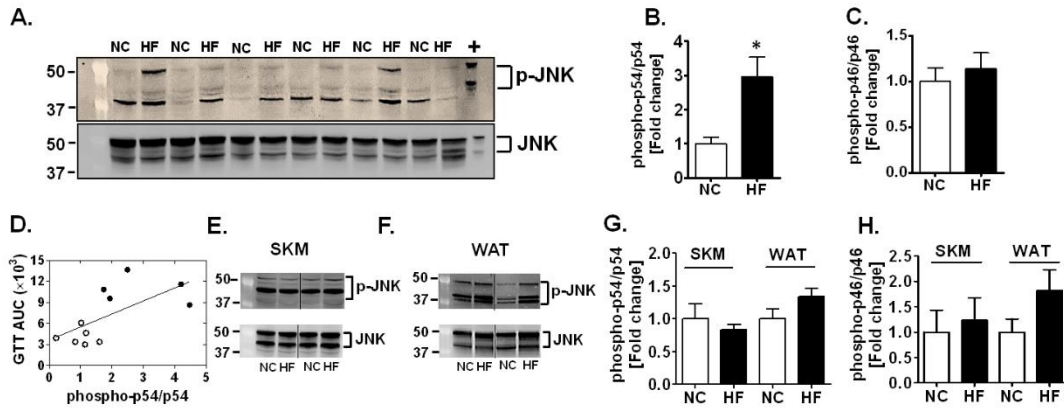
Given that GSTP limits JNK activation and signaling [102, 107] and that activated JNK inhibits insulin signaling [139], we assessed JNK phosphorylation status in HFD-fed mice. As shown in Fig. 11A-C, hepatic phospho-p54 JNK (but not phospho-p46) abundance was increased ~3-fold in livers of HFD-fed mice vs NC-fed mice. Hepatic phospho-p54 JNK abundance was also correlated positively with GTT AUC (Fig. 11D) – an unsurprising finding given the known inhibitory role of JNK and insulin signaling [139].

Collectively, these data support a model wherein, the lean to obese transition results in impaired glucose tolerance, fasting hyperinsulinemia and increased HOMA-IR, coincident with hepatic GSTP downregulation, increased JNK phosphorylation and protein-acrolein adduct formation. However, because multiple GSTs were downregulated by even a short-term feeding of HFD, it is unclear whether metabolic derangements can be solely attributed to a decrease in GSTP alone. Therefore, we next tested whether GSTP deficiency alone (GSTP-null mice) could recapitulate the phenotypic effects of short-term HFD on glucose tolerance as described in chapter IV.

FIG. 11. High-fat diet-induced phosphorylation of JNK in WT mice.

Representative Western blots for phospho-JNK (Thr183/Tyr185) and total JNK (p54/p46) in **(A)** liver, **(E)** gastrocnemius skeletal muscle, and **(F)** epididymal white adipose tissue from NC- and HF-fed WT mice and respective densitometric analyses **(B, C, G, H)**. **(D)** Hepatic phospho-p54 JNK protein band density was plotted against GTT AUC ($r^2=0.3$, $p<0.05$). Values are mean \pm SEM ($n=5$ per group). * $P<0.05$, NC vs. HF by Mann-Whitney U-test. NC, open symbols or bars; HF, filled symbols or bars.

Figure 11. Effect of HFD on JNK phosphorylation in WT mice



DISCUSSION

The major findings of this study are that short-term high fat diet feeding in mice significantly downregulates several GST proteins including GSTP (by an as yet undefined mechanism). Glucose intolerance in HFD-fed mice is correlated with amount of hepatic phospho-p54-JNK (activated). Furthermore, obese mice demonstrate markedly elevated hepatic protein-acrolein adducts, in agreement with the known function of GSTP in acrolein metabolism. Collectively, we conclude that downregulation of hepatic GSTP selectively increases JNK activation and induces deficits in aldehyde detoxification that, in turn, alters liver metabolism to promote glucose intolerance. We believe this scenario represents an early event that begets a “domino” type cascade of deleterious events leading from diet-induced obesity to diabetes.

In the current study, we provide evidence that hepatic GSTs are involved in the early derangements in obesity. High fat diet suppressed GSTP isozyme in the liver but not in the epididymal adipose or the skeletal muscle of WT mice. GSTA protein was selectively downregulated in adipose tissue of obese mice, suggesting a tissue-specific metabolic role of GSTs in obesity and diabetes [45, 46]. Second, we show that, phospho-JNK abundance (p54 but not p46) is selectively increased in the livers of HFD-fed (only 3.5 weeks) WT mice. Moreover, the level of phospho-JNK is positively correlated with the level of glucose intolerance (see Fig. 11D). Because GSTP inhibits JNK *in vivo* [107], we infer that hepatic GSTP downregulation contributes to hepatic JNK activation and progression towards IGT in obesity. Although augmented JNK activation in

peripheral tissues is known to mediate glucose intolerance and IR [139], these models do not address the earliest events that precede established systemic IR.

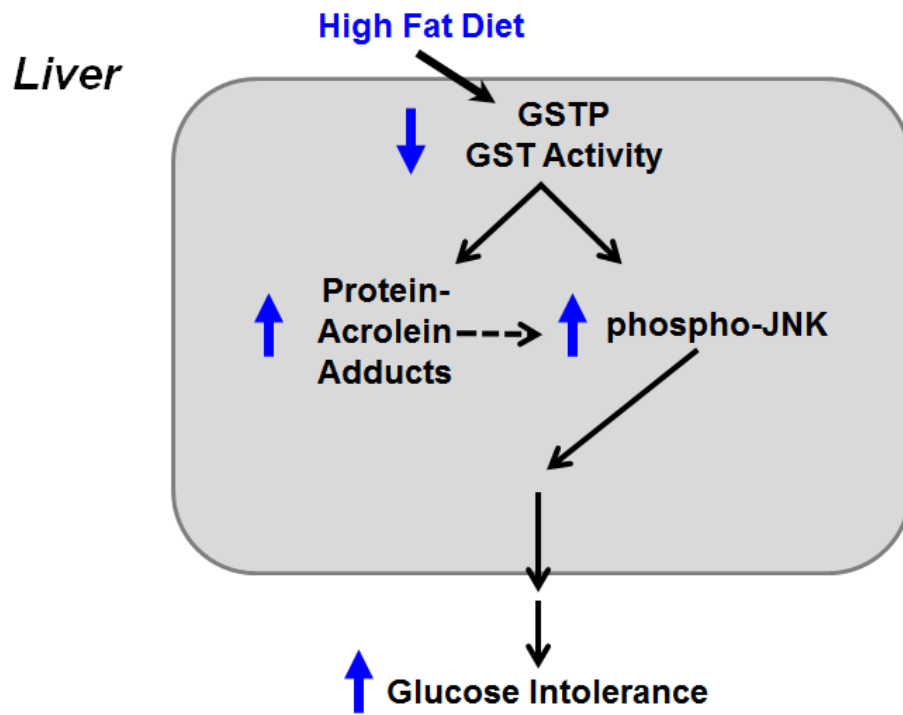
A potential factor known to induce JNK activation is the accumulation of aldehyde-modified proteins (carbonylated proteins), and protein-aldehyde adducts are considered determinants of inflammation and IR [30, 46]. A primary role for GSTP is as an antioxidant enzyme, quenching acrolein in the cell. Because GSTP activity selectively conjugates GSH with acrolein [52], we measured and found increases in protein-acrolein adducts in liver (but not in skeletal muscle nor in adipose) of short-term HFD-fed WT mice compared with NC-fed mice (Figs 10A). Interestingly, a general pattern of protein-acrolein adducts (5 prominent M_r bands: 125, 90, 77, 75, 27 kDa) appears following HFD and some of these bands are significantly increased. While the role of these adducts in JNK activation is unclear, the accumulation of these adducts reflects a loss of acrolein removal capacity that is consistent with the decreased overall GSTP abundance and GST activity (using CDNB as substrate), in livers of HFD-fed WT mice. Previously, we used organ-specific protein-acrolein adducts as both a metric of acrolein exposure (as with tobacco smoke; [59]) but also as an arbiter of cardiac injury in models of ischemia-reperfusion [61] and cyclophosphamide toxicity [62]. Whereas other studies have demonstrated an increase in oxidative stress markers such as hepatic malondialdehyde and ROS measurements [141], to our knowledge this is the first report of direct protein modification by acrolein in liver, linked to obesity. Modest but multiple protein modifications common to a pathway or process has been deemed sufficient to

alter overall metabolic flux in an organ [46]. Acrolein-adduction can inhibit protein function or affect protein folding leading to ER stress and the UPR [98]. ER stress-activation of JNK is a link between obesity, inflammation and IR. The potential direct relationship between protein-acrolein adducts and JNK activation remains to be investigated. Further studies should determine targets of acrolein crosslinking in liver, the specific modification and its functional consequences.

FIG. 12. Schematic illustrating the effect of high fat diet on GSTP abundance and function in WT mice.

Effects of high fat (HF) diet in wild-type (WT) are shown with blue arrows. HF diet results in glucose intolerance in WT mice, typical of this commonly utilized model of diet-induced obesity [127]. In the liver, HF feeding decreases GSTP protein and total GST activity concomitant with increased protein-acrolein adduct and phospho-JNK abundance, in agreement with the known functions of GSTP [36, 102]. Hepatic phospho-p54 JNK positively correlates with glucose intolerance in HF-fed mice. Because GSTP is an *in vivo* JNK inhibitor [107], decreased hepatic GSTP could augment JNK activation following early diet-induced obesity

Figure 12. Scheme: Effect of HFD on hepatic GSTP in WT mice



In summary, we show that short-term HFD-induced glucose intolerance in mice is concomitant with decreased GSTP abundance and increased phospho-p54 JNK and accumulation of protein-acrolein adducts in murine livers. Because GSTP is normally expressed at low levels in human liver [54] and is highly polymorphic [36], further studies of diet-induced hepatic GSTP dysregulation in human obesity, NAFLD and diabetes are warranted. Preventing even small changes in hepatic GSTP abundance or activity may have potentially important consequences for addressing dramatic inter-individual variation in disease susceptibility.

CHAPTER IV

GLUTATHIONE-S-TRANSFERASE-P IN GLUCOSE HOMEOSTASIS: ROLE OF JNK ACTIVATION

INTRODUCTION

Glucose metabolism lies at the heart of type 2 diabetes (T2D). T2D is characterized by deregulation of glucose homeostasis through the development of insulin resistance, manifested as diminished glucose uptake in peripheral tissues and increased glucose production in the liver. The phenomenon of insulin resistance encompasses a precise sequence of events that mediate the hormone signal into action in peripheral tissues.

Insulin Signaling

Binding of insulin to the insulin receptor, a membrane tyrosine kinase, leads to its dimerization and self-phosphorylation of specific intracellular tyrosine residues. This phosphorylation event initiates a protein signaling cascade in peripheral tissues that culminates in mediating the effects of insulin on multiple cellular metabolic pathways. Akt is a serine threonine kinase which lies at the distal end of the insulin signaling cascade and mediates many of insulin's metabolic effects through phosphorylation of various targets including protein kinases, transcription factors and enzymes.

Insulin action in the liver is pivotal for the control of glucose metabolism. The effect of insulin to inhibit hepatic glucose production (HGP) is essential for glucose homeostasis. Hepatic insulin resistance and impaired suppression of HGP underlies the hyperglycemia in patients with diabetes [142].

Biochemistry of Hepatic Glucose Production

Two metabolic pathways contribute to glucose production in vivo: glycogenolysis in the liver and gluconeogenesis in the liver and kidney. As prolonged fasting depletes the glycogen stores, gluconeogenesis provides the required glucose from multiple metabolic sources. I will describe the pathway of gluconeogenesis alone to remain within the confines of the experimental framework of this thesis.

Gluconeogenesis

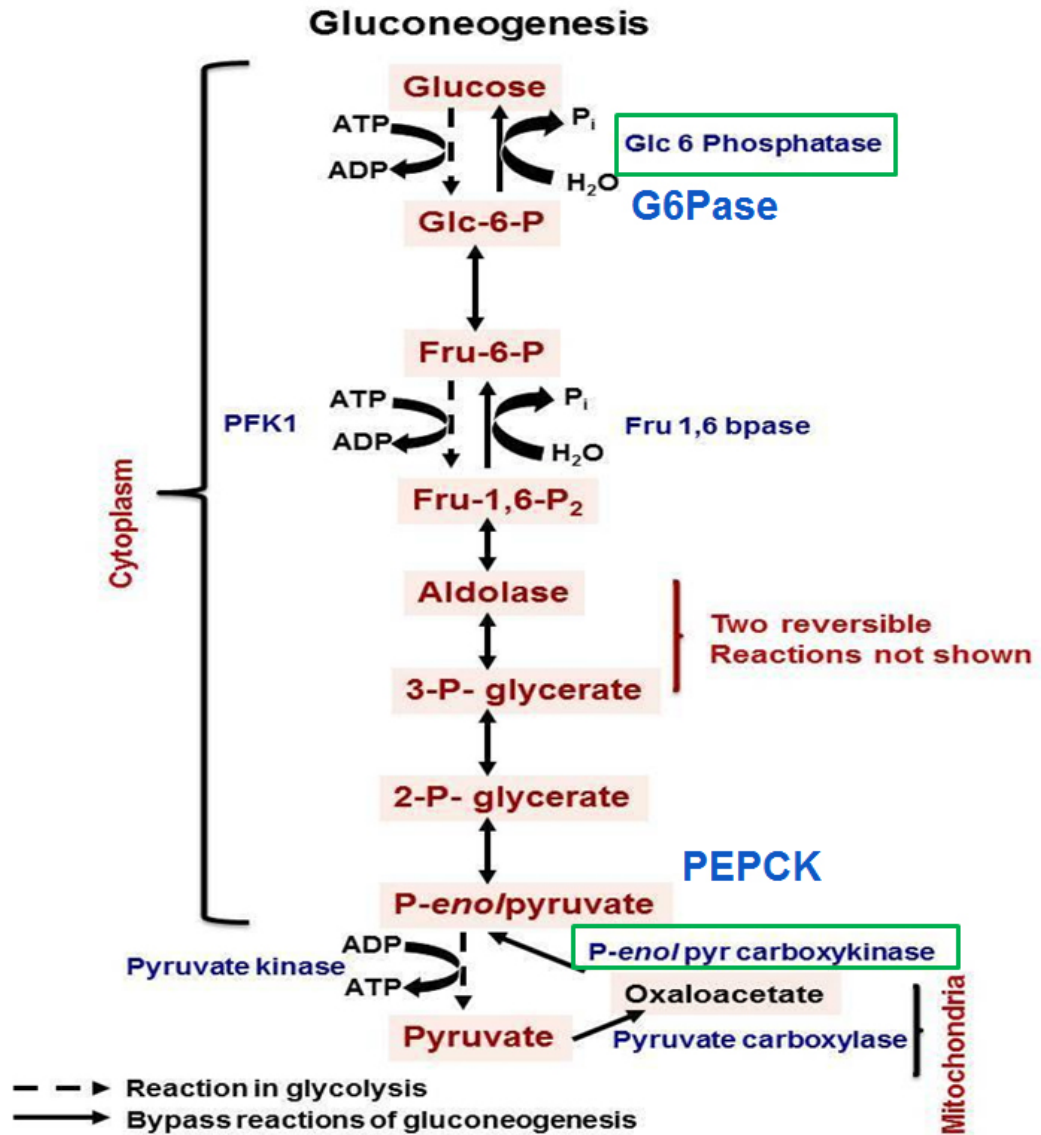
Hepatic gluconeogenesis is responsible for the de novo production of glucose from three carbon precursors such as glycerol, lactate, pyruvate and alanine. Gluconeogenesis operates exclusively in the hepatocytes and the renal cortex. Figure 13 highlights the reactions within the pathway. Gluconeogenesis is often described as the “reverse of glycolysis”. Glycolysis is highly exergonic resulting in the generation of pyruvate, ATP and NADH with several enzymes catalyzing thermodynamically irreversible reactions. Gluconeogenesis utilizes a combination of glycolytic and pathway-specific enzymes to produce glucose at the expense of pyruvate and ATP.

FIG. 13. Schematic showing the biochemical reactions of the gluconeogenesis pathway (adapted from Voet and Voet).

Gluconeogenic pathway enzymes are analogous to their glycolytic counterparts, with exception of reaction steps that are thermodynamically unfavorable. In the first committed step of gluconeogenesis, pyruvate carboxylase (EC 6.4.1.1) catalyzes the synthesis of phosphoenolpyruvate (PEP) from pyruvate.

Phosphoenolpyruvate carboxykinase (PEPCK, EC 4.1.1.32) catalyzes the decarboxylation of cytosolic oxaloacetate into phosphoenolpyruvate, after transport from the mitochondria through the oxaloacetate-malate shuttle. At this point, PEP undergoes the reversible reactions of gluconeogenesis into the triose phosphate pool, condensation through aldolase and formation of fructose-1,6-bisphosphate. Fructose-1,6-bisphosphatase (EC 3.1.3.11) catalyzes the removal of the C1 phosphate and formation of fructose-6-phosphate. The last step in the metabolic pathway of gluconeogenesis is the dephosphorylation of glucose-6-phosphate through the action of glucose-6-phosphatase (EC 3.1.3.9).

Figure 13. Scheme: Biochemical pathway of gluconeogenesis



Gluconeogenic pathway enzymes are analogous to their glycolytic complements, with exception of reaction steps that are thermodynamically unfavorable. In the first committed step of gluconeogenesis, pyruvate carboxylase (EC 6.4.1.1), found in liver and kidney but not muscle, catalyzes the synthesis of phosphoenolpyruvate (PEP) from pyruvate. Phosphoenolpyruvate carboxykinase (PEPCK, EC 4.1.1.32) catalyzes the decarboxylation of cytosolic oxaloacetate into phosphoenolpyruvate, after transport from the mitochondria through the oxaloacetate-malate shuttle. As with pyruvate carboxylase, PEPCK is found in liver and kidney cells. PEP undergoes the reversible reactions of gluconeogenesis into the triose phosphate pool, condensation through aldolase and formation of fructose-1,6-bisphosphate. Fructose-1,6-bisphosphatase (EC 3.1.3.11) catalyzes the removal of the C1 phosphate and formation of fructose-6-phosphate. This enzyme is again found in the liver and kidney. The last step in the pathway of gluconeogenesis is the dephosphorylation of glucose-6-phosphate through the action of glucose-6-phosphatase (EC 3.1.3.9). This enzyme is again exclusive to liver and kidney. These enzymes are used as markers for gluconeogenesis given their distinctive presence in this pathway. Excess hepatic glucose output has been attributed to dysregulation of the gluconeogenic enzymes, PEPCK and G6Pase [143]. Insulin inhibits the transcriptional expression of both of these enzymes through Akt-mediated phosphorylation of FoxO1 [144]. Phosphorylation of the FoxO proteins resulting in their translocation from the nucleus and sequestration in the cytoplasm results in the inhibition of gluconeogenic gene expression. The promoters of both the

PEPCK and G6Pase genes contain so called insulin responsive elements (IREs) that are essential for the effect of insulin on the regulation of those genes.

During the initial stages of fasting, gluconeogenesis accounts for roughly 25% of the glucose output. Upon exhaustion of glycogen reserves, gluconeogenesis becomes the principal source of glucose. The primary glucose sources include lactate from cellular respiration, alanine from protein breakdown and glycerol from triglyceride breakdown. Precise mechanisms of control for gluconeogenesis have been postulated which include: availability of precursors and their initial conversion to the first metabolic intermediate, conversion of pyruvate to phosphoenolpyruvate and the conversion of fructose-1,6-bisphosphate to fructose-6-phosphate.

Glucose-stimulated Insulin Secretion

Pancreatic insulin secretion from the β -cells follows a biphasic pattern, in which an initial peak minutes after stimulation by glucose is followed by a lower magnitude sustained phase over the duration of glucose stimulation. This phenomenon is contributed by the interaction of two signaling pathways: the triggering pathway and the amplifying pathway [145, 146]. In the triggering phase of insulin secretion, mitochondrial glucose metabolism leads to an increase in cytosolic ATP/ADP ratio, which causes the closure of the ATP-sensitive K channel (KATP channel) and membrane depolarization. The resulting membrane depolarization opens voltage-dependent calcium channels, allowing an influx of extracellular Ca^{2+} and stimulation of calcium-induced calcium release from the endoplasmic reticulum. This leads to ATP-dependent exocytosis of a readily

releasable pool of insulin granules. The amplifying pathway of insulin secretion is also dependent on glucose but does not elevate the intracellular Ca^{2+} concentrations and is therefore referred to as the KATP channel-independent pathway [147].

STUDY OBJECTIVE

Our previous work (Chapter III) shows that obesity-induced insulin resistance and impaired glucose tolerance is concurrent with hepatic GSTP downregulation and increased JNK phosphorylation and protein-acrolein adducts. However, multiple GSTs were dysregulated by even a short-term feeding of HFD. To more fully explore the role of GSTP in glucose homeostasis, we compared the glucose metabolic phenotype of GSTP-null mice with that of WT mice. Through the combination of glucose, insulin and C-peptide levels, glucose and pyruvate tolerance tests, high fat feeding, insulin signaling and secretion, we explored the changes to glucose production and utilization in GSTP-null mice, and found evidence for a novel role of GSTP in hepatic gluconeogenesis and insulin secretion to account for the glucose intolerance observed in this mouse model.

RESULTS

GSTP-null mice are glucose tolerant on normal chow diet.

A key concern with gene knockout in animals is the possibility of compensatory changes in the expression of related or alternative genes. Since GSTs are inducible enzymes and most tissues express several GST isoforms, gene deletion of GSTP may be offset by increased expression of other GSTs.

However, studies using GSTP-null mice have confirmed lack of compensatory activation of other GSTs in major tissues such as lung, liver and heart. Kitteringham et al. performed a systematic comparison of the protein expression profiles of livers from GSTP-null and WT mice by proteomic techniques in an attempt to identify possible targets that explain the resistance of GSTP-null mice to acetaminophen-induced hepatotoxicity [55]. The authors demonstrated that deletion of *mGstp1/2* was not compensated for by changes in the expression of other GST isoforms in the liver. Moreover, the authors found significant similarity in expression of approximately 200 proteins analyzed quantitatively in the liver supporting a highly selective nature of the phenotype of GSTP-null mice. Similar results have been reported in the hearts of GSTP-null mice [61]. Taken together, GSTP-null mice are a suitable model for investigating GSTP-specific effects.

Although age-matched WT and GSTP-null male mice fed NC were similar in body weight, body composition (fat and lean mass), organ weights (including liver), fasting blood glucose, fasting plasma insulin, HOMA-IR, HOMA- β and other plasma measures (Fig. 14A-D; Table 1), the GSTP-null mice were significantly more glucose intolerant than WT mice (Fig. 14E-F) as determined by i.p. GTT. After 6 h of fasting, blood glucose levels were similar among the genotypes (indicated at 0 min) (Fig. 14E). Following glucose administration, GSTP-null mice exhibited severe hyperglycemia resulting in significantly greater AUC for glucose values from 0–120 min (Fig. 14F) compared with WT mice. This glucose-intolerant phenotype (~70-120% increase in glucose AUC) was repeated in multiple independent experiments to a similar extent in mice of several lines

and was observed in animals as early as 11 weeks of age. No differences were noted in metabolic profile between the genotypes (Fig. 14G-L). These data suggest a novel role for GSTP in glucose homeostasis and sets forth the possibility that altered GSTP predisposes to a pre-diabetic phenotype.

Table 2. Metabolic and plasma parameters of male WT and GSTP-null mice on normal chow diet.

Values are mean \pm SEM. Abbreviations: BW, body weight; EWAT, epididymal white adipose tissue; BAT, brown adipose tissue; TC, total cholesterol; HDL-C, high-density lipoprotein cholesterol; LDL-C, low-density lipoprotein cholesterol; TG, triglycerides; CK, creatine kinase; LDH, lactate dehydrogenase; ALT, alanine aminotransferase; AST, aspartate aminotransferase. * $P < 0.05$, WT vs. Null by Student's t-test or Mann-Whitney U test as appropriate.

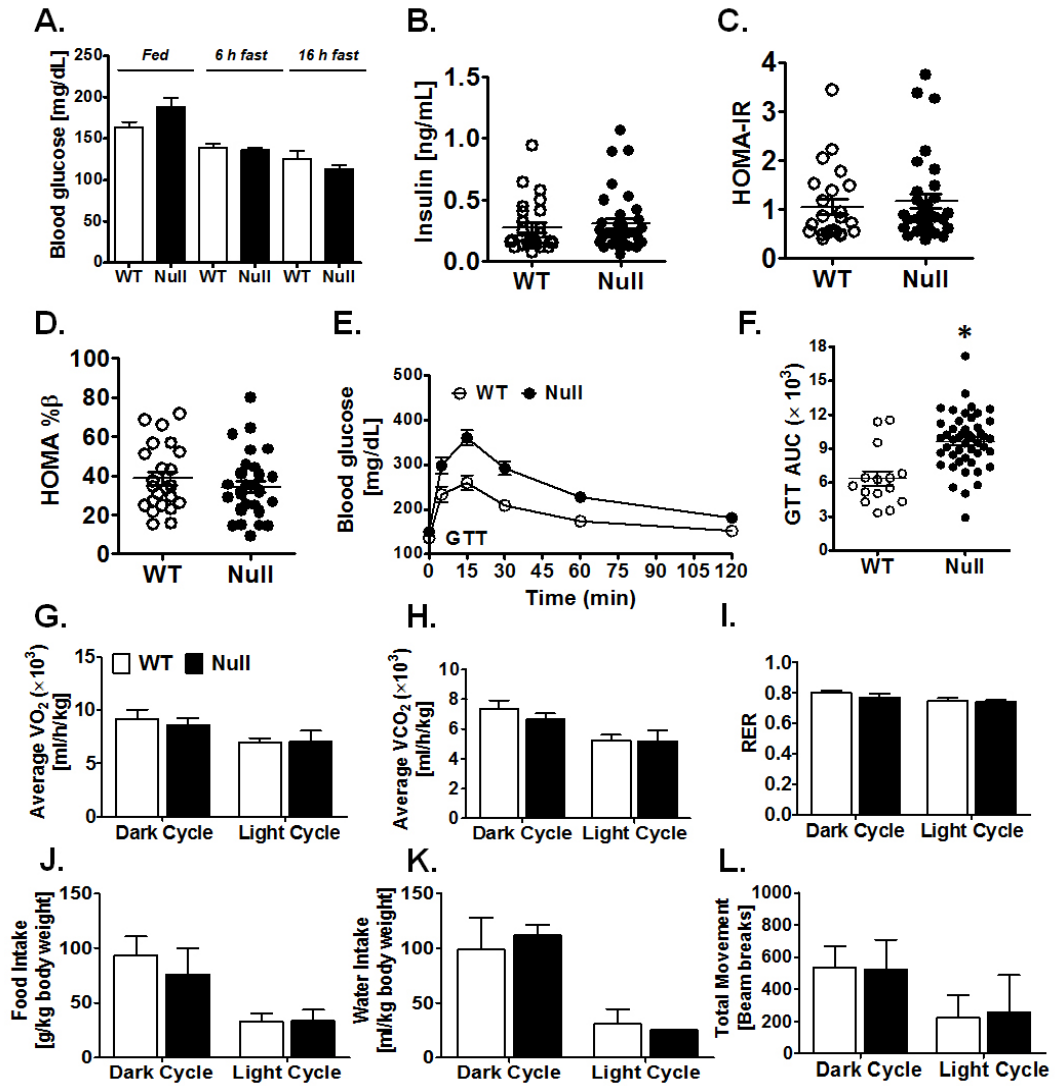
Table 2. Metabolic and plasma parameters of WT and GSTP-null mice

Parameter	Wild-Type (<i>n</i>)	GSTP-null (<i>n</i>)
Body composition (g)		
Body weight	29.57 ± 0.36 (24)	29.36 ± 0.40 (23)
Lean mass	21.04 ± 0.32 (24)	21.34 ± 0.31 (23)
Fat mass	4.88 ± 0.14 (24)	4.56 ± 0.17 (23)
Organ weights (% of BW)		
Liver	4.33 ± 0.11 (16)	4.26 ± 0.09 (17)
EWAT	1.03 ± 0.09 (16)	1.24 ± 0.08 (17)
BAT	0.18 ± 0.02 (16)	0.28 ± 0.01 (17)*
Plasma lipids (mg/dL)		
TC	72.74 ± 1.90 (8)	73.64 ± 1.68 (18)
HDL-C	75.65 ± 2.70 (8)	74.97 ± 2.48 (18)
LDL-C	11.67 ± 0.54 (8)	12.84 ± 0.54 (18)
TG	44.42 ± 2.73 (8)	40.20 ± 2.12 (18)
Plasma biochemistry		
Albumin (g/dL)	2.579 ± 0.07 (8)	2.501 ± 0.03 (18)
Total protein (g/dL)	4.384 ± 0.08 (8)	4.285 ± 0.05 (18)
CK (U/L)	234.7 ± 57.31 (6)	190.8 ± 27.87 (15)
LDH (U/L)	205.6 ± 25.46 (6)	164.8 ± 10.89 (15)
ALT (U/L)	55.95 ± 6.99 (6)	35.49 ± 3.10 (15)*
AST (U/L)	79.98 ± 13.82 (6)	57.18 ± 6.85 (15)

FIG. 14. GSTP-deletion in mice causes glucose intolerance.

Glucose tolerance test (GTT), glycemic indices and indirect calorimetry measurements shown for WT and GSTP-null mice fed NC diet. **(A)** Fasting blood glucose; **(B)** Fasting plasma insulin; **(C)** HOMA-IR, and **(D)** HOMA-% β values in WT and GSTP-null mice. For GTT, **(E)** Blood glucose levels were measured before and after glucose bolus (1 mg/g lean mass, i.p.) in WT and GSTP-null mice, and **(F)** GTT area under the curve (AUC) values were calculated. Metabolic parameters were measured by indirect calorimetry in 12 week-old WT and GSTP-null mice using a PhenoMaster system: **(G)** oxygen consumption (VO₂); **(H)** carbon dioxide production (VCO₂); **(I)** respiratory exchange ratio (RER); **(J, K)** food and water intake; and, **(L)** total activity (movement). Values are mean \pm SEM (n=5-50 per group). **P* < 0.05, WT vs. GSTP-null by Student's t-test or by Mann-Whitney U-test where appropriate. WT, open symbols or bars; GSTP-null, filled symbols or bars.

Figure 14. GTT and indirect calorimetry in GSTP-null mice on NC diet



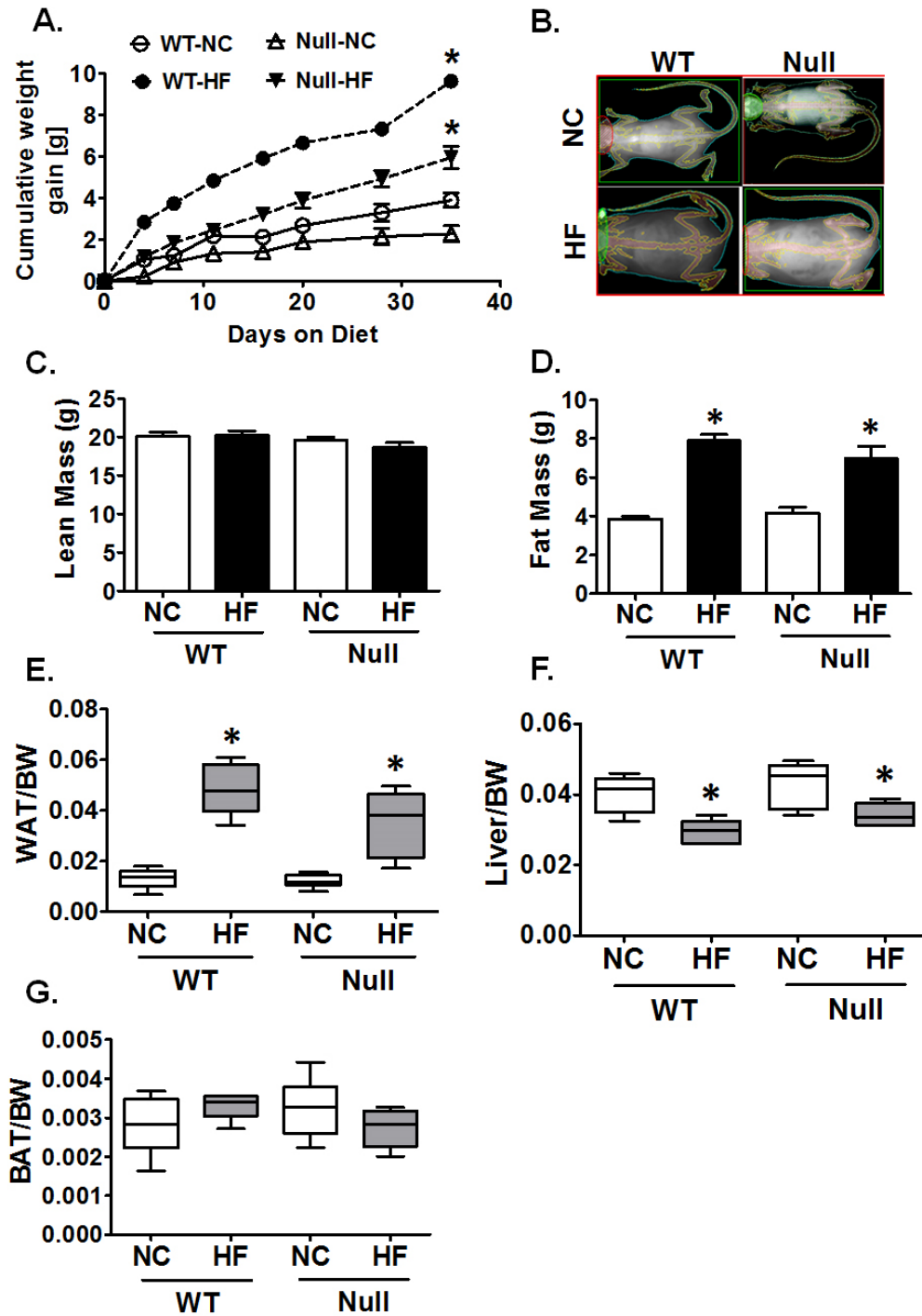
Short-term high fat diet does not further exacerbate obesity and glucose intolerance in GSTP-null mice.

Obesity and T2D are each characterized by a strong interaction of genetics and environment. We investigated whether HFD aggravated metabolic derangements in GSTP-null mice compared with WT mice. To that end, weight gain, glucose tolerance and energy metabolism was examined in chow and HF-fed mice of both genotypes. Interestingly, following a short-term HFD feeding (60% kcal; 3.5 weeks), weight gain was lower in GSTP-null mice compared with WT mice (Fig. 15A). The differences persisted throughout the six-week study resulting in a small but statistically significant lesser cumulative weight gain in GSTP-null mice (6.38 ± 0.72 g in WT and 3.35 ± 0.68 g in GSTP-null mice, $p < 0.05$, $n = 5-7$ per group). However, this difference in weight gain was not accounted for by differences in HFD-induced changes in lean and fat mass or organ weights between genotypes (Fig. 15B-G). To investigate this point further, we subjected mice to indirect calorimetry to determine whether an increase in energy expenditure accounted for the surplus in energy intake that was not stored in adipose tissue of GSTP-null mice. However, both genotypes showed similar alterations in energy expenditure, caloric intake, locomotor movement and respiratory quotient following HFD (Fig. 16A-F).

FIG. 15. Short-term diet-induced obesity in WT and GSTP-null mice.

(A) Cumulative body weight (BW) of mice fed normal chow (NC) and high-fat diet (HF, 60% kcal fat) ad libitum for 6 weeks. Dual-energy X-ray absorptiometry (DEXA) analysis and glucose tolerance test (GTT) were performed at 3 or 3.5 weeks of diet study, respectively (see arrows). **(B)** Lean and fat mass content as measured by DEXA. *Inset:* Representative DEXA images. **(C)** Fed and **(D)** Fasting (6h) blood glucose at weeks 2 and 3 of diet study measured by tail vein. **(E-G)** Organ to body weight ratios at the end of the diet study. Values are mean \pm SEM ($n = 5$ per group). BW, body weight; EWAT, epididymal white adipose tissue; SubQ WAT, subcutaneous white adipose tissue; BAT, brown adipose tissue (interscapular); PVAT, perivascular adipose tissue. * $P < 0.05$, NC vs. HF by Mann-Whitney U test. NC, open symbols or bars; HF, filled symbols or grey bars.

Figure 15. Diet-induced obesity in GSTP-null mice



Although short-term HFD feeding in GSTP-null mice increased adiposity, yet it did not increase GTT AUC over that of GSTP-null mice fed NC (Fig. 16G-H). Moreover, the GTT AUC of GSTP-null mice (regardless of diet) was similar to the GTT AUC of HFD-fed WT mice suggesting that the glucose intolerance effects of HFD in WT mice may be attributable solely to the downregulation of hepatic GSTP. Consistent with this hypothesis, although lacking GSTP, the hepatic protein levels of GSTA and GSTM in GSTP-null were similar to their levels in age-matched, NC-fed WT mice (Fig. 17A-E) indicating no compensatory upregulation in GSTP-null mice of these abundant GST isoforms. The total hepatic GST activity in GSTP-null mice was decreased by only about 24% (CDNB substrate; Fig. 17F) -- a decrease in GST activity that was similar (surprisingly) to the decreased hepatic GST activity measured in HFD-fed WT mice (see Fig. 8, Chapter III). Moreover, and despite the idea that fat accumulation in the liver causes hepatic IR [148, 149] and subsequently peripheral IR and glucose intolerance [150-152], levels of hepatic triglycerides and cholesterol were similar in WT and GSTP-null mice whether fed NC or HFD (Fig. 18). These data indicate that GSTP deficiency exerted a specific defect perhaps selectively hepatic that led to glucose intolerance.

FIG. 16. Short-term diet-induced obesity and glucose intolerance in WT and GSTP-null mice.

Indirect calorimetry and glucose tolerance test (GTT) measurements are shown for WT and GSTP-null mice fed NC and HF diet. Metabolic parameters were measured by indirect calorimetry in 12 week-old WT and GSTP-null mice using a PhenoMaster system: **(A)** oxygen consumption (VO_2); **(B)** carbon dioxide production (VCO_2); **(C)** respiratory exchange ratio (RER); **(D)** total activity (movement); and **(E, F)** food and water intake. **(G)** For GTT, mice were fasted for 6 h and injected intraperitoneally with glucose bolus (1 mg/g of lean mass). Blood glucose was measured by tail vein, and **(H)** the area under the curve (AUC) was calculated. Values are mean \pm SEM ($n = 5-7$ per group). HOMA-IR and HOMA-% β , homeostasis model assessment-estimated insulin resistance and β -cell function indices. * $P < 0.05$, NC vs. HF or WT vs Null by Mann-Whitney U test and *One-way ANOVA* analysis as appropriate

Figure 16. GTT and indirect calorimetry in GSTP-null mice on HFD

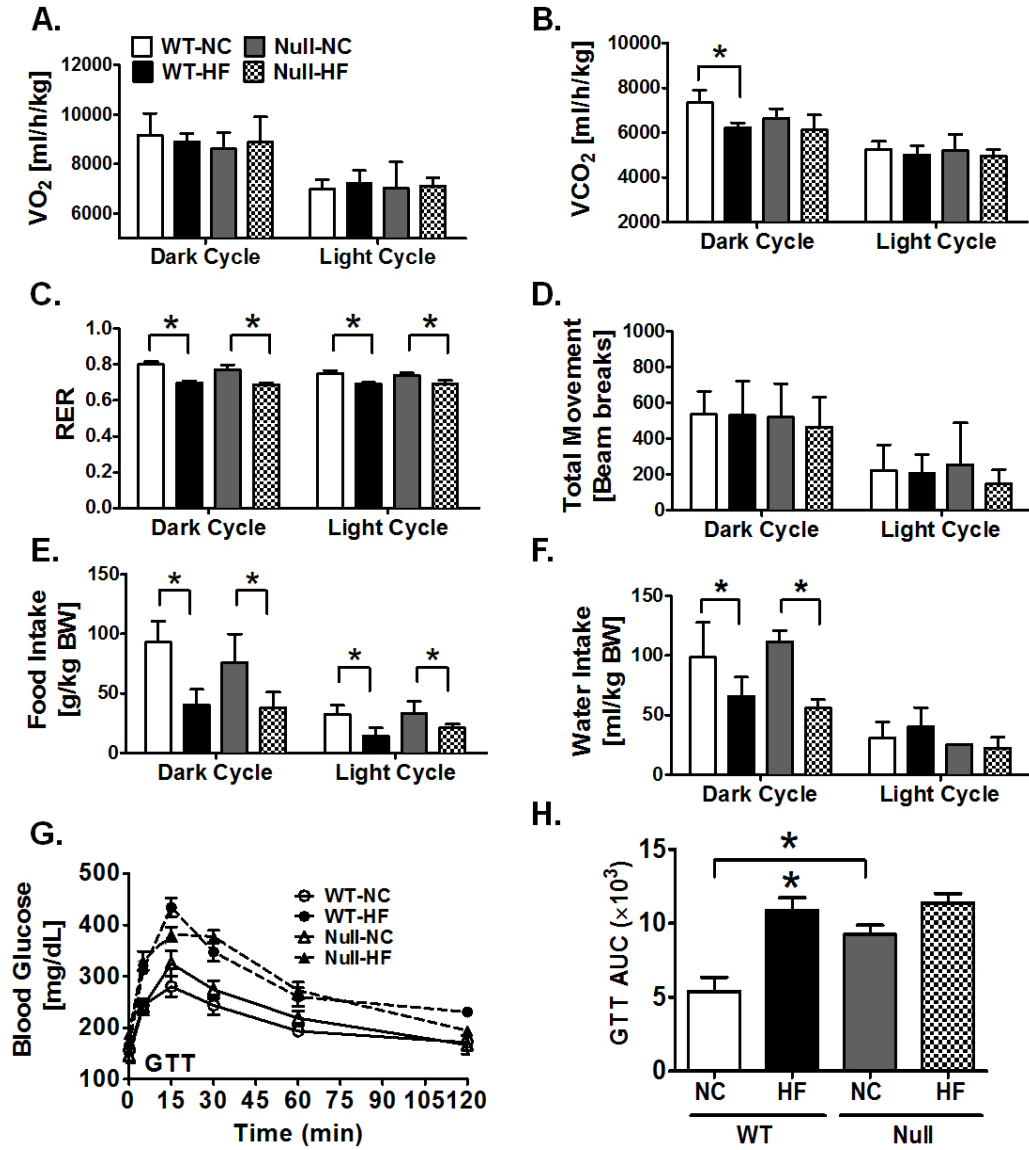


Fig. 17. Glutathione S-transferases expression and activity in liver of WT and GSTP-null mice.

(A) *Gsta4*, *Gstm4.1*, and *Gstp1* mRNA expression (normalized to *Rplp0*) in liver of WT and GSTP-null mice fed NC ($n=6-8$ per group). **(B)** Representative Western blots of liver lysates for GSTA, GSTM and GSTP and respective **(C)** densitometric analyses ($n=3$ per group). **(D, E)** Liver sections from WT and GSTP-null mice stained with anti-GSTP antibody. **(F)** Hepatic GST activity measured with 1-chloro-dinitrobenzene (CDNB) as substrate ($n=10-11$ per group). Values are mean \pm SEM. * $P < 0.05$, by Mann-Whitney U test. NC, open symbols or bars; HF, filled symbols or bars.

Figure 17. Hepatic GSTA and GSTM abundance in GSTP-null mice

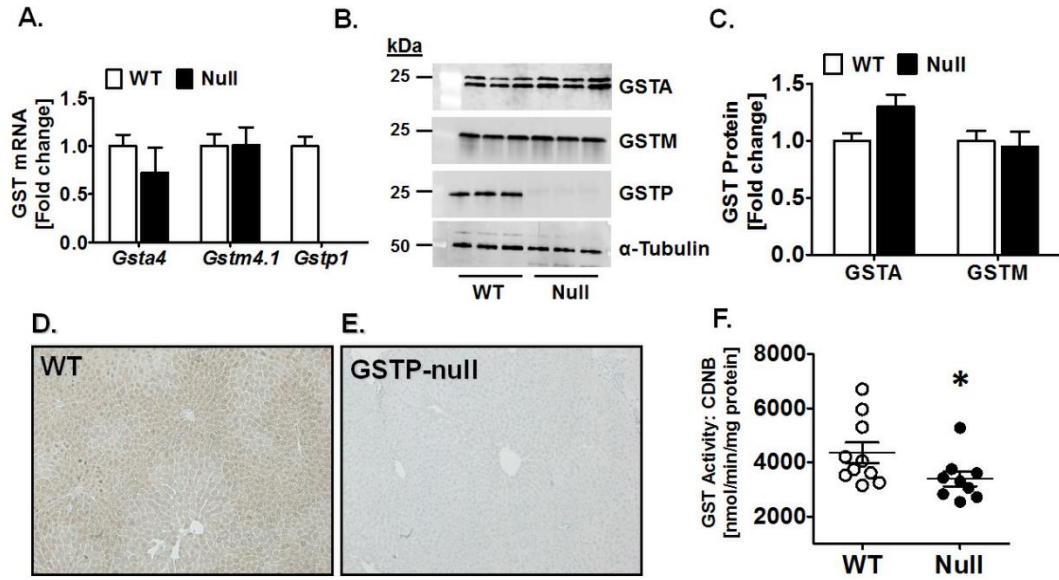
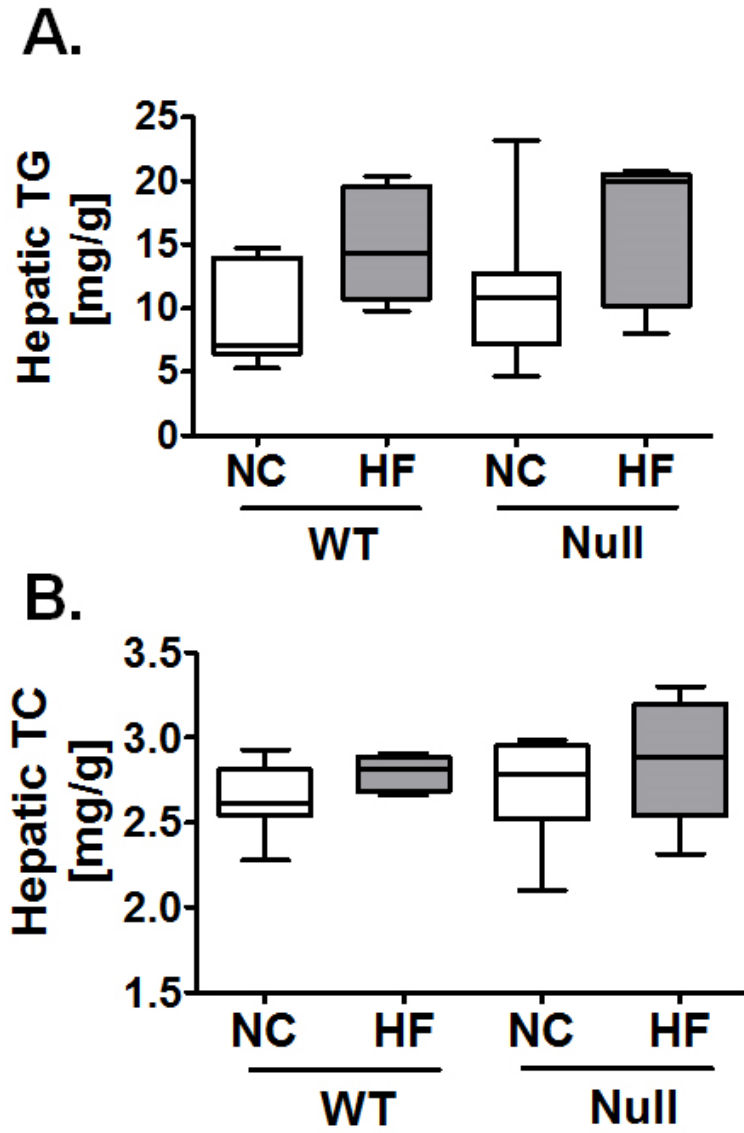


Fig. 18. Short-term diet-induced obesity and hepatic lipids in WT and GSTP-null mice.

Measurements were made in WT and GSTP-null mice fed normal chow (NC) and high-fat diet (HF, 60% kcal fat) ad libitum for 6 weeks. **(A)** Total triglycerides (TG) and **(B)** cholesterol (TC) were measured on livers collected at the end of the diet study. Values are mean \pm SEM (WT $n = 5$ and GSTP-null $n=7$ animals per group). * $P < 0.05$, NC vs. HF and WT vs. GSTP-null by Mann-Whitney U test. NC, open bars; HF, grey bars.

Figure 18. Hepatic triglycerides and cholesterol in GSTP-null mice on HFD



These characteristics of GSTP-null mice are reminiscent of the natural history of T2D in certain populations which develop diabetic complications independent of obesity and carry polymorphic GSTP variants. Thus, GSTP-null mice represent a relevant animal model for gaining insights into pathophysiological mechanisms operative in human T2D.

GSTP-null mice exhibit increased hepatic phospho-JNK abundance and protein-acrolein adduct formation.

Because GSTP-null mice have both diminished acrolein metabolism and increased JNK activation under basal and stressful conditions [59, 107], we measured both protein-acrolein adducts and JNK phosphorylation status in the major glucose disposal organs (liver, skeletal muscle and adipose). Under basal conditions, a single protein-acrolein adduct band (i.e., $M_r \cong 90$ kDa, +1.3 fold; $p < 0.05$; Fig. 19A-B) was statistically increased in liver of NC-fed GSTP-null and WT mice. No differences in adduct levels were observed in skeletal muscle and adipose of GSTP-null and WT mice fed either NC or HFD (Fig 19C-F). High fat feeding did not have an additive effect in increasing protein-acrolein adducts in GSTP-null mice compared with WT mice (Fig. 20 and 21).

Fig. 19. Protein-acrolein adducts in WT and GSTP-null mice.

Representative Western blots of protein-acrolein adduct bands in **(A)** liver, **(C)** gastrocnemius skeletal muscle, and **(E)** epididymal white adipose tissue and respective **(B, D, F)** densitometric analyses. Values are mean \pm SEM ($n=6$ per group). * $P < 0.05$, NC vs. HF by Mann-Whitney U-test. NC, open bars; GSTP-null, filled bars.

Figure 19. Protein-acrolein adducts in GSTP-null mice on NC diet

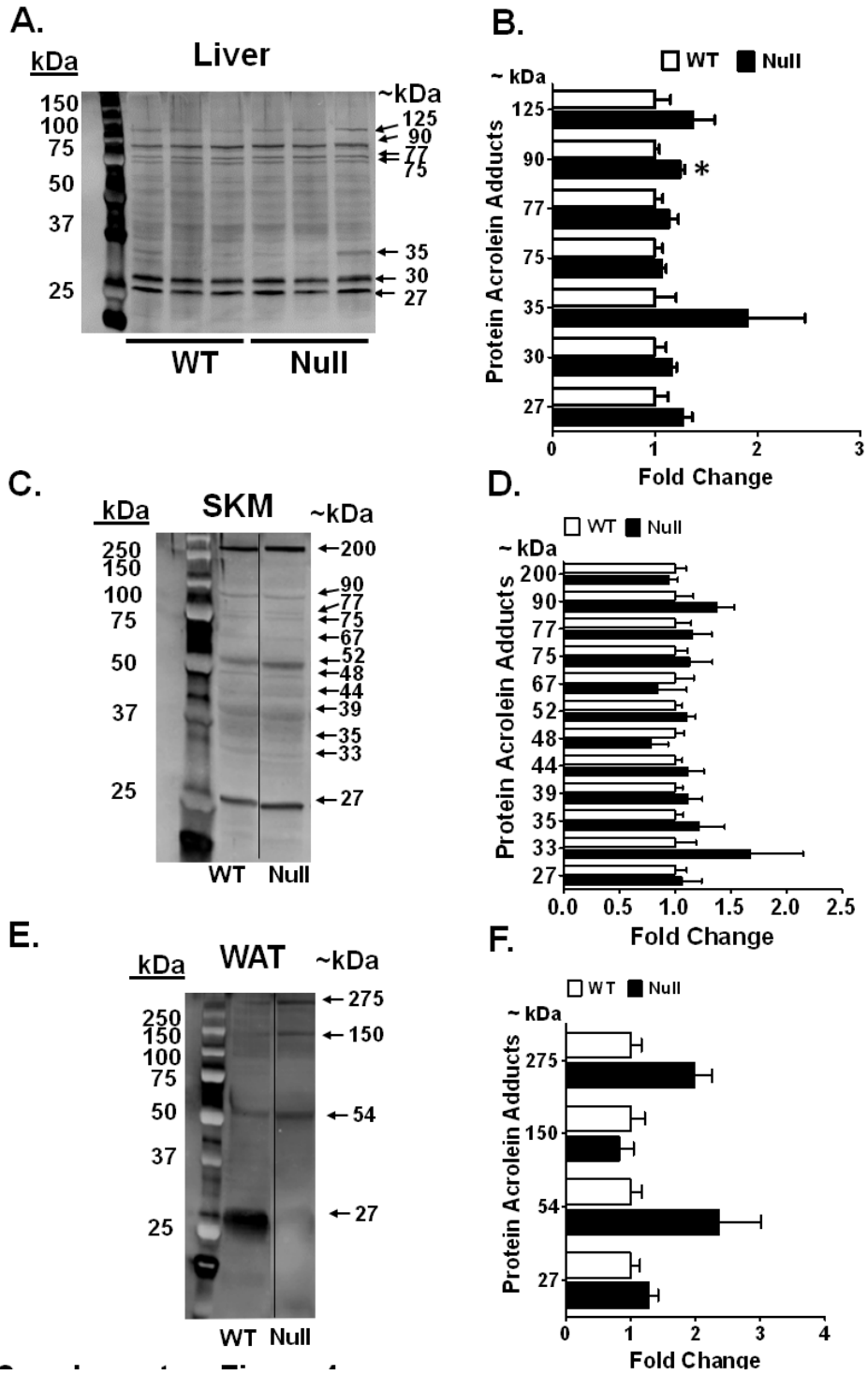


Fig 20. Protein-acrolein adducts in normal chow and high-fat diet fed GSTP-null mice.

Representative Western blots of protein-acrolein adduct bands in liver of **(A)** GSTP-null mice fed NC and HFD; **(C)** WT and GSTP-null mice fed HFD, and respective **(B, D)** densitometric analyses. Values are mean \pm SEM ($n=5-6$ per group). * $P < 0.05$, NC vs. HF by Mann-Whitney U-test. NC, open bars; HF, filled bars.

Figure 20. Protein-acrolein adducts in GSTP-null mice on HFD

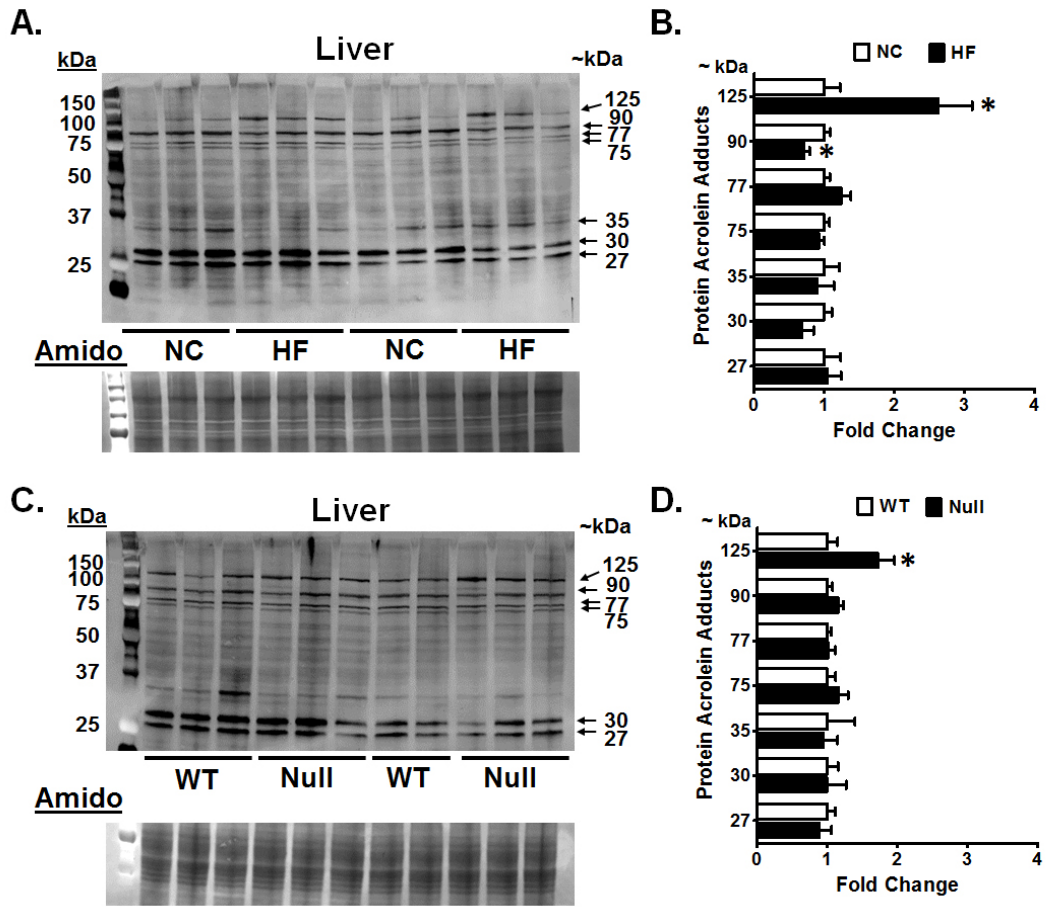
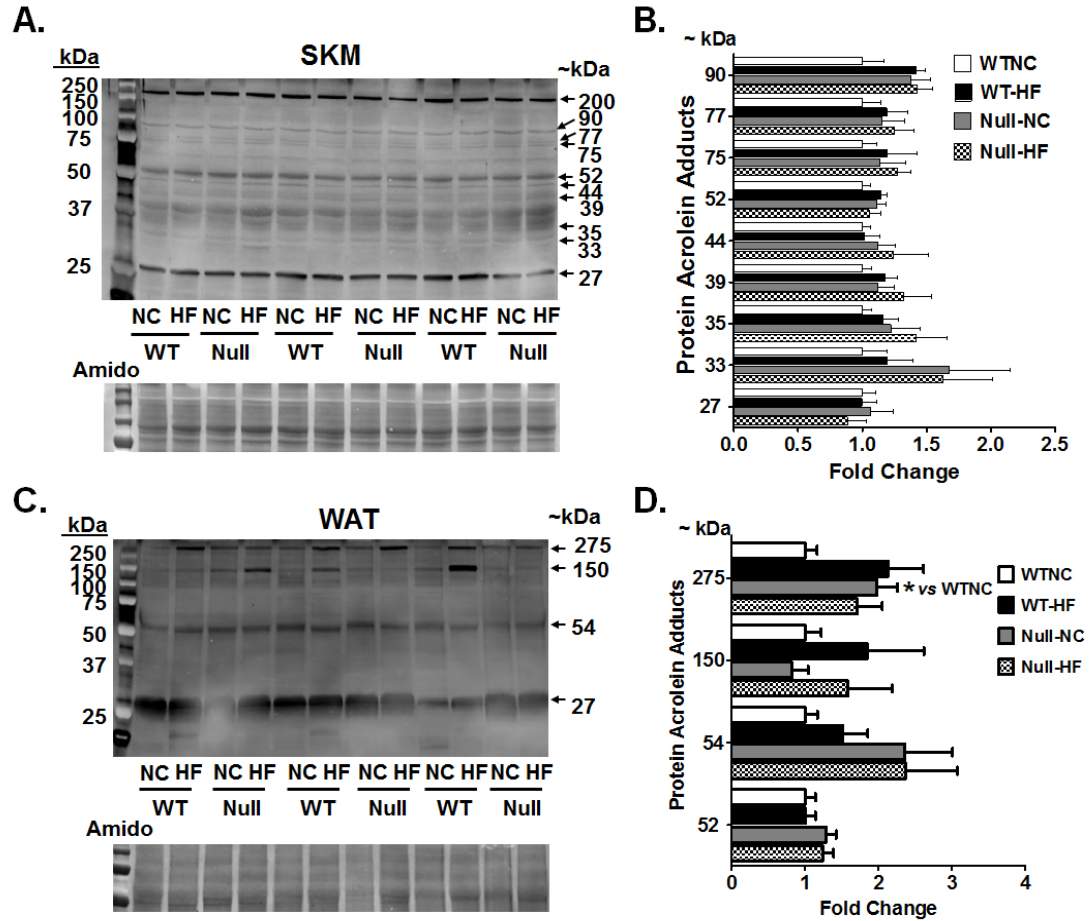


Fig 21. Protein-acrolein adducts in normal chow and high-fat diet fed WT mice.

Representative Western blots of protein-acrolein adduct bands in **(A)** gastrocnemius skeletal muscle, and **(C)** epididymal adipose tissue and respective **(B, D)** densitometric analyses. Values are mean \pm SEM ($n=5$ per group). * $P < 0.05$, NC vs. HF by Mann-Whitney U-test.

Figure 21. Protein-acrolein adducts in GSTP-null mice on HFD



Because acrolein (and other unsaturated aldehydes) can induce protein-aldehyde adducts and endoplasmic reticulum stress (ER-stress; [99]) that can activate JNK [6, 140], the hepatic levels of XBP-1 splicing and known ER-stress markers, HERP and GRP78 [153], were measured. The levels of these ER stress markers were similar in livers of GSTP-null and WT mice (Fig. 22). However, as observed in WT mice fed HFD, hepatic abundance of phospho-p54 JNK (but not phospho-p46) was greater in GSTP-null than in WT mice (Fig. 23A-C). In adipose and skeletal muscle, however, the levels of phospho-JNK (p54, p46) were similar in GSTP-null and WT mice (Fig. 23D-G). Furthermore, hepatic phospho-JNK abundance was increased to a similar degree in HFD-GSTP-null mice compared with HFD-WT mice. Collectively, these data show GSTP deficiency had selective effects on hepatic accumulation of protein-acrolein adducts and JNK (p54) activation in the absence of ER stress – effects not observed in the other major insulin-sensitive organs.

Fig. 22. Hepatic ER stress markers in WT and GSTP-null mice.

Xbp-1 splicing was assessed by RT-PCR, and *Herp* and *Grp78* mRNA expression (normalized to *Rplp0*) in livers of 6 h fasted WT and GSTP-null mice was assessed. Values are mean \pm SEM ($n=6$ animals per group). * $P < 0.05$, WT vs. GSTP-null by Mann-Whitney U-test. WT, open bars; GSTP-null, filled bars.

Figure 22. Hepatic ER-stress markers in GSTP-null mice

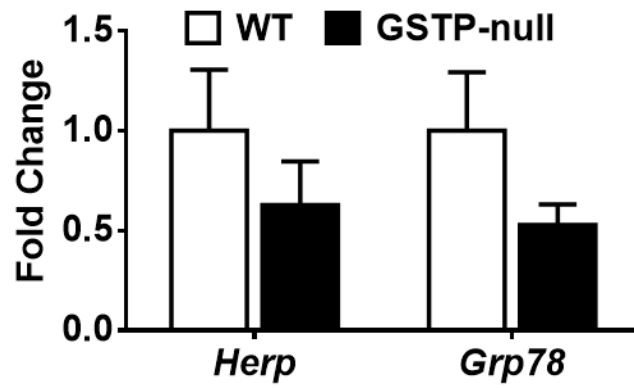
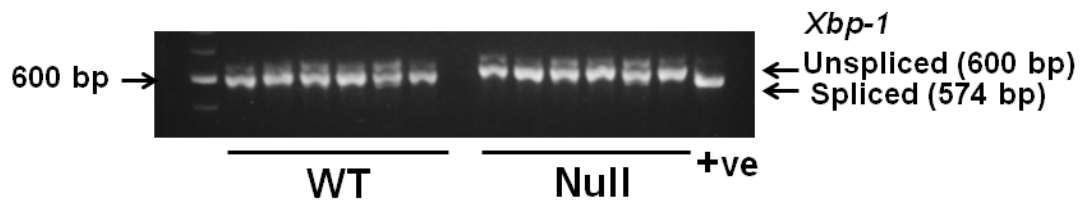


FIG. 23. JNK phosphorylation in WT and GSTP-null mice on NC diet.

Representative Western blots for phospho-JNK (Thr183/Tyr185) and total JNK (p54/p46) in **(A)** liver, **(D)** gastrocnemius skeletal muscle, and **(E)** epididymal white adipose tissue and respective **(B, C, F, G)** densitometric analyses. Values are mean \pm SEM ($n=6$ per group). * $P < 0.05$, WT vs. null by Mann-Whitney U-test. NC, open bars; GSTP-null, filled bars.

Figure 23. JNK phosphorylation in GSTP-null mice on NC diet

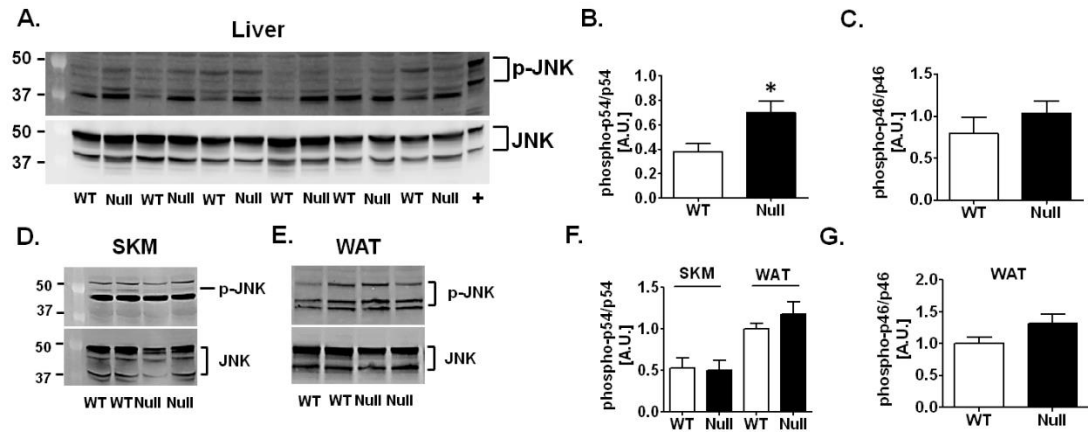
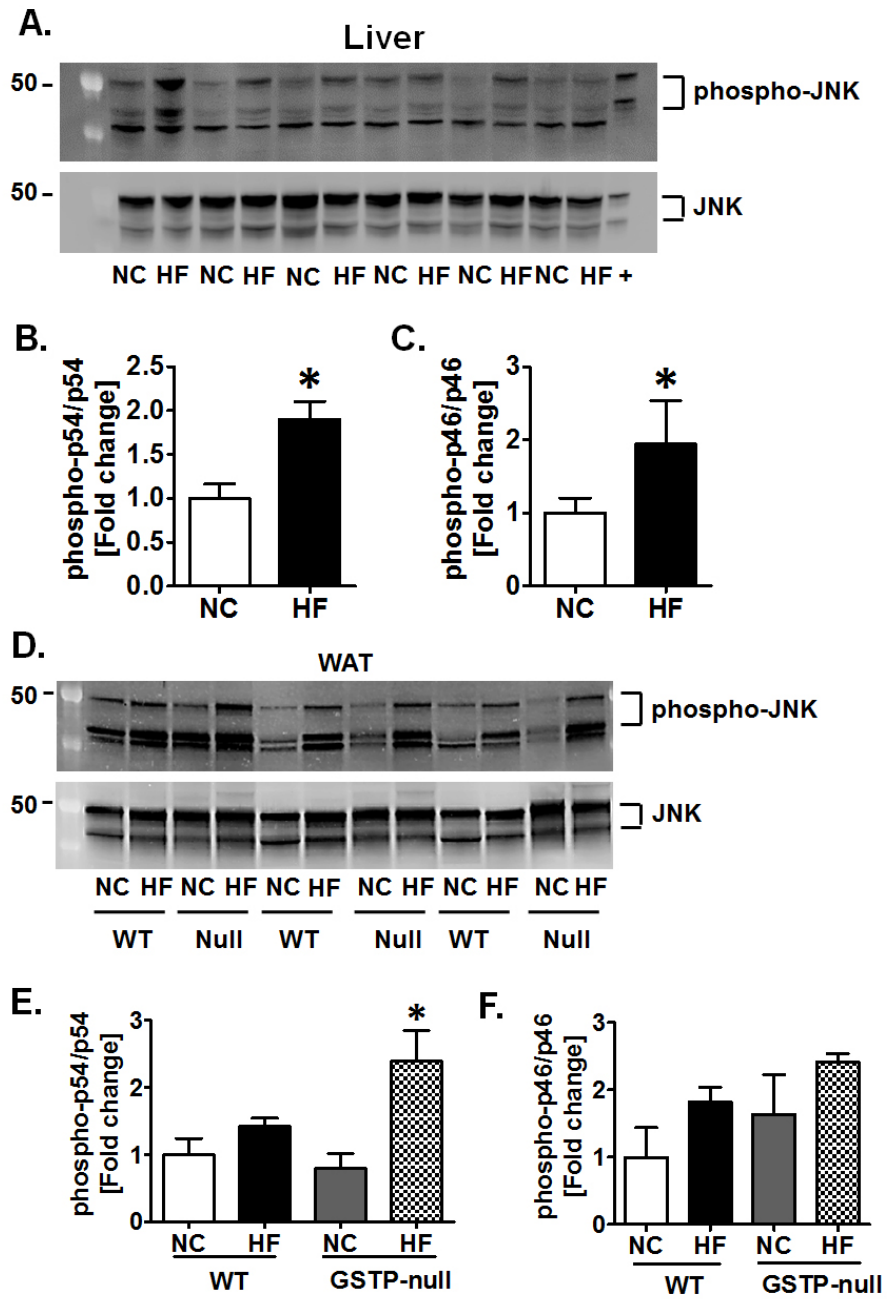


FIG. 24. JNK phosphorylation in WT and GSTP-null mice fed high-fat diet.

Representative Western blots for phospho-JNK (Thr183/Tyr185) and total JNK (p54/p46) in **(A)** liver of GSTP-null mice fed HF-diet; and **(D)** epididymal white adipose tissue from NC- and HF-fed WT and GSTP-null mice and respective densitometric analyses **(B, C, E, F)**. Values are mean \pm SEM ($n=5$ per group).

* $P < 0.05$, NC vs. HF for each genotype by Mann-Whitney U-test.

Figure 24. JNK phosphorylation in GSTP-null mice on HFD



Insulin sensitivity and increased gluconeogenesis in GSTP-null mice.

JNK activation impairs insulin signaling in diabetes [139], but how hepatic JNK activation in GSTP-null mice increases glucose intolerance is unclear. To assess insulin signaling in GSTP-null mice, glucose disposal and Akt phosphorylation was measured after insulin injection. The fall in glycemia at 15 min after insulin injection was similar in both genotypes, suggesting insulin sensitivity was preserved in GSTP-null mice (*data not shown*). Consistent with this interpretation, insulin stimulated robust Akt phosphorylation (pSer⁴⁷³-Akt) in liver, skeletal muscle and adipose tissue with no differences between GSTP-null and WT mice (Fig. 25). Because the level of blood glucose (as in a GTT) is a consequence of the opposing forces of glucose uptake and glucose output, we tested whether GSTP-null mice had increased hepatic glucose output. To test this, we conducted a pyruvate tolerance test (PTT). Mice were challenged with the gluconeogenic precursor, pyruvate and hepatic glucose output (HGP) was estimated. As shown in Fig. 26A, following pyruvate injection, GSTP-null mice exhibited enhanced blood glucose excursion during the first 30 min (Fig. 26B), suggesting a higher gluconeogenic potential in the absence of GSTP. These differences persisted throughout the 120 mins of the PTT (Fig. 26C) and resulted in a significantly greater glucose AUC in GSTP-null mice compared with WT mice (Fig. 26D).

Fig. 25. Insulin signaling in WT and GSTP-null mice.

(A-F) Total Akt and phospho-Akt (Ser473) following saline or insulin (1.5U/kg lean mass, ip) bolus in NC-fed WT and GSTP-null mice after a 6 h fast. Representative blots are shown for liver, gastrocnemius skeletal muscle and epididymal adipose tissue (top, middle and lower panels respectively) along with respective **(B, D, F)** densitometric analyses. Bar values = mean \pm SEM from 3 independent experiments ($n = 6$ animals per group). * $P < 0.05$, WT vs. GSTP-null by Mann-Whitney U-test.

Figure 25. Insulin signaling in peripheral tissues in GSTP-null mice

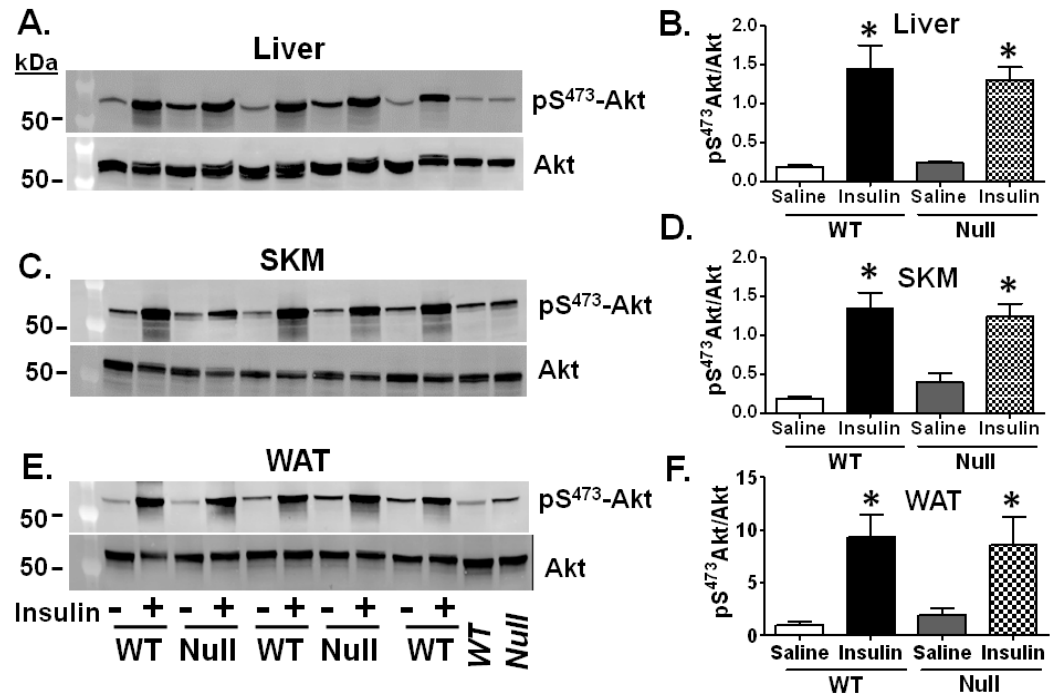
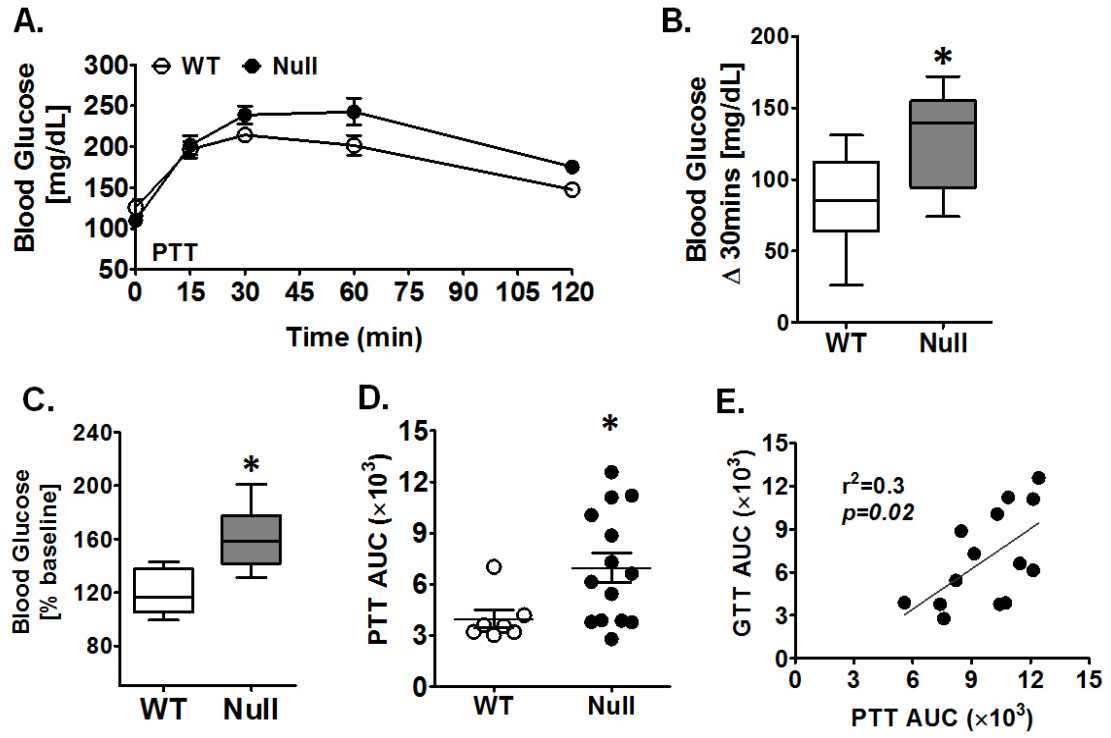


FIG. 26. GSTP-null mice have increased gluconeogenesis.

Pyruvate tolerance test (PTT) measurements are shown. **(A)** Blood glucose levels were measured before and after pyruvate bolus (2 mg/g lean mass, i.p.) in WT and GSTP-null mice (WT $n=7$; GSTP-null $n=15$). **(B)** Delta 30 min blood glucose values relative to baseline for vehicle and JNKI-treated GSTP-null mice (also referred to as the “*glucose appearance rate*”). **(C)** Blood glucose values percent of baseline at 120 min of the PTT for each genotype; **(D)** PTT area under the curve (AUC) values. **(E)** GTT AUC was plotted relative to PTT AUC for GSTP-null mice. Values are mean \pm SEM. * $P < 0.05$, WT vs. GSTP-null by Mann-Whitney U-test. WT, open symbols; GSTP-null, filled symbols.

Figure 26. Hepatic gluconeogenesis by PTT in GSTP-null mice



Additionally, the PTT AUC was significantly correlated with the GTT AUC ($r^2=0.3$, $p=0.02$) in GSTP-null mice (Fig. 14E), further supporting the idea that hepatic glucose output was contributing to overall elevated glucose intolerance in GSTP-null mice.

Glucose homeostasis in rodents, as in humans, is a function of the rate of insulin release in response to glycemia and insulin sensitivity of peripheral organs. The balance between these two factors determines the overall physiological tolerance to glucose and the capacity to sustain glucose homeostasis within the normal physiological range. Because GSTP-null mice exhibited robust Akt phosphorylation in peripheral tissues, we inferred that impaired glucose tolerance (and increased gluconeogenesis) in GSTP-null mice is not likely explained by insulin resistance. Therefore, we tested whether glucose-stimulated insulin secretion (GSIS) is altered in GSTP-null mice.

GSTP-null mice exhibit decreased glucose-stimulated insulin secretion (GSIS).

The peak insulin secretion and action is reported in the literature to be within ~25-30 min following glucose bolus administration in mice. The half-life of insulin in mice is ~10-15 min and that of the pro-insulin cleavage product, C-peptide is ~30 min. Endogenous measurement of plasma C-peptide is a clinically validated assessment of β -cell function. We measured glucose-stimulated plasma insulin and C-peptide levels at 20 and 30 min post glucose challenge in independent cohorts of age-matched WT and GSTP-null mice. Fasting plasma glucose and C-peptide levels were similar in WT and GSTP-null mice. In contrast, plasma insulin

levels were decreased by ~10-fold in GSTP-null mice compared with WT mice at 20 min post glucose bolus, yet the difference was normalized at 30 min post glucose injection (Fig. 27A). C-peptide levels also were decreased in GSTP-null versus WT mice (Fig. 27B), consistent with the decreased insulin secretion. In contrast, the C-peptide/insulin ratio, which reflects insulin clearance, was unaltered in GSTP-null mice compared with WT mice (Fig. 27E). Together, these findings indicate that the hyperglycemia of GSTP-null mice results, at least in part from insulin hyposecretion rather than from differences in insulin resistance or clearance, which were unaltered in GSTP-null mice.

GSTP-null mice exhibit decreased pyruvate-stimulated insulin secretion (PSIS).

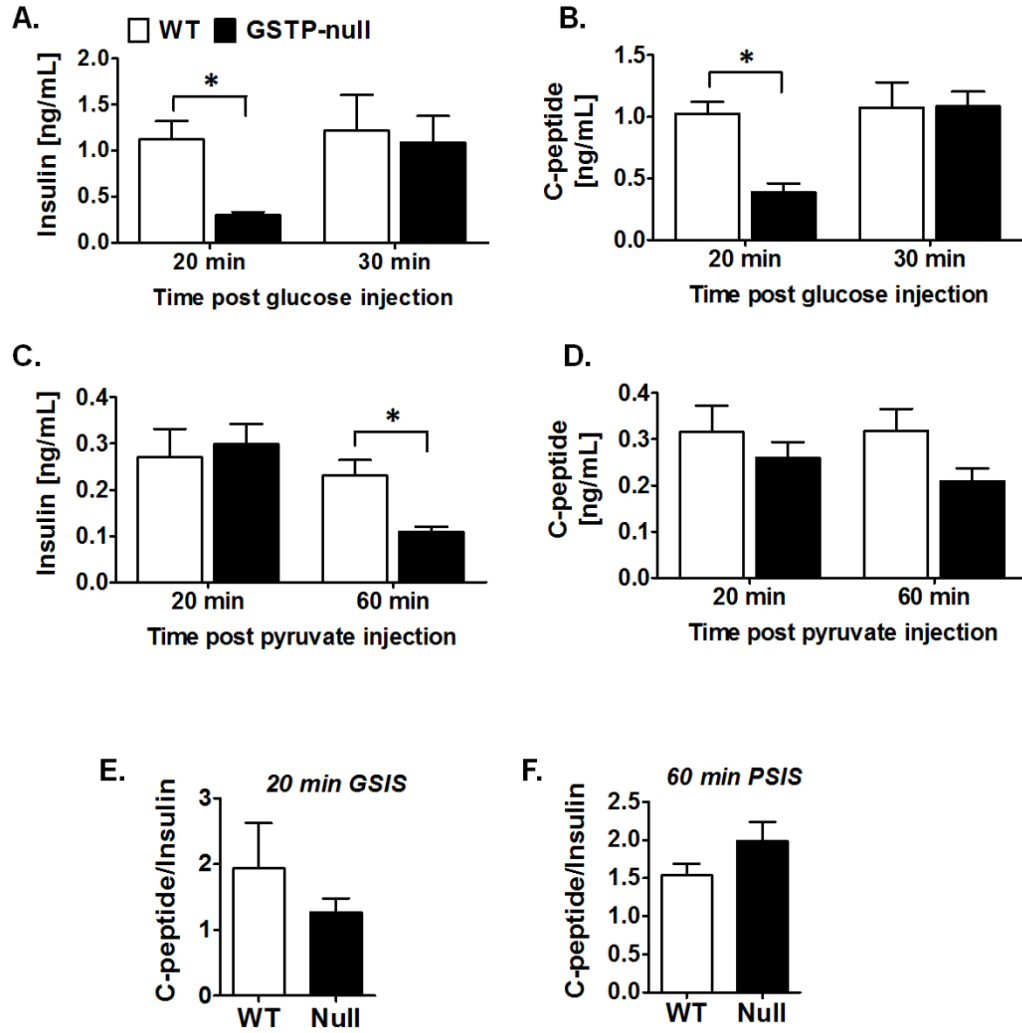
Next, we asked whether altered insulin responses could account for the divergent PTT curves of WT and GSTP-null mice, which would link insulin secretion, rather than hepatic insulin resistance to increased gluconeogenesis in GSTP-null mice. The effect of injection of a gluconeogenic substrate on the hormonal response was determined in GSTP-null mice. Plasma insulin concentrations were measured from blood samples collected before and after pyruvate bolus at precise time points (20 and 60 min respectively) based on literature reports of PSIS studies in mice. GSTP-null mice did not display altered plasma insulin and C-peptide levels in the plasma sample taken 20 min after the pyruvate load (Fig. 27C-D); however, compared with WT mice, GSTP-null mice exhibited significantly decreased plasma insulin levels at 60 min after the pyruvate bolus (Fig. 27C-D). Similar to GSIS, the C-peptide/insulin ratio was

unaltered in GSTP-null mice compared with WT mice (Fig. 27F). These data suggest that decreased insulin secretion could account for the increased gluconeogenesis (by PTT) of the GSTP-null mice.

FIG. 27. Glucose and pyruvate-stimulated insulin and C-peptide secretion in WT and GSTP-null mice.

For detailed experimental design, see Fig. 3. **(A)** Plasma insulin and **(E)** C-peptide values are shown for plasma samples collected at 20 and 30 min post glucose injection. **(D)** Plasma insulin and **(E)** C-peptide values are shown for plasma samples collected at 20 and 60 min post pyruvate injection. **(C)** C-peptide to insulin ratio in plasma samples collected at 30 min post glucose injection; **(F)** C-peptide to insulin ratio in plasma samples collected at 60 min post pyruvate injection; Values are means \pm SEM, n=10-12 animals per group, *P< 0.05, WT vs. GSTP-null by Student's t-test or by Mann-Whitney U-test where appropriate. WT, open bars; GSTP-null, filled bars.

Figure 27. Glucose and pyruvate-stimulated insulin secretion in GSTP-null mice



Hepatic gluconeogenesis and inflammation.

Because hepatic glucose output is a function of gluconeogenesis and the abundance of its rate limiting enzymes, phosphoenolpyruvate carboxykinase (PEPCK) and glucose-6-phosphatase (G6Pase) [153], we examined hepatic mRNA levels of *Pepck* and *G6pc*. Surprisingly, we found no differences in hepatic mRNA levels of *Pepck* and *G6pc* between 6 h fasted GSTP-null and WT mice (Fig. 28A). Because activated JNK is linked with inflammatory signaling, hepatic inflammatory genes were measured. Hepatic mRNA levels of *Mip-1alpha* (~6 fold) but not of *Il-6*, *Mcp-1* and *Il-1beta* were significantly greater in GSTP-null compared with WT mice (Fig. 28B). Significant relationships between hepatic gluconeogenesis and inflammation markers were revealed in GSTP-null but not in WT mice using Spearman's rank correlation (Fig. 28D-E). For example, the following pairs of gene mRNAs were highly correlated: 1) *Mcp1* and *Pepck* ($p=0.05$); 2) *Mcp-1* and *Il-1beta* ($p=0.00$); and, 3) *Il-1beta* and *Pepck* ($p=0.02$) (Table 3). Although the signaling relationship between activated JNK, gluconeogenesis and cytokines in the liver is complicated, these data likely support a coordinating role of JNK in the glucose intolerance of GSTP-null mice.

FIG. 28. Gluconeogenic and inflammatory mRNA markers in WT and GSTP-null mice.

(A) Hepatic gluconeogenic markers; and inflammatory markers mRNA expression in (B) liver and (C) epididymal adipose tissue (normalized to Rppo) of NC-fed WT and GSTP-null mice; (D, E) Spearman's correlation analyses between hepatic inflammatory and gluconeogenic markers in NC-fed WT and GSTP-null mice are shown. Colors of spheres represent strength of correlation, with brown representing a positive association and blue representing a negative association. In each case, dark colors show a high degree of association. Values are means \pm SEM ($n=6-8$ animals per group). * $P < 0.05$, WT vs. GSTP-null by Mann-Whitney U-test. WT, open bars; GSTP-null, filled bars.

Figure 28. Gluconeogenic and inflammatory markers in GSTP-null mice

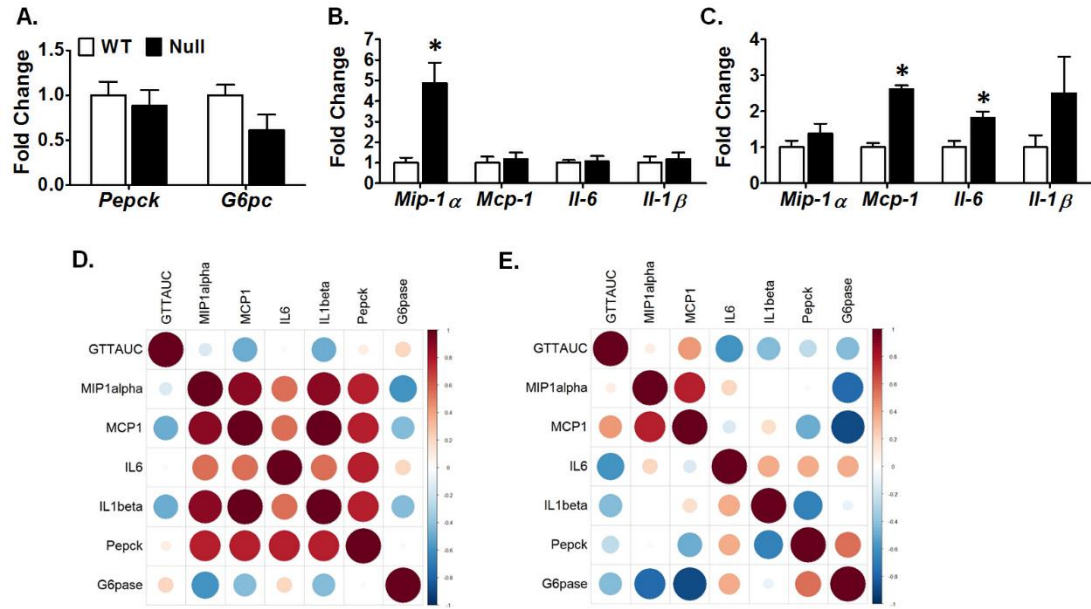


Table 3. Spearman's correlation co-efficients of gluconeogenic and inflammatory markers in GSTP-null mice

Spearman's Rank Correlation Coefficients of hepatic gluconeogenic and inflammatory marker mRNAs in WT and GSTP-null mice fed normal chow diet.

Inflammatory markers	Gluconeogenic markers					
	<i>G6pc</i>			<i>Pepck</i>		
	r		P	r		P
	WT	Null		WT	Null	
<i>Mcp-1</i>	-0.429	-0.886	N.S.	0.771	-0.486	<0.05
<i>Mip-1alpha</i>	-0.6	-0.771	N.S.	0.771	-0.029	N.S.
<i>Il-1beta</i>	-0.429	-0.087	N.S.	0.771	-0.667	<0.05
<i>Il-6</i>	0.2	0.371	N.S.	0.771	0.371	N.S.

JNK and hepatic gluconeogenesis.

Thus, to test the hypothesis that activated JNK was promoting glucose intolerance (via increased gluconeogenesis) in GSTP-null mice, we inhibited JNK phosphorylation *in vivo* using SP600125, a competitive inhibitor of ATP-binding site in JNK. Following 7 consecutive days of treatment, JNK inhibitor had no effect on fasting blood glucose and body weight indicating no untoward toxicity (Fig. 29A and $t = 0$ of Fig. 17B). Compared with vehicle, SP600125 suppressed glucose production from pyruvate in GSTP-null mice (PTT; Fig. 29B-E). The PTT AUC was reduced by $45 \pm 7\%$ ($p < 0.05$, $n = 11$; Fig. 29E) in SP600125-treated mice compared with vehicle-treated littermate controls. This percentage decrease was calculated taking into account the GSTP-attributable effect on PTTAUC, as known from previous PTT experiments in WT and GSTP-null mice. To test what hepatic targets were altered by JNK inhibition, we re-assessed hepatic mRNA levels and their inter-relationships using Spearman's Rank Correlation Coefficients. Surprisingly, we found no differences between hepatic mRNA levels (including for *Mip-1alpha*) between JNK inhibitor and saline-treated mice (Fig. 30A-B), however, the SP600125 treatment significantly altered the correlations between hepatic *Mcp-1* and *G6pc* mRNAs and *Mcp-1* and *Pepck* mRNAs (Fig. 30C-D; Table 4) indicating that JNK activation was coordinating the basal levels of these mRNAs in GSTP-null mice. These data support the contention that JNK activation is, at least in part, responsible for the increased hepatic gluconeogenesis (perhaps via regulation of inflammatory and gluconeogenic genes) in GSTP-null mice

FIG. 29. Increased gluconeogenesis was reversed by JNK inhibitor in GSTP-null mice.

Pyruvate tolerance test (PTT) measurements are shown for vehicle and JNK inhibitor (JNKI; i.p. 5 mg/kg, 7 days, once daily)-treated GSTP-null mice ($n=11$ per group). For experimental design of inhibitor study, see Fig. 3, Chapter II. **(A)** Body weights of mice are shown for the 7 consecutive days of injection. **(B)** Blood glucose levels were measured before and after pyruvate bolus (2 mg/g lean mass, i.p.). **(C)** Delta 30 min blood glucose values relative to baseline for vehicle and JNKI-treated GSTP-null mice (also referred to as the “*glucose appearance rate*”). **(D)** Blood glucose values at 120 min of PTT expressed as percent of baseline values for each treatment group. **(E)** PTT area under the curve (AUC) values. Values are mean \pm SEM. * $P < 0.05$, Vehicle vs JNKI by Mann-Whitney U-test. Vehicle, open symbols; JNKI, filled symbols or grey bars.

Figure 29. Effect of JNK inhibitor on hepatic gluconeogenesis by PTT in GSTP-null mice

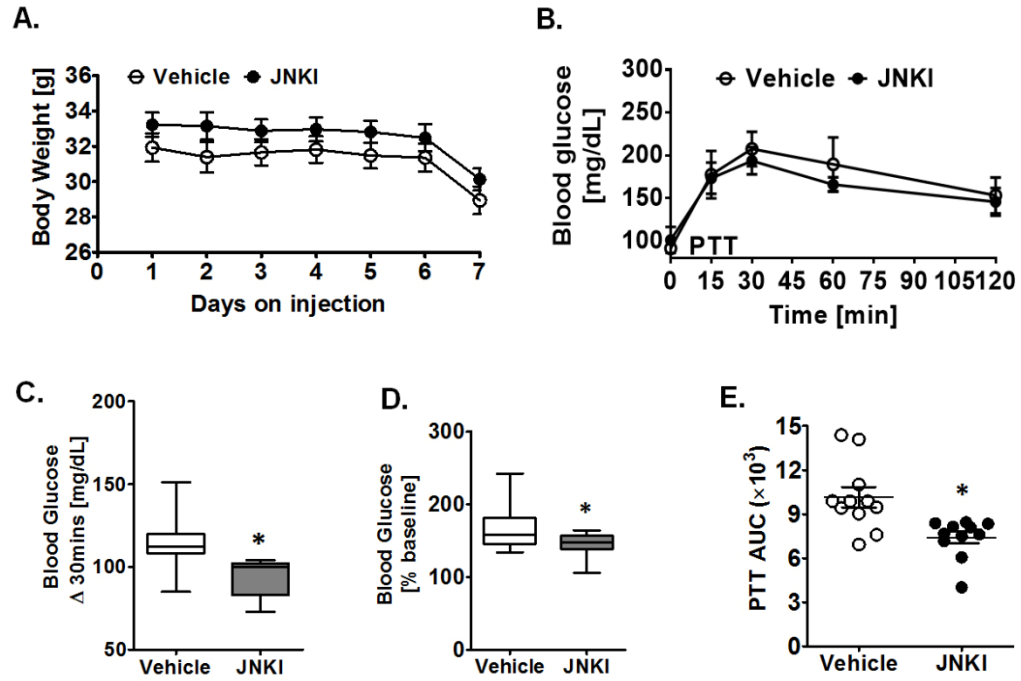


Fig. 30. Hepatic gluconeogenic and inflammatory mRNA markers in GSTP-null mice treated with vehicle or JNK inhibitor.

(A) Hepatic gluconeogenic markers and **(B)** inflammatory markers mRNA expression (normalized to Rppo) in vehicle or JNK inhibitor (JNKI, SP600125, 5 mg/day/kg body weight, 7 days)-treated GSTP-null mice; **(C, D)** Spearman's correlation analyses between hepatic inflammatory and gluconeogenic markers are shown. Colors of spheres represent strength of correlation, with brown representing a positive association and blue representing a negative association. In each case, dark colors show a high degree of association. Values are means \pm SEM ($n=6-8$ animals per group). * $P < 0.05$, Vehicle vs. JNKI by Mann-Whitney U-test. Vehicle, open bars; JNKI, filled bars.

Figure 30. Effect of JNK inhibitor on gluconeogenic and inflammatory markers in GSTP-null mice

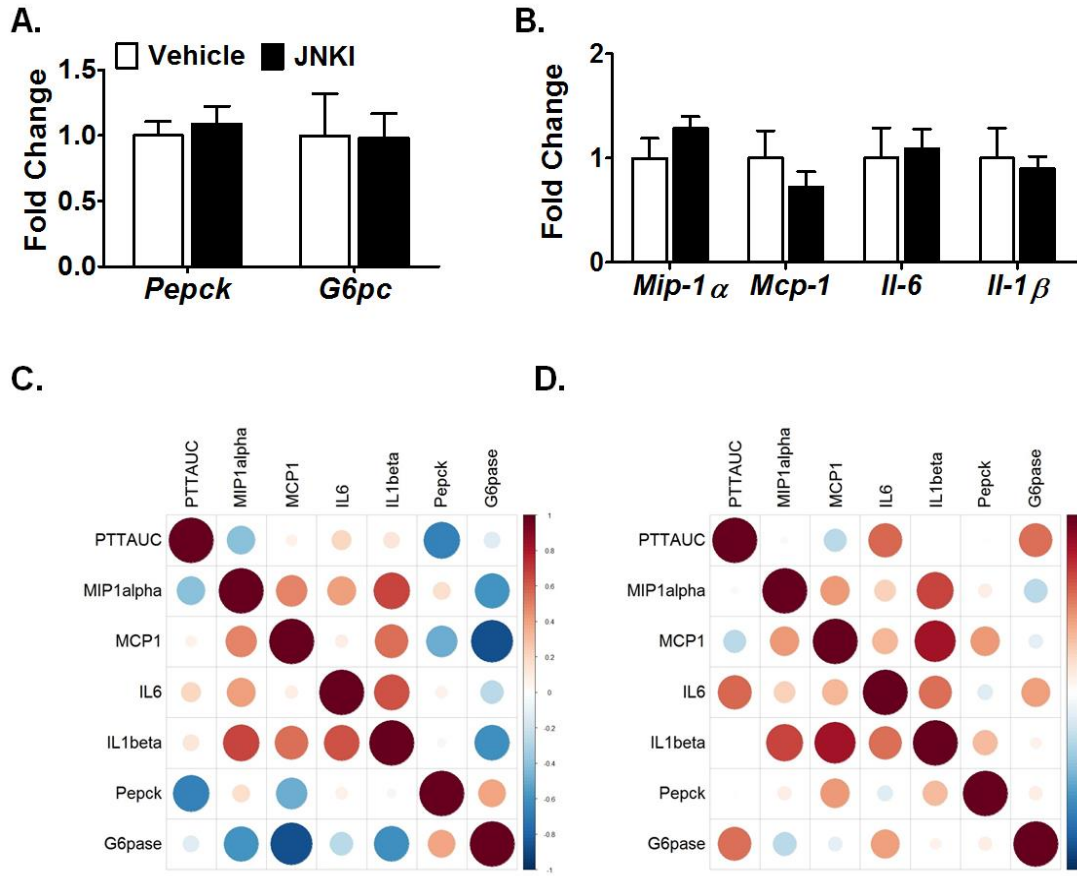


Table 4. Effect of JNK inhibitor on Spearman's correlation co-efficients of gluconeogenic and inflammatory markers in GSTP-null mice

Spearman's Rank Correlation Coefficients of hepatic gluconeogenic and inflammatory marker mRNAs in GSTP-null mice fed normal chow diet and treated for 7 days with either vehicle or JNK inhibitor (JNKI).

Inflammatory markers	Gluconeogenic markers					
	<i>G6pc</i>			<i>Pepck</i>		
	r		P	r		P
	Vehicle	JNKI		Vehicle	JNKI	
<i>Mcp-1</i>	-0.867	-0.105	<0.05	-0.491	0.42	<0.05
<i>Mip-1alpha</i>	-0.6	-0.280	N.S.	0.164	0.098	N.S.
<i>Il-1beta</i>	-0.612	0.063	N.S.	-0.042	0.308	N.S.
<i>Il-6</i>	-0.273	0.413	N.S.	0.079	-0.126	N.S.

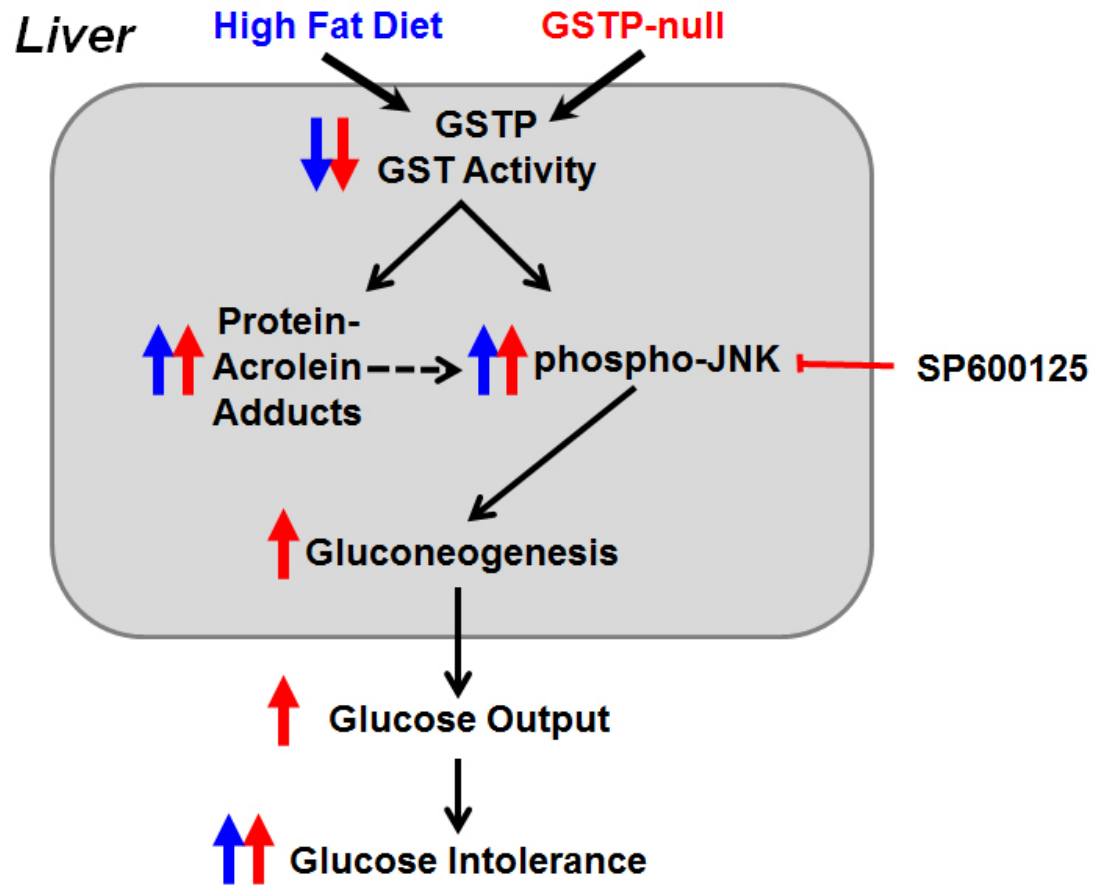
DISCUSSION

It is appreciated that both β -cell dysfunction and insulin resistance are early and necessary events in the development and progression of glucose intolerance to type 2 diabetes [154]. The novel finding of this study is the role of hepatic GSTP in glucose homeostasis via its effect on hepatic gluconeogenesis and insulin secretion. GSTP-null mice fed normal chow diet were glucose intolerant. Furthermore, glucose intolerance in GSTP-null mice is unchanged by HFD feeding and appears to be a function of JNK activity. We confirmed the role of JNK (i.e., reversed by SP600125, a JNK inhibitor) in glucose intolerance, and that JNK-dependent glucose output results from increased hepatic gluconeogenesis. Collectively, we conclude that downregulation of hepatic GSTP (whether by HFD or genetic manipulation or gene polymorphism) selectively increases JNK activation that, in turn, alters hepatic signaling to promote gluconeogenesis and intolerance (see Schematic, Fig. 19). The GSTP-null genotype thus recapitulates the early deleterious events leading from diet-induced obesity to diabetes.

FIG. 31. . Schematic showing how high fat diet or GSTP-null genotype affects glucose intolerance via liver-specific JNK activation in mice.

Effects of high fat (HF) diet in wild-type (WT) are shown with blue arrows. Effects of the GSTP-deficient genotype (GSTP-null) occurring independently of obesity are shown with red arrows. HF diet results in glucose intolerance in WT mice, typical of this commonly utilized model of diet-induced obesity [127]. In the liver, HF feeding decreases GSTP protein and total GST activity concomitant with increased protein-acrolein adduct and phospho-JNK abundance, in agreement with the known functions of GSTP [36, 102]. Hepatic phospho-p54 JNK positively correlates with glucose intolerance in HF-fed mice. Because GSTP is an *in vivo* JNK inhibitor [107], decreased hepatic GSTP could augment JNK activation following early diet-induced obesity. Consistent with this, GSTP-null genotype elicits similar metabolic derangements. GSTP-null mice exhibit positively correlated glucose and pyruvate-intolerance on normal chow diet, suggesting that increased hepatic glucose contributes to glucose intolerance. Livers of GSTP-null mice show increased protein-acrolein adduct and phospho-JNK abundance, thereby recapitulating the HF-induced sequelae in WT mice. Treatment with JNK inhibitor, SP600125, alleviates hepatic glucose output in GSTP-null mice, thus illustrating a novel role for GSTP in glucose tolerance via JNK regulation.

Figure 31. Scheme illustrating the summary of project findings



In the current study, we provide evidence that hepatic JNK activation contributes to the early derangements in glucose control. First, we show that phospho-JNK abundance (p54 but not p46) is selectively increased in the livers of GSTP-null mice on normal chow, like was observed in obese WT livers. Second, increased hepatic glucose output was associated with a pyruvate bolus in GSTP-null on normal chow diet. Third, the JNK inhibitor, SP600125, significantly corrected glucose intolerance associated with a pyruvate bolus. This experiment shows that JNK activation augments hepatic gluconeogenesis (i.e., pyruvate fuels reverse glycolysis in liver [155]) and that this can occur in the absence of HFD, obesity or a genetic model of obesity and IR (e.g., *db/db* mice). Thus, the absence of GSTP is sufficient to promote JNK activation [107], and hepatic gluconeogenesis, a known mediator of enhanced glycemia in T2D [156]. Although augmented JNK activation in peripheral tissues is known to mediate glucose intolerance and IR [139], these models do not address the earliest events that precede established systemic insulin resistance. In fact, our study shows that insulin signaling is intact and robust in liver, skeletal muscle and adipose of GSTP-null mice *despite hepatic JNK activation* showing that increased hepatic glucose output precedes hepatic insulin resistance *per se*. Although we used whole body GSTP-null mice, these mice are identical to WT mice in body composition, metabolism, activity, fasting blood glucose and insulin and food and water intake (see Fig. 4 and Table 1) indicating a selective effect of GSTP-deletion on hepatic glucose output likely important in glucose excursions after feeding. Moreover, despite using whole body GSTP-deficient mice, we

observed a continuum of glucose intolerance (see Fig. 4E) that likely reflects a currently unidentified stress factor in these mice.

A potential factor known to induce JNK activation is the accumulation of aldehyde-modified proteins (carbonylated proteins), and protein-aldehyde adducts are considered determinants of inflammation and IR [30, 46]. Because GSTP activity selectively conjugates GSH with acrolein [52], we measured and found increases in protein-acrolein adducts in liver (but not in skeletal muscle nor in adipose) of both short-term HFD-fed WT and NC-fed GSTP-null mice compared with NC-fed WT mice. Although acrolein-modified and unfolded proteins can trigger ER stress and the unfolded protein response (UPR) that can initiate JNK activation [98], we did not find obvious evidence of ER stress-induced UPR in GSTP-null mice. Interestingly, a general pattern of protein-acrolein adducts (5 prominent M_r bands: 125, 90, 77, 75, 27 kDa) appears in both HFD-fed WT and GSTP-null mice and some of these bands are significantly increased although not the same ones in both models. While the role of these adducts in JNK activation is unclear, the accumulation of these adducts reflects diminished acrolein detoxification capacity that is consistent with the decreased overall GSTP abundance and GST activity (using CDNB as substrate), which is surprisingly similar (approx. 25% loss) in livers of both HFD-fed WT and GSTP-null mice. The prospect of protein-acrolein adducts as perpetrators of hepatic JNK activation and glucose intolerance remains to be investigated.

Hepatic JNK activation has been shown to play a pivotal role in causing IR and glucose intolerance in diabetic animal models [126]. Although we did not

definitely reveal a single mechanism how JNK (or if it was JNK1 or JNK2) augments hepatic gluconeogenesis, we did reveal potential relationships between rate limiting gluconeogenic enzymes and inflammatory mediators using Spearman's Rank Correlation Coefficient analyses in glucose intolerant GSTP-null mice. Supporting this approach, cytokines, IL-1 β and IL-10, exert influence over hepatocyte PEPCK mRNA, protein and enzyme activity demonstrating an interaction between Kupffer cells and hepatocyte gluconeogenesis [157]. Similarly, hepatic and circulating chemokines such as MIP-1 α and MCP-1 are potential candidates linking obesity with IR [158, 159] in humans and mice. In our present study, JNK inhibitor significantly disrupted the relationship between hepatic *Mcp-1* and *G6pc* mRNAs and *Mcp-1* and *Pepck* mRNAs. We did not see a change in *Mip-1alpha* mRNA after SP600125, which suggests that MIP-1 α lies upstream of JNK rather than as a consequence of JNK activity. Further analyses of specific signaling (e.g., cell type, JNK isoform) events and targets of JNK (independent of insulin signaling) are required to define the complicated role of activated JNK in regulation of hepatic gluconeogenesis as an early event in diet-induced glucose intolerance.

In summary, these are the first studies to demonstrate that deletion of the murine *Gstp1/2* genes results in glucose intolerance, decreased insulin release and increased hepatic glucose production independently of obesity. These findings in a mouse model of GSTP-deficiency recapitulate the early deleterious events observed following HFD feeding in WT mice. Glucose intolerance in GSTP-null mice is manifest in the absence of defects in insulin signaling in major

glucose disposal organs – skeletal muscle, adipose and liver and may be ascribed, at least in part, to an inability to raise plasma insulin levels in response to hyperglycemia. JNK appears to orchestrate relationships between hepatic cytokine and rate-limiting gluconeogenic enzymes that predispose the liver of GSTP-null mice to increase glucose output. These data predict that variation(s) in GSTP abundance or function may modulate diabetes susceptibility and/or severity in human populations and merits future investigation.

CHAPTER V

CONCLUSIONS AND FUTURE DIRECTIONS

This project was designed to achieve new understanding of how the glutathione-S-transferase pi isozyme (GSTP) contributes to glucose homeostasis. In Chapter I, we put forth the ***hypothesis that GSTP is downregulated in obesity and diabetes and is a key modulator of glucose tolerance via its role (s) in aldehyde metabolism and JNK regulation (Figure 1)***. We used two different animal models to address the hypothesis. First, the effect of obesity on GSTP was assessed by high-fat diet (HFD) feeding in C57BL/6J mice (Chapter III), as it remains the most well accepted model for studying impaired glucose tolerance and early type 2 diabetes [127]. Second, the *in vivo* effect of GSTP deficiency on glucose homeostasis was investigated by using whole-body GSTP-deficient (GSTP-null) mice (Chapter IV). Through the work in this thesis, we have 1) elucidated the effect of diet-induced obesity on GSTP expression and function in insulin-responsive tissues as it relates to the development of glucose intolerance and insulin resistance, 2) identified a glucose intolerance phenotype in GSTP-null mice, 3) uncovered a potentially novel pathway of hepatic gluconeogenesis that likely operates via JNK activation and inflammation in GSTP-null mice and 4) illustrated that glucose-stimulated insulin secretion is decreased in GSTP-null mice. We propose that hepatic GSTP

contributes to glucose homeostasis in mammals by modulating hepatic glucose production; reduced hepatic expression of GSTP might be a critical instigator of hyperglycemia in type 2 diabetes, thus adding a new player to our evolving understanding of this physiology.

We assessed the impact of HFD feeding on GSTP abundance, protein-acrolein adducts and JNK phosphorylation in insulin-sensitive tissues. As discussed in Chapter III, HFD induced significant weight gain and adiposity as early as 3.5 weeks. Glucose tolerance test showed marked glucose intolerance in HF-fed animals. Systemic metabolic parameters were significantly altered by HF feeding as expected. HF feeding induced marked elevations in fasting plasma insulin and HOMA-IR and HOMA- β indices, consistent with obesity-induced insulin resistance. In examining the relationship between these early metabolic derangements and GSTs, abundance of GSTP was greatly diminished selectively in the livers of diet-induced and genetic mouse models of glucose intolerance and insulin resistance. Such tissue-specific dysregulation has been documented for other GST isozymes in human and animal studies of obesity, diabetes and NAFLD [45, 135]. As functional indices of decreased GSTP abundance, hepatic protein-acrolein adducts and phospho-JNK abundance (p54 but not p46) were significantly elevated in obese mice. Collectively, we conclude that downregulation of hepatic GSTP selectively increases JNK activation and induces deficits in aldehyde detoxification that, in turn affects pathways of glucose storage and/or production to promote glucose intolerance. Dietary nutrients or phytochemicals have been reported to restore GSTP protein

expression and have been studied in cancer. For instance, phytoestrogens, phenethyl isothiocyanate, a phytochemical found in large amounts in cruciferous vegetables, green tea polyphenols and lycopene have been studied. It is interesting to postulate that using such compounds to restore hepatic GSTP levels and functionality in obesity may have beneficial effects on glucose handling in mouse models. Furthermore, *in vitro* and *in vivo* studies are needed to understand the mechanisms that underlie GSTP downregulation following HFD feeding. Multiple mechanisms are plausible as outlined in Chapter I (such as transcriptional, hormonal, epigenetics, microRNA).

To delineate the role of GSTP in glucose metabolism, we used GSTP-null mice. Compared with WT mice, GSTP-null mice are identical in body composition; metabolism, fasting glycemia and insulin and food and water intake (see Fig. 14 and Table 2). However, GSTP-null mice were glucose and pyruvate intolerant on normal chow (NC) diet, indicating a selective effect of GSTP-deletion on hepatic glucose output likely important in glucose excursions after feeding. Furthermore, GSTP-null mice exhibited decreased glucose-stimulated insulin secretion at an early time point of 20 min post glucose injection. JNK activation, which is known to impair both insulin signaling and insulin secretion in diabetes, was an important physiological correlate of glucose intolerance in both WT-HFD and in GSTP-null mice. First, we showed that phospho-JNK abundance was selectively increased in the livers of GSTP-null mice on normal chow, similar to that observed in obese WT livers. Second, treatment with JNK inhibitor,

SP600125, significantly attenuated hepatic glucose output in GSTP-null mice confirming the role of JNK in GSTP-mediated glucose regulation.

A global gene knockout approach, as embodied by GSTP-null mice, allows us to test GSTP requirement but not GSTP sufficiency while also not identifying the tissue that contributes to the phenotype. Future studies of adenoviral vector-mediated liver-specific GSTP re-expression in GSTP-knockout mice that improves the glucose intolerance phenotype would further corroborate our current results.

We found increases in hepatic protein-acrolein adduct in both short-term HFD-fed WT and NC-fed GSTP-null mice compared with NC-fed WT mice. The accumulation of acrolein adducts indicate deficits in acrolein detoxification capacity that was consistent with the observations of decreased overall GST activity in livers of both HFD-fed WT and GSTP-null mice. Measurement of free acrolein in tissues remains a tricky endeavor, due to acrolein being highly volatile and reactive. Accurate detection and quantification of endogenous acrolein relies on complicated methods using carbonyl derivatizing reagents [61]. Additional studies are needed to quantify HFD-induced acrolein generation in rodent livers. Acrolein-modified proteins can trigger ER stress and the unfolded protein response (UPR) that can initiate JNK activation (10). As indicators of ER-stress we measured *Xbp-1* splicing, *Herp* and *Grp78* mRNA and found that they were no different in the WT and GSTP-null livers. Future studies are warranted to elucidate a potential direct relationship between protein-acrolein adducts and JNK activation.

Hepatic JNK activation has been shown to play a causal role in IR and glucose intolerance in diabetic animal models [126]. Our study shows that insulin signaling is intact and robust in peripheral tissues of GSTP-null mice *despite hepatic JNK activation* suggesting that increased gluconeogenesis is independent of hepatic IR in the GSTP-null model of glucose intolerance. Although JNK inhibitor data revealed potential relationships between rate limiting gluconeogenic enzymes and inflammatory mediators using Spearman's Rank Correlation Coefficient analyses, further studies are essential to define the mechanism how JNK (and JNK1 or JNK2) augments hepatic gluconeogenesis in GSTP-deficient mice. To identify potential factors that regulate gluconeogenesis in GSTP-null livers, and to determine the site and mechanism of their actions as well as substrate utilization and flux through the pathway, future studies could utilize isolated perfused liver preparations that would provide a milieu similar to that in vivo while retaining the advantages of a system operating in vitro.

In the present study, we assessed and found no differences in mRNA for *Pepck* and *G6pc*. Increased hepatic gluconeogenesis is often ascribed to transcriptional regulation of *Pepck* and *G6pc* [160] [161] [162] [163]. Yet, it has been demonstrated that the control they exert over gluconeogenic flux is relatively weak [164-167]. It has recently been reported that hepatic expression of *Pepck* and *G6pc* mRNA was not related to fasting hyperglycemia in humans and in rodent models of T2D [168]. The authors revealed a strong association between pyruvate carboxylase protein expression and glycemia in humans [169]. Pyruvate carboxylase is allosterically activated by acetyl-CoA [170].

Enhanced expression of pyruvate carboxylase has been reported in rodent models of type 1 diabetes [171, 172] and in obese Zucker Diabetic Fatty (ZDF) rats [173]. Thus, future studies could examine effects of GSTP deletion on such additional regulatory mechanisms of the gluconeogenic pathway.

Although a PTT can be useful in cases of severe alterations in hepatic gluconeogenesis, it is highly dependent on the variables that influence the outcome of a GTT, including glucose-stimulated insulin secretion (GSIS) and insulin sensitivity. It is thus important to analyze results from a PTT in light of data obtained from GSIS and ITT. Metabolic tests such as GTT and PTT mimic the conditions of a physiological meal intake. From our current study, glucose intolerance in GSTP-null mice cannot be attributed solely to increased gluconeogenesis in vivo due to the observed defect in insulin secretion. Our finding of the decreased glucose-stimulated insulin levels adds a layer of complexity to the glucose metabolic phenotype and reinforces that the biologic function of GSTP in pancreatopathy and insulin secretion needs to be investigated further. In this regard, ex vivo studies of GSIS with isolated pancreatic islets are warranted. It is not known whether HFD decreases pancreatic GSTP function in WT mice or if GSTP deletion activates JNK in the pancreas. Pancreatic JNK activation could explain the decreased GSIS in GSTP-null mice to contribute to the overall systemic phenotype. Ex vivo studies could test whether JNK inhibitor improves decreased GSIS in GSTP-null mice.

Through this work, we have delineated a direct involvement of GSTP in hepatic glucose output and GSIS in mice; future genome-wide association

studies in diverse population groups may reveal whether GSTP is indeed a type 2 diabetes candidate gene to further corroborate our present animal studies.

In summary, this thesis continues the research efforts of our group to elucidate the link between detoxification mechanisms (GSTP), aldehydes and metabolic disease. Our general goal envisions identifying novel factors that govern interindividual susceptibility to obesity and diabetes. T2D is characterized by defects in both insulin sensitivity and insulin secretion that result in glucose intolerance, increased gluconeogenesis and hyperglycemia with severe consequences [154]. The genetic and environmental factors that promote inappropriate homeostatic control in diabetes remain inadequately understood. Given its role in cellular detoxification and stress kinase regulation, the redox sensor GSTP is unquestionably capable of influencing glucose homeostasis, probably through acrolein generation and adduction of critical proteins, but perhaps more importantly through JNK activation. This project adds to our knowledge of the possible pathways by which GSTP may affect glucose regulation. GSTP is highly polymorphic in humans. Further investments in understanding diet-induced GST dysregulation in human obesity, NAFLD and diabetes could have potentially important consequences for addressing inter-individual variation to disease susceptibility.

REFERENCES

1. Finucane, M.M., et al., *National, regional, and global trends in body-mass index since 1980: systematic analysis of health examination surveys and epidemiological studies with 960 country-years and 9.1 million participants*. Lancet, 2011. **377**(9765): p. 557-67.
2. Browning, J.D., et al., *Prevalence of hepatic steatosis in an urban population in the United States: impact of ethnicity*. Hepatology, 2004. **40**(6): p. 1387-95.
3. Smits, M.M., et al., *Non-alcoholic fatty liver disease as an independent manifestation of the metabolic syndrome: results of a US national survey in three ethnic groups*. J Gastroenterol Hepatol, 2013. **28**(4): p. 664-70.
4. Rathmann, W. and G. Giani, *Global prevalence of diabetes: estimates for the year 2000 and projections for 2030*. Diabetes Care, 2004. **27**(10): p. 2568-9; author reply 2569.
5. Ogden, C.L., et al., *Prevalence of Obesity Among Adults and Youth: United States, 2011-2014*. NCHS Data Brief, 2015(219): p. 1-8.
6. Hotamisligil, G.S., *Inflammation and metabolic disorders*. Nature, 2006. **444**(7121): p. 860-7.
7. Tolman, K.G., et al., *Spectrum of liver disease in type 2 diabetes and management of patients with diabetes and liver disease*. Diabetes Care, 2007. **30**(3): p. 734-43.
8. Hui, J.M., et al., *Long-term outcomes of cirrhosis in nonalcoholic steatohepatitis compared with hepatitis C*. Hepatology, 2003. **38**(2): p. 420-7.
9. Ratziu, V., et al., *A position statement on NAFLD/NASH based on the EASL 2009 special conference*. J Hepatol, 2010. **53**(2): p. 372-84.
10. Chan, J.C., et al., *Diabetes in Asia: epidemiology, risk factors, and pathophysiology*. Jama, 2009. **301**(20): p. 2129-40.
11. Amarapurkar, D.N., et al., *How common is non-alcoholic fatty liver disease in the Asia-Pacific region and are there local differences?* J Gastroenterol Hepatol, 2007. **22**(6): p. 788-93.

12. Nanditha, A., et al., *Diabetes in Asia and the Pacific: Implications for the Global Epidemic*. *Diabetes Care*, 2016. **39**(3): p. 472-85.
13. Ramachandran, A., R.C. Ma, and C. Snehalatha, *Diabetes in Asia*. *Lancet*, 2010. **375**(9712): p. 408-18.
14. Zimmet, P.Z., et al., *Diabetes: a 21st century challenge*. *Lancet Diabetes Endocrinol*, 2014. **2**(1): p. 56-64.
15. Gluckman, P.D., et al., *Effect of in utero and early-life conditions on adult health and disease*. *N Engl J Med*, 2008. **359**(1): p. 61-73.
16. Sherwin, R.S., et al., *Prevention or delay of type 2 diabetes*. *Diabetes Care*, 2004. **27 Suppl 1**: p. S47-54.
17. Chan, J.C., et al., *Diabetes in the Western Pacific Region--past, present and future*. *Diabetes Res Clin Pract*, 2014. **103**(2): p. 244-55.
18. Gauthier, M.S. and N.B. Ruderman, *Adipose tissue inflammation and insulin resistance: all obese humans are not created equal*. *Biochem J*, 2010. **430**(2): p. e1-4.
19. Wildman, R.P., et al., *The obese without cardiometabolic risk factor clustering and the normal weight with cardiometabolic risk factor clustering: prevalence and correlates of 2 phenotypes among the US population (NHANES 1999-2004)*. *Arch Intern Med*, 2008. **168**(15): p. 1617-24.
20. Petersen, K.F., et al., *Increased prevalence of insulin resistance and nonalcoholic fatty liver disease in Asian-Indian men*. *Proc Natl Acad Sci U S A*, 2006. **103**(48): p. 18273-7.
21. Das, K., et al., *Nonobese population in a developing country has a high prevalence of nonalcoholic fatty liver and significant liver disease*. *Hepatology*, 2010. **51**(5): p. 1593-602.
22. *Classification and diagnosis of diabetes mellitus and other categories of glucose intolerance*. *National Diabetes Data Group*. *Diabetes*, 1979. **28**(12): p. 1039-57.
23. Ito, C., K. Mito, and H. Hara, *Review of criteria for diagnosis of diabetes mellitus based on results of follow-up study*. *Diabetes*, 1983. **32**(4): p. 343-51.
24. Gregor, M.F. and G.S. Hotamisligil, *Inflammatory mechanisms in obesity*. *Annu Rev Immunol*, 2011. **29**: p. 415-45.

25. Houstis, N., E.D. Rosen, and E.S. Lander, *Reactive oxygen species have a causal role in multiple forms of insulin resistance*. *Nature*, 2006. **440**(7086): p. 944-8.
26. Uchida, K., *4-Hydroxy-2-nonenal: a product and mediator of oxidative stress*. *Prog Lipid Res*, 2003. **42**(4): p. 318-43.
27. Miyake, H., A. Kadoya, and T. Ohyashiki, *Increase in molecular rigidity of the protein conformation of brain Na⁺-K⁺-ATPase by modification with 4-hydroxy-2-nonenal*. *Biol Pharm Bull*, 2003. **26**(12): p. 1652-6.
28. Carbone, D.L., J.A. Doorn, and D.R. Petersen, *4-Hydroxynonenal regulates 26S proteasomal degradation of alcohol dehydrogenase*. *Free Radic Biol Med*, 2004. **37**(9): p. 1430-9.
29. Medina-Navarro, R., et al., *Formation of an adduct between insulin and the toxic lipoperoxidation product acrolein decreases both the hypoglycemic effect of the hormone in rat and glucose uptake in 3T3 adipocytes*. *Chem Res Toxicol*, 2007. **20**(10): p. 1477-81.
30. Grimsrud, P.A., et al., *Carbonylation of adipose proteins in obesity and insulin resistance: identification of adipocyte fatty acid-binding protein as a cellular target of 4-hydroxynonenal*. *Mol Cell Proteomics*, 2007. **6**(4): p. 624-37.
31. Uzun, H., et al., *Plasma protein carbonyl and thiol stress before and after laparoscopic gastric banding in morbidly obese patients*. *Obes Surg*, 2007. **17**(10): p. 1367-73.
32. Sledzinski, T., et al., *Decrease in serum protein carbonyl groups concentration and maintained hyperhomocysteinemia in patients undergoing bariatric surgery*. *Obes Surg*, 2009. **19**(3): p. 321-6.
33. Codoner-Franch, P., et al., *Oxidative markers in children with severe obesity following low-calorie diets supplemented with mandarin juice*. *Acta Paediatr*, 2010. **99**(12): p. 1841-6.
34. Itoh, K., et al., *An Nrf2/small Maf heterodimer mediates the induction of phase II detoxifying enzyme genes through antioxidant response elements*. *Biochem Biophys Res Commun*, 1997. **236**(2): p. 313-22.
35. Nguyen, T., P. Nioi, and C.B. Pickett, *The Nrf2-antioxidant response element signaling pathway and its activation by oxidative stress*. *J Biol Chem*, 2009. **284**(20): p. 13291-5.
36. Hayes, J.D., J.U. Flanagan, and I.R. Jowsey, *Glutathione transferases*. *Annu Rev Pharmacol Toxicol*, 2005. **45**: p. 51-88.

37. Armstrong, R.N., *Structure, catalytic mechanism, and evolution of the glutathione transferases*. Chem Res Toxicol, 1997. **10**(1): p. 2-18.
38. Litwack, G., B. Ketterer, and I.M. Arias, *Ligandin: a hepatic protein which binds steroids, bilirubin, carcinogens and a number of exogenous organic anions*. Nature, 1971. **234**(5330): p. 466-7.
39. Dulhunty, A., et al., *The glutathione transferase structural family includes a nuclear chloride channel and a ryanodine receptor calcium release channel modulator*. J Biol Chem, 2001. **276**(5): p. 3319-23.
40. Merrell, M.D. and N.J. Cherrington, *Drug metabolism alterations in nonalcoholic fatty liver disease*. Drug Metab Rev, 2011. **43**(3): p. 317-34.
41. Rouer, E. and J.P. Leroux, *Liver microsomal cytochrome P-450 and related monooxygenase activities in genetically hyperglycemic (ob/ob and db/db) and lean streptozotocin-treated mice*. Biochem Pharmacol, 1980. **29**(13): p. 1959-62.
42. Agius, C. and A.S. Gidari, *Effect of streptozotocin on the glutathione S-transferases of mouse liver cytosol*. Biochem Pharmacol, 1985. **34**(6): p. 811-9.
43. Thomas, H., et al., *Effect of diabetes and starvation on the activity of rat liver epoxide hydrolases, glutathione S-transferases and peroxisomal beta-oxidation*. Biochem Pharmacol, 1989. **38**(23): p. 4291-7.
44. Kim, S.K., K.J. Woodcroft, and R.F. Novak, *Insulin and glucagon regulation of glutathione S-transferase expression in primary cultured rat hepatocytes*. J Pharmacol Exp Ther, 2003. **305**(1): p. 353-61.
45. Curtis, J.M., et al., *Downregulation of adipose glutathione S-transferase A4 leads to increased protein carbonylation, oxidative stress, and mitochondrial dysfunction*. Diabetes, 2010. **59**(5): p. 1132-42.
46. Frohnert, B.I., et al., *Increased adipose protein carbonylation in human obesity*. Obesity (Silver Spring), 2011. **19**(9): p. 1735-41.
47. Boden, G., et al., *Increase in endoplasmic reticulum stress-related proteins and genes in adipose tissue of obese, insulin-resistant individuals*. Diabetes, 2008. **57**(9): p. 2438-44.
48. Grant, R.W., et al., *Adipose tissue transcriptome changes during obesity development in female dogs*. Physiol Genomics, 2011. **43**(6): p. 295-307.
49. Kirpich, I.A., et al., *Integrated hepatic transcriptome and proteome analysis of mice with high-fat diet-induced nonalcoholic fatty liver disease*. J Nutr Biochem, 2011. **22**(1): p. 38-45.

50. Lopez, I.P., et al., *DNA microarray analysis of genes differentially expressed in diet-induced (cafeteria) obese rats*. *Obes Res*, 2003. **11**(2): p. 188-94.
51. Miller, R.S., et al., *Adipocyte gene expression is altered in formerly obese mice and as a function of diet composition*. *J Nutr*, 2008. **138**(6): p. 1033-8.
52. Berhane, K., et al., *Detoxication of base propenals and other alpha, beta-unsaturated aldehyde products of radical reactions and lipid peroxidation by human glutathione transferases*. *Proc Natl Acad Sci U S A*, 1994. **91**(4): p. 1480-4.
53. Tew, K.D., et al., *The role of glutathione S-transferase P in signaling pathways and S-glutathionylation in cancer*. *Free Radic Biol Med*, 2011. **51**(2): p. 299-313.
54. Hayes, P.C., et al., *Glutathione S-transferases in human liver cancer*. *Gut*, 1991. **32**(12): p. 1546-9.
55. Kitteringham, N.R., et al., *Protein expression profiling of glutathione S-transferase pi null mice as a strategy to identify potential markers of resistance to paracetamol-induced toxicity in the liver*. *Proteomics*, 2003. **3**(2): p. 191-207.
56. Henderson, C.J., et al., *Increased skin tumorigenesis in mice lacking pi class glutathione S-transferases*. *Proc Natl Acad Sci U S A*, 1998. **95**(9): p. 5275-80.
57. Henderson, C.J., et al., *Increased resistance to acetaminophen hepatotoxicity in mice lacking glutathione S-transferase Pi*. *Proc Natl Acad Sci U S A*, 2000. **97**(23): p. 12741-5.
58. Zhou, J., et al., *Glutathione transferase P1: an endogenous inhibitor of allergic responses in a mouse model of asthma*. *Am J Respir Crit Care Med*, 2008. **178**(12): p. 1202-10.
59. Conklin, D.J., et al., *Glutathione-S-transferase P protects against endothelial dysfunction induced by exposure to tobacco smoke*. *Am J Physiol Heart Circ Physiol*, 2009. **296**(5): p. H1586-97.
60. Conklin, D.J., et al., *Increased sensitivity of glutathione S-transferase P-null mice to cyclophosphamide-induced urinary bladder toxicity*. *J Pharmacol Exp Ther*, 2009. **331**(2): p. 456-69.
61. Conklin, D.J., et al., *Genetic Deficiency of Glutathione S-Transferase P Increases Myocardial Sensitivity to Ischemia-Reperfusion Injury*. *Circ Res*, 2015. **117**(5): p. 437-49.

62. Conklin, D.J., et al., *Glutathione S-transferase P protects against cyclophosphamide-induced cardiotoxicity in mice*. Toxicol Appl Pharmacol, 2015. **285**(2): p. 136-48.
63. Ma, Q., *Role of nrf2 in oxidative stress and toxicity*. Annu Rev Pharmacol Toxicol, 2013. **53**: p. 401-26.
64. Lo, H.W. and F. Ali-Osman, *Genetic polymorphism and function of glutathione S-transferases in tumor drug resistance*. Curr Opin Pharmacol, 2007. **7**(4): p. 367-74.
65. Xia, C., et al., *The organization of the human GSTP1-1 gene promoter and its response to retinoic acid and cellular redox status*. Biochem J, 1996. **313 (Pt 1)**: p. 155-61.
66. Zhang, R., et al., *Epigenetic alterations are involved in the overexpression of glutathione S-transferase pi-1 in human colorectal cancers*. Int J Oncol, 2014. **45**(3): p. 1275-83.
67. Patron, J.P., et al., *MiR-133b targets antiapoptotic genes and enhances death receptor-induced apoptosis*. PLoS One, 2012. **7**(4): p. e35345.
68. Zhang, X., et al., *miR-513a-3p sensitizes human lung adenocarcinoma cells to chemotherapy by targeting GSTP1*. Lung Cancer, 2012. **77**(3): p. 488-94.
69. Mutallip, M., et al., *Glutathione S-transferase P1 (GSTP1) suppresses cell apoptosis and its regulation by miR-133alpha in head and neck squamous cell carcinoma (HNSCC)*. Int J Mol Med, 2011. **27**(3): p. 345-52.
70. Uchida, Y., et al., *MiR-133a induces apoptosis through direct regulation of GSTP1 in bladder cancer cell lines*. Urol Oncol, 2013. **31**(1): p. 115-23.
71. Moriya, Y., et al., *Tumor suppressive microRNA-133a regulates novel molecular networks in lung squamous cell carcinoma*. J Hum Genet, 2012. **57**(1): p. 38-45.
72. Wang, Y., et al., *Autocrine production of interleukin-6 confers cisplatin and paclitaxel resistance in ovarian cancer cells*. Cancer Lett, 2010. **295**(1): p. 110-23.
73. Mizutani, Y., et al., *Sensitization of human renal cell carcinoma cells to cis-diamminedichloroplatinum(II) by anti-interleukin 6 monoclonal antibody or anti-interleukin 6 receptor monoclonal antibody*. Cancer Res, 1995. **55**(3): p. 590-6.

74. Perry, R.J., et al., *Hepatic acetyl CoA links adipose tissue inflammation to hepatic insulin resistance and type 2 diabetes*. Cell, 2015. **160**(4): p. 745-58.
75. Han, M.S., et al., *JNK expression by macrophages promotes obesity-induced insulin resistance and inflammation*. Science, 2013. **339**(6116): p. 218-22.
76. Board, P.G., G.C. Webb, and M. Coggan, *Isolation of a cDNA clone and localization of the human glutathione S-transferase 3 genes to chromosome bands 11q13 and 12q13-14*. Ann Hum Genet, 1989. **53**(Pt 3): p. 205-13.
77. Duggirala, R., et al., *Further evidence for a type 2 diabetes susceptibility locus on chromosome 11q*. Genet Epidemiol, 2003. **24**(3): p. 240-2.
78. Baier, L.J. and R.L. Hanson, *Genetic studies of the etiology of type 2 diabetes in Pima Indians: hunting for pieces to a complicated puzzle*. Diabetes, 2004. **53**(5): p. 1181-6.
79. Ji, X., et al., *Structure and function of the xenobiotic substrate-binding site and location of a potential non-substrate-binding site in a class pi glutathione S-transferase*. Biochemistry, 1997. **36**(32): p. 9690-702.
80. Pal, A., et al., *Catalytic efficiencies of allelic variants of human glutathione S-transferase Pi in the glutathione conjugation of alpha, beta-unsaturated aldehydes*. Cancer Lett, 2000. **154**(1): p. 39-43.
81. Thevenin, A.F., et al., *GST pi modulates JNK activity through a direct interaction with JNK substrate, ATF2*. Protein Sci, 2011. **20**(5): p. 834-48.
82. Godschalk, R.W., et al., *Impact of GSTM1 on aromatic-DNA adducts and p53 accumulation in human skin and lymphocytes*. Pharmacogenetics, 2001. **11**(6): p. 537-43.
83. Bid, H.K., et al., *Association of glutathione S-transferase (GSTM1, T1 and P1) gene polymorphisms with type 2 diabetes mellitus in north Indian population*. J Postgrad Med, 2010. **56**(3): p. 176-81.
84. Gonul, N., et al., *The role of GSTM1, GSTT1, GSTP1, and OGG1 polymorphisms in type 2 diabetes mellitus risk: a case-control study in a Turkish population*. Gene, 2012. **505**(1): p. 121-7.
85. McIlwain, C.C., D.M. Townsend, and K.D. Tew, *Glutathione S-transferase polymorphisms: cancer incidence and therapy*. Oncogene, 2006. **25**(11): p. 1639-48.

86. Moasser, E., et al., *Study of the association between glutathione S-transferase (GSTM1, GSTT1, GSTP1) polymorphisms with type II diabetes mellitus in southern of Iran*. Mol Biol Rep, 2012. **39**(12): p. 10187-92.
87. Pinheiro, D.S., et al., *Evaluation of glutathione S-transferase GSTM1 and GSTT1 deletion polymorphisms on type-2 diabetes mellitus risk*. PLoS One, 2013. **8**(10): p. e76262.
88. Stoian, A., et al., *Influence of GSTM1, GSTT1, and GSTP1 Polymorphisms on Type 2 Diabetes Mellitus and Diabetic Sensorimotor Peripheral Neuropathy Risk*. Dis Markers, 2015. **2015**: p. 638693.
89. Wang, G., L. Zhang, and Q. Li, *Genetic polymorphisms of GSTT1, GSTM1, and NQO1 genes and diabetes mellitus risk in Chinese population*. Biochem Biophys Res Commun, 2006. **341**(2): p. 310-3.
90. Yalin, S., et al., *Glutathione S-transferase gene polymorphisms in Turkish patients with diabetes mellitus*. Cell Biochem Funct, 2007. **25**(5): p. 509-13.
91. Zaki, M.A., et al., *Glutathione S-transferase M1, T1 and P1 gene polymorphisms and the risk of developing type 2 diabetes mellitus in Egyptian diabetic patients with and without diabetic vascular complications*. Alexandria Journal of Medicine, 2015. **51**(1): p. 73-82.
92. Ramprasath, T., et al., *Potential risk modifications of GSTT1, GSTM1 and GSTP1 (glutathione-S-transferases) variants and their association to CAD in patients with type-2 diabetes*. Biochem Biophys Res Commun, 2011. **407**(1): p. 49-53.
93. Rao, D.K., et al., *Variations in the GST activity are associated with single and combinations of GST genotypes in both male and female diabetic patients*. Mol Biol Rep, 2014. **41**(2): p. 841-8.
94. Amer, M.A., et al., *Evaluation of glutathione S-transferase P1 genetic variants affecting type-2 diabetes susceptibility and glycemic control*. Arch Med Sci, 2012. **8**(4): p. 631-6.
95. Habig, W.H., M.J. Pabst, and W.B. Jakoby, *Glutathione S-transferases. The first enzymatic step in mercapturic acid formation*. J Biol Chem, 1974. **249**(22): p. 7130-9.
96. Witz, G., *Biological interactions of alpha,beta-unsaturated aldehydes*. Free Radic Biol Med, 1989. **7**(3): p. 333-49.

97. Esterbauer, H., R.J. Schaur, and H. Zollner, *Chemistry and biochemistry of 4-hydroxynonenal, malonaldehyde and related aldehydes*. Free Radic Biol Med, 1991. **11**(1): p. 81-128.
98. Moghe, A., et al., *Molecular mechanisms of acrolein toxicity: relevance to human disease*. Toxicol Sci, 2015. **143**(2): p. 242-55.
99. Aldini, G., M. Orioli, and M. Carini, *Protein modification by acrolein: relevance to pathological conditions and inhibition by aldehyde sequestering agents*. Mol Nutr Food Res, 2011. **55**(9): p. 1301-19.
100. Baba, S.P., et al., *Aldose reductase (AKR1B3) regulates the accumulation of advanced glycosylation end products (AGEs) and the expression of AGE receptor (RAGE)*. Chem Biol Interact, 2011. **191**(1-3): p. 357-63.
101. Daimon, M., et al., *Increased urinary levels of pentosidine, pyrroline and acrolein adduct in type 2 diabetes*. Endocr J, 2003. **50**(1): p. 61-7.
102. Adler, V., et al., *Regulation of JNK signaling by GSTp*. Embo j, 1999. **18**(5): p. 1321-34.
103. Ishisaki, A., et al., *Glutathione S-transferase Pi is a dopamine-inducible suppressor of dopamine-induced apoptosis in PC12 cells*. J Neurochem, 2001. **77**(5): p. 1362-71.
104. Bernardini, S., et al., *Modulation of GST P1-1 activity by polymerization during apoptosis*. J Cell Biochem, 2000. **77**(4): p. 645-53.
105. Singh, S.V., et al., *Gender-related differences in susceptibility of A/J mouse to benzo[a]pyrene-induced pulmonary and forestomach tumorigenesis*. Cancer Lett, 1998. **128**(2): p. 197-204.
106. Wang, T., et al., *Glutathione S-transferase P1-1 (GSTP1-1) inhibits c-Jun N-terminal kinase (JNK1) signaling through interaction with the C terminus*. J Biol Chem, 2001. **276**(24): p. 20999-1003.
107. Elsby, R., et al., *Increased constitutive c-Jun N-terminal kinase signaling in mice lacking glutathione S-transferase Pi*. J Biol Chem, 2003. **278**(25): p. 22243-9.
108. Ruscoe, J.E., et al., *Pharmacologic or genetic manipulation of glutathione S-transferase P1-1 (GSTpi) influences cell proliferation pathways*. J Pharmacol Exp Ther, 2001. **298**(1): p. 339-45.
109. Wetzelberger, K., et al., *Postischemic deactivation of cardiac aldose reductase: role of glutathione S-transferase P and glutaredoxin in regeneration of reduced thiols from sulfenic acids*. J Biol Chem, 2010. **285**(34): p. 26135-48.

110. McGarry, D.J., et al., *Proteome-wide identification and quantification of S-glutathionylation targets in mouse liver*. *Biochem J*, 2015. **469**(1): p. 25-32.
111. McGarry, D.J., et al., *Altered protein S-glutathionylation identifies a potential mechanism of resistance to acetaminophen-induced hepatotoxicity*. *J Pharmacol Exp Ther*, 2015. **355**(2): p. 137-44.
112. Davis, R.J., *Signal transduction by the JNK group of MAP kinases*. *Cell*, 2000. **103**(2): p. 239-52.
113. Sabio, G., et al., *A stress signaling pathway in adipose tissue regulates hepatic insulin resistance*. *Science*, 2008. **322**(5907): p. 1539-43.
114. Samuel, V.T. and G.I. Shulman, *Mechanisms for insulin resistance: common threads and missing links*. *Cell*, 2012. **148**(5): p. 852-71.
115. Das, M., et al., *Induction of hepatitis by JNK-mediated expression of TNF-alpha*. *Cell*, 2009. **136**(2): p. 249-60.
116. Kaneto, H., et al., *Possible novel therapy for diabetes with cell-permeable JNK-inhibitory peptide*. *Nat Med*, 2004. **10**(10): p. 1128-32.
117. Solinas, G., et al., *Saturated fatty acids inhibit induction of insulin gene transcription by JNK-mediated phosphorylation of insulin-receptor substrates*. *Proc Natl Acad Sci U S A*, 2006. **103**(44): p. 16454-9.
118. Kim, W.H., et al., *Synergistic activation of JNK/SAPK induced by TNF-alpha and IFN-gamma: apoptosis of pancreatic beta-cells via the p53 and ROS pathway*. *Cell Signal*, 2005. **17**(12): p. 1516-32.
119. Varona-Santos, J.L., et al., *c-Jun N-terminal kinase 1 is deleterious to the function and survival of murine pancreatic islets*. *Diabetologia*, 2008. **51**(12): p. 2271-80.
120. Bonny, C., et al., *Cell-permeable peptide inhibitors of JNK: novel blockers of beta-cell death*. *Diabetes*, 2001. **50**(1): p. 77-82.
121. Noguchi, H., et al., *Activation of c-Jun NH2-terminal kinase (JNK) pathway during islet transplantation and prevention of islet graft loss by intraportal injection of JNK inhibitor*. *Diabetologia*, 2007. **50**(3): p. 612-9.
122. Noguchi, H., et al., *Cell permeable peptide of JNK inhibitor prevents islet apoptosis immediately after isolation and improves islet graft function*. *Am J Transplant*, 2005. **5**(8): p. 1848-55.
123. Diaz-Delfin, J., M. Morales, and C. Caelles, *Hypoglycemic action of thiazolidinediones/peroxisome proliferator-activated receptor gamma by*

- inhibition of the c-Jun NH2-terminal kinase pathway*. Diabetes, 2007. **56**(7): p. 1865-71.
124. Abdelli, S., et al., *Intracellular stress signaling pathways activated during human islet preparation and following acute cytokine exposure*. Diabetes, 2004. **53**(11): p. 2815-23.
 125. Ammendrup, A., et al., *The c-Jun amino-terminal kinase pathway is preferentially activated by interleukin-1 and controls apoptosis in differentiating pancreatic beta-cells*. Diabetes, 2000. **49**(9): p. 1468-76.
 126. Nakatani, Y., et al., *Modulation of the JNK pathway in liver affects insulin resistance status*. J Biol Chem, 2004. **279**(44): p. 45803-9.
 127. Winzell, M.S. and B. Ahren, *The high-fat diet-fed mouse: a model for studying mechanisms and treatment of impaired glucose tolerance and type 2 diabetes*. Diabetes, 2004. **53 Suppl 3**: p. S215-9.
 128. McGuinness, O.P., et al., *NIH experiment in centralized mouse phenotyping: the Vanderbilt experience and recommendations for evaluating glucose homeostasis in the mouse*. Am J Physiol Endocrinol Metab, 2009. **297**(4): p. E849-55.
 129. Maianti, J.P., et al., *Anti-diabetic activity of insulin-degrading enzyme inhibitors mediated by multiple hormones*. Nature, 2014. **511**(7507): p. 94-8.
 130. Livak, K.J. and T.D. Schmittgen, *Analysis of relative gene expression data using real-time quantitative PCR and the 2(-Delta Delta C(T)) Method*. Methods, 2001. **25**(4): p. 402-8.
 131. Schiza, V., et al., *N-alpha-terminal acetylation of histone H4 regulates arginine methylation and ribosomal DNA silencing*. PLoS Genet, 2013. **9**(9): p. e1003805.
 132. Bligh, E.G. and W.J. Dyer, *A rapid method of total lipid extraction and purification*. Can J Biochem Physiol, 1959. **37**(8): p. 911-7.
 133. Team, R.C., *R: A language and environment for statistical computing*. Vienna, Austria: R Foundation for Statistical Computing; 2014. 2014.
 134. Cefalu, W.T., M.P. Petersen, and R.E. Ratner, *The alarming and rising costs of diabetes and prediabetes: a call for action!* Diabetes Care, 2014. **37**(12): p. 3137-8.
 135. Hardwick, R.N., et al., *Diversity in antioxidant response enzymes in progressive stages of human nonalcoholic fatty liver disease*. Drug Metab Dispos, 2010. **38**(12): p. 2293-301.

136. Petrovic, D. and B. Peterlin, *GSTM1-null and GSTT1-null genotypes are associated with essential arterial hypertension in patients with type 2 diabetes*. Clin Biochem, 2014. **47**(7-8): p. 574-7.
137. Haberzettl, P., et al., *Role of endoplasmic reticulum stress in acrolein-induced endothelial activation*. Toxicol Appl Pharmacol, 2009. **234**(1): p. 14-24.
138. Hirosumi, J., et al., *A central role for JNK in obesity and insulin resistance*. Nature, 2002. **420**(6913): p. 333-6.
139. Lee, Y.H., et al., *c-Jun N-terminal kinase (JNK) mediates feedback inhibition of the insulin signaling cascade*. J Biol Chem, 2003. **278**(5): p. 2896-902.
140. Hotamisligil, G.S., *Endoplasmic reticulum stress and the inflammatory basis of metabolic disease*. Cell, 2010. **140**(6): p. 900-17.
141. Zhao, L., et al., *Chronic inflammation aggravates metabolic disorders of hepatic fatty acids in high-fat diet-induced obese mice*. Sci Rep, 2015. **5**: p. 10222.
142. DeFronzo, R.A., *Banting Lecture. From the triumvirate to the ominous octet: a new paradigm for the treatment of type 2 diabetes mellitus*. Diabetes, 2009. **58**(4): p. 773-95.
143. Puigserver, P., et al., *Insulin-regulated hepatic gluconeogenesis through FOXO1-PGC-1alpha interaction*. Nature, 2003. **423**(6939): p. 550-5.
144. Barthel, A. and D. Schmolli, *Novel concepts in insulin regulation of hepatic gluconeogenesis*. Am J Physiol Endocrinol Metab, 2003. **285**(4): p. E685-92.
145. Henquin, J.C., et al., *Signals and pools underlying biphasic insulin secretion*. Diabetes, 2002. **51 Suppl 1**: p. S60-7.
146. Szollosi, A., et al., *Glucose stimulates Ca²⁺ influx and insulin secretion in 2-week-old beta-cells lacking ATP-sensitive K⁺ channels*. J Biol Chem, 2007. **282**(3): p. 1747-56.
147. Straub, S.G. and G.W. Sharp, *Glucose-stimulated signaling pathways in biphasic insulin secretion*. Diabetes Metab Res Rev, 2002. **18**(6): p. 451-63.
148. Seppala-Lindroos, A., et al., *Fat accumulation in the liver is associated with defects in insulin suppression of glucose production and serum free fatty acids independent of obesity in normal men*. J Clin Endocrinol Metab, 2002. **87**(7): p. 3023-8.

149. Samuel, V.T., et al., *Mechanism of hepatic insulin resistance in non-alcoholic fatty liver disease*. J Biol Chem, 2004. **279**(31): p. 32345-53.
150. Kraegen, E.W., et al., *Development of muscle insulin resistance after liver insulin resistance in high-fat-fed rats*. Diabetes, 1991. **40**(11): p. 1397-403.
151. Kim, J.K., et al., *Tissue-specific overexpression of lipoprotein lipase causes tissue-specific insulin resistance*. Proc Natl Acad Sci U S A, 2001. **98**(13): p. 7522-7.
152. Kim, S.P., et al., *Primacy of hepatic insulin resistance in the development of the metabolic syndrome induced by an isocaloric moderate-fat diet in the dog*. Diabetes, 2003. **52**(10): p. 2453-60.
153. Kokame, K., et al., *Herp, a new ubiquitin-like membrane protein induced by endoplasmic reticulum stress*. J Biol Chem, 2000. **275**(42): p. 32846-53.
154. Kahn, S.E., *The relative contributions of insulin resistance and beta-cell dysfunction to the pathophysiology of Type 2 diabetes*. Diabetologia, 2003. **46**(1): p. 3-19.
155. Hers, H.G. and L. Hue, *Gluconeogenesis and related aspects of glycolysis*. Annu Rev Biochem, 1983. **52**: p. 617-53.
156. Firth, R.G., et al., *Postprandial hyperglycemia in patients with noninsulin-dependent diabetes mellitus. Role of hepatic and extrahepatic tissues*. J Clin Invest, 1986. **77**(5): p. 1525-32.
157. Yerkovich, S.T., et al., *Kupffer cell cytokines interleukin-1beta and interleukin-10 combine to inhibit phosphoenolpyruvate carboxykinase and gluconeogenesis in cultured hepatocytes*. Int J Biochem Cell Biol, 2004. **36**(8): p. 1462-72.
158. Watanabe, C., et al., *Remodeling of hepatic metabolism and hyperaminoacidemia in mice deficient in proglucagon-derived peptides*. Diabetes, 2012. **61**(1): p. 74-84.
159. Westerbacka, J., et al., *Genes involved in fatty acid partitioning and binding, lipolysis, monocyte/macrophage recruitment, and inflammation are overexpressed in the human fatty liver of insulin-resistant subjects*. Diabetes, 2007. **56**(11): p. 2759-65.
160. Jurado, L.A., et al., *Conserved amino acids within CCAAT enhancer-binding proteins (C/EBP(alpha) and beta) regulate phosphoenolpyruvate carboxykinase (PEPCK) gene expression*. J Biol Chem, 2002. **277**(31): p. 27606-12.

161. Koo, S.H., et al., *The CREB coactivator TORC2 is a key regulator of fasting glucose metabolism*. Nature, 2005. **437**(7062): p. 1109-11.
162. O'Brien, R.M., et al., *Hepatic nuclear factor 3- and hormone-regulated expression of the phosphoenolpyruvate carboxykinase and insulin-like growth factor-binding protein 1 genes*. Mol Cell Biol, 1995. **15**(3): p. 1747-58.
163. Yoon, J.C., et al., *Control of hepatic gluconeogenesis through the transcriptional coactivator PGC-1*. Nature, 2001. **413**(6852): p. 131-8.
164. Burgess, S.C., et al., *Cytosolic phosphoenolpyruvate carboxykinase does not solely control the rate of hepatic gluconeogenesis in the intact mouse liver*. Cell Metab, 2007. **5**(4): p. 313-20.
165. Le Lay, J., et al., *CRTC2 (TORC2) contributes to the transcriptional response to fasting in the liver but is not required for the maintenance of glucose homeostasis*. Cell Metab, 2009. **10**(1): p. 55-62.
166. Ramnanan, C.J., et al., *Molecular characterization of insulin-mediated suppression of hepatic glucose production in vivo*. Diabetes, 2010. **59**(6): p. 1302-11.
167. Sloop, K.W., et al., *Specific reduction of hepatic glucose 6-phosphate transporter-1 ameliorates diabetes while avoiding complications of glycogen storage disease*. J Biol Chem, 2007. **282**(26): p. 19113-21.
168. Samuel, V.T., et al., *Fasting hyperglycemia is not associated with increased expression of PEPCK or G6Pc in patients with Type 2 Diabetes*. Proc Natl Acad Sci U S A, 2009. **106**(29): p. 12121-6.
169. Kumashiro, N., et al., *Targeting pyruvate carboxylase reduces gluconeogenesis and adiposity and improves insulin resistance*. Diabetes, 2013. **62**(7): p. 2183-94.
170. Jitrapakdee, S., et al., *Structure, mechanism and regulation of pyruvate carboxylase*. Biochem J, 2008. **413**(3): p. 369-87.
171. Weinberg, M.B. and M.F. Utter, *Effect of streptozotocin-induced diabetes mellitus on the turnover of rat liver pyruvate carboxylase and pyruvate dehydrogenase*. Biochem J, 1980. **188**(3): p. 601-8.
172. Large, V. and M. Beylot, *Modifications of citric acid cycle activity and gluconeogenesis in streptozotocin-induced diabetes and effects of metformin*. Diabetes, 1999. **48**(6): p. 1251-7.
173. Jitrapakdee, S., et al., *Regulation of rat pyruvate carboxylase gene expression by alternate promoters during development, in genetically*

obese rats and in insulin-secreting cells. Multiple transcripts with 5'-end heterogeneity modulate translation. J Biol Chem, 1998. **273**(51): p. 34422-8.

CURRICULUM VITAE

Shubha Ghosh Dastidar

University of Louisville, School of Medicine
Diabetes and Obesity Center
580 S Preston Street, Baxter II, Rm. 409
Louisville, KY 40202
shubha.ghoshdastidar@louisville.edu
Alt. Email: shubhaghosh83@gmail.com
Phone: 502-657-9013 (Cell)
Citizenship: India

EDUCATION AND TRAINING

Ph.D. Candidate - Biochemistry and Molecular Genetics, GPA 3.82
University of Louisville, School of Medicine, Louisville, KY, USA.

2012-Current

Advisors: Dr. Aruni Bhatnagar Ph.D.

Dr. Daniel J. Conklin Ph.D.

Dissertation Title: "GLUTATHIONE-S-TRANSFERASE P IN GLUCOSE HOMEOSTASIS IN MICE"

Graduation Expected: December 2016

M.S. - Biochemistry and Molecular Biology

University of Louisville, School of Medicine, Louisville, KY, USA.

2010-2012

M.Sc. - Microbiology

Bangalore University, Bangalore, India

2004-2006

B.Sc. - Microbiology

University of Pune, Pune, India

2001-2004

RESEARCH EXPERIENCE

Graduate Research Assistant

Diabetes and Obesity Center, University of Louisville

August 2011 – Current

Summary of Dissertation Research:

My dissertation project was designed to achieve new understanding of how the antioxidant enzyme, Glutathione-S-transferase P (GSTP) contributes to glucose homeostasis via its role (s) in aldehyde metabolism and JNK regulation. Hepatic and adipose glutathione S-transferases are dysregulated in obesity, non-alcoholic fatty liver disease (NAFLD) and type 2 diabetes (T2D). Through the work in my thesis, I have elucidated a novel role of GSTP in glucose homeostasis via its effect on hepatic glucose output and insulin secretion. Using high-fat diet feeding in mice, I have delineated the effect of obesity on GSTP abundance and function(s) in metabolic tissues as it relates to the development of glucose intolerance and insulin resistance. Furthermore, I have identified a glucose intolerance phenotype in GSTP-null mice and uncovered a potentially novel pathway of hepatic gluconeogenesis that likely operates via JNK activation and inflammation in GSTP-null mice. Overall, my data suggests that reduced hepatic GSTP might be a crucial instigator of hyperglycemia in T2D and preventing even small changes in hepatic GSTP abundance or activity may have potentially important consequences for addressing inter-individual variation to disease susceptibility.

Technical Expertise:

Animal Techniques (Murine models):

- High fat feeding and intervention studies: Planned and performed diet studies with varying composition and duration, and completed JNK inhibitor (SP600125) intervention studies.
- Body composition assessment via dual energy X-ray absorptiometry (DEXA)
- Metabolic phenotyping- measurement of indirect gas calorimetry, food and water intake and locomotor activity
- Genomic DNA isolation and genotyping
- Organ harvest and blood collection by left ventricular heart puncture from euthanized mice
- Glucose, insulin and pyruvate tolerance tests

Molecular Biology Techniques:

- Adipocyte and Stromal Vascular Fraction isolation
- RNA isolation from tissues (lung, liver, heart, adipose depots, skeletal muscle), cDNA preparation and quantitative RT-PCR
- Western blotting and immunoprecipitation
- Assays for oxidative stress (GSH:GSSG ratio)
- General assays for diabetes and obesity research: Performed ELISAs to assess plasma insulin, C-peptide and glucagon
- Bligh and Dyer extraction of hepatic lipids for steatosis studies

Data Analyses and Presentation:

MS Word, Excel, PowerPoint, GraphPad Prism, SigmaPlot, Adobe Photoshop, Adobe Photoshop Sketch

Lab Trainee

Department of Biochemistry and Molecular Biology, University of Louisville

Principal Investigator: Dr. Yong Li

January 2011-August 2011

Project: Examining the role of NF-kB pathway proteins in miR301a and miR-21 activation in pancreatic carcinoma

Project Intern

Department of Virology, Calcutta School of Tropical Medicine, Kolkata, India

Supervisor: Dr. Srima Adhikari

January 2006-March 2006

Project: Screening and sero-diagnosis of Hepatitis B, Hepatitis C, HIV/AIDS virus

AWARDS/SCHOLORSHIPS

- Professional Development Stipend, Graduate Teaching Assistant Academy, School of Interdisciplinary and Graduate Studies, University of Louisville, August 2016
- Graduate Student Travel Award, Department of Biochemistry and Molecular Genetics and PGXL Laboratories, Louisville, KY, to attend *Experimental Biology*, San Diego, CA, April 2016
- International Student Tuition Support Award, International Center, University of Louisville, Spring 2016
- 2nd Place Award, Graduate Student Research Poster Competition; *The Sixth University of Louisville Biochemistry and Molecular Genetics Colloquium*, Louisville KY, 2015
- Integrated Program in Biomedical Sciences Fellowship (IPIBS) Award, University of Louisville, August 2010-July, 2012

PUBLICATIONS AND ABSTRACTS

- **Ghosh Dastidar S**, Jagatheesan G, Haberzettl P, Bhatnagar A, Conklin DJ. Glutathione S-transferase P Deficiency Increases Hepatic Gluconeogenesis via JNK Activation. *Manuscript in preparation*.
- **Shubha Ghosh Dastidar**, Ganapathy Jagatheesan, Aruni Bhatnagar and Daniel J. Conklin. Glutathione S-transferase P and JNK Activation in Glucose Intolerance in Mice. *FASEB J.* April 2016 Vol 30. (Meeting Abstract Supplement) 956.2

PRESENTATIONS

Oral Presentations

- DOC Trainee Project Presentation (Biannual), Diabetes and Obesity Center, Univ. of Louisville. 2012-Present.
- “Glucose Intolerance in Glutathione-S-Transferase P-Deficient Mice: Role of JNK Activation, Inflammation and Enhanced Hepatic Gluconeogenesis”. Research Conference, Department of Biochemistry and Molecular Genetics, Univ. of Louisville. September 28, 2015.
- “Glutathione-S-transferase-P in Diet-induced Obesity and Insulin Resistance”. Research Conference, Department of Biochemistry and Molecular Biology, Univ. of Louisville. April 7, 2014
- “Protein Carbonylation and Glutathione-S-transferases in Adipose Tissue: Implications for Obesity and Insulin Resistance”. Seminar Series, Department of Biochemistry and Molecular Biology, Univ. of Louisville. September 16, 2013.
- “Cardiovascular Pathology in Hutchinson-Gilford Progeria Syndrome - Implications for Human Aging”. Seminar Series, Department of Biochemistry and Molecular Biology, Univ. of Louisville. April 9, 2012
- “Examination of NF- κ B pathway proteins in miR-301a and miR-21 activation in pancreatic carcinoma”. Lab Rotation Report, Department of Biochemistry and Molecular Biology, Univ. of Louisville. June 13, 2011

Abstracts and Posters at National/Local Conferences

- *Glutathione-S-transferase-P and JNK Activation in Glucose Intolerance in Mice*; **Shubha Ghosh Dastidar**, Ganapathy Jagatheesan, Aruni

Bhatnagar and Daniel J. Conklin. *Experimental Biology* San Diego, CA, April 2016.

- *Glucose Intolerance in Mice: Role of Glutathione-S-transferase-P, JNK Activation, Inflammation and Increased Hepatic Gluconeogenesis*; **Ghosh Dastidar S.**, Bhatnagar A. and Conklin DJ.
 - Research! Louisville 2015, Louisville, KY
 - The Sixth University of Louisville Biochemistry and Molecular Genetics Colloquium, Louisville, KY, August 2015
- *Phenotyping Humanized (hGSTP1) Mice to Explore the Role of GST-P in Glucose Intolerance, Obesity and Diabetes*; David Logan, **Shubha Ghosh Dastidar** and Daniel J. Conklin. Summer Undergraduate Cardiovascular Research Poster Session, Dept. of Physiology, University of Louisville, July 2015
- *Glutathione-S-transferase-P deficiency leads to Glucose Intolerance in Mice*; **Shubha Ghosh Dastidar**, Aruni Bhatnagar and Daniel J. Conklin. Research! Louisville 2014, Louisville, KY
- *Adipose Depot-specific Modulation of Glutathione-S-transferases in Diet-induced Obesity in Mice*; **Shubha Ghosh Dastidar**, Aruni Bhatnagar and Daniel J. Conklin.
 - Research! Louisville 2013, Louisville, KY
 - The Fifth University of Louisville Biochemistry and Molecular Biology Colloquium, Louisville, KY, August 2013

TEACHING/MENTORING EXPERIENCE

- Teaching Assistant, Advanced Biochemistry-II (BIOC 647)-Spring 2012, University of Louisville.
Course: Cellular metabolism of carbohydrates, amino acids and lipids.
-Aided in tutoring students and grading assignments
- Participated in journal club facilitation and student peer mentoring in the Dept. of Biochemistry
- Trained lab members in planning and executing high fat diet studies in mice including techniques for DEXA scanning, blood glucose measurement from tail snips, glucose tolerance tests, metabolic phenotyping, data acquisition and analyses

CERTIFICATION

Graduate Teaching Assistant Academy

School of Interdisciplinary and Graduate Studies and Delphi Center for Teaching and Learning, University of Louisville, August 2015-April 2016

ACADEMIC SERVICE

- Served on Graduate Student Panel for PLAN workshop, “Succeeding in the US University” School of Interdisciplinary and Graduate Studies, University of Louisville, October 2016
- Served as GTA (Graduate Teaching Assistant) Academy Alumni Mentor, 2016-2017 GTA Academy
- Participated in Department of Biochemistry Student Body Meetings and Recruitment Week for prospective Biochemistry students
- Met in interviews with Dept. of Biochemistry Graduate School Candidates

PROFESSIONAL MEMBERSHIPS

- American Society of Biochemistry and Molecular Biology
- International Society for Biocuration

PAST PROFESSIONAL EXPERIENCE

Principal Scientific Analyst

Molecular Connections Pvt. Ltd, Bangalore, India
August 2006-June 2010

Project Area: Biocuration

The intent of the project was curation, interpretation, abstraction, and annotation of published scientific literature for the development and content enrichment of knowledge bases either for providing custom services to client or for in-house product development. The goal was to enable efficient and flexible data retrieval with simple queries.

Performed manual curation of biological data from published literature in the following areas:

- Pathology: Identified genes and variants and their relationship to the disease phenotype, evaluated diagnostic and prognostic biomarkers and extracted protein interactions implicated in disease etiology. MeSH and other NCBI databases were referred to and cross-referenced with for incorporating extracted data in the curation tool using pre-defined keywords and synopsis statements for each article.
- Pharmacology: Used standard thesauri to index drug-related adverse events, safety and efficacy data, contraindications and pharmacokinetics.

- Epigenetics: Mined data related to DNA methylation, histone modification, enzymes and genes involved, and the cellular/physiological phenotype. The extracted data was integrated in an in-house database for product development.

VOLUNTEER WORK

- Member and Volunteer, Organization Assisting and Serving International Students (OASIS), Louisville, KY, 08/2010-Current
- Attendee and Volunteer (booth for providing BMI and body fat measurements), American Diabetes Association (ADA) STEP OUT WALK, Louisville, KY, 2011, 2016
- Attendee and Volunteer (Logistics), American Heart Association (AHA) Heart Walk, Louisville, KY, 2012, 2014 and 2016
- Member and Volunteer, Louisville Bicycle Club, 2014-Current

REFERENCES

Aruni Bhatnagar, Ph.D. F.A.H.A

Professor of Medicine
 Director, Diabetes and Obesity Center
 U. Louisville, Louisville, USA
 Email: a0bhat01@louisville.edu

Daniel J. Conklin, Ph.D.

Professor of Medicine
 Division of Cardiovascular Medicine
 U. Louisville, Louisville, USA
 Email: dj.conklin@louisville.edu

Russell A. Prough, Ph.D.

Professor Emeritus/Adjunct Professor (Gratis)
 Dept. of Biochemistry & Molecular Genetics
 U. Louisville, Louisville, USA
 raprou01@louisville.edu

Barbara J. Clark, Ph.D.

Associate Professor
 Director of Graduate Studies
 Dept. of Biochemistry & Molecular Genetics

U. Louisville, Louisville, USA
Email: bjclar01@louisville.edu

Priti Ramamohan, Ph.D.

Principal Scientist
Molecular Connections Pvt. Ltd.
Bangalore, India
Email: pritisrikanth@gmail.com